LIST OF PUBLICATIONS

1. Kabita, K.; Maibam, J.; Sharma, B.I.; Singh, R.K.; Thapa, R.K. (2016). First principles phase transition, elastic properties and electronic structure calculations for cadmium telluride under induced pressure: density functional theory, LDA, GGA and modified Becke–Johnson potential. *Materials Research Express*, Vol. 3, No. 1, pp. 015901 (1-11).
2. Kabita, K.; Jameson, M.; Sharma, B.I.; Brojen, R.K.; Thapa, R.K. (2015). A detailed first principle study on the structural, elastic, and electronic properties of indium arsenide (InAs) under induced pressure. *Canadian Journal of Physics*, Vol. 94, No. 3, pp. 254-261.
3. Kabita, K.; Maibam, J.; Sharma, I.; Singh, R.K.; Thapa, R.K. (2015). Elastic Properties and Electronic Structures of Pressure Induced Zinc Sulphide (ZnS): A Density Functional Theory Study. *Advanced Science Letters*, Vol. 21, No. 9, pp. 2906-2910.
4. Kabita, K.; Maibam, J.; Sharma, B.I.; Thapa, R.K.; Singh, R.K. (2015). First principle study on pressure-induced electronic structure and elastic properties of indium phosphide (InP). *Indian Journal of Physics*, Vol. 89, No. 12, pp. 1265-1271.
5. Kabita, K.; Sharma, B. I. (2015). Electronic Structures of GaX (X=P, As) under Induced Pressure: A First Principle Study. *Jounal of Basic and Applied Engineering Research,* Vol. 2, No. 13, pp. 1064-1067.
6. Kabita, K.; Sharma, B. I. (2015). Structural Phase Transition of Indium Arsenide under Induced Pressure: A Density Functional Theory Study. *Journal of Applied and Fundamental Sciences*, Vol. 1, No. 1, pp.7-10.
7. Kabita, K.; Maibam, J.; Sharma, B.I.; Singh, R.K.; Thapa, R.K. (2014). Density functional theory study on pressure induced structural transformation, elastic properties and electronic structure of gallium

arsenide (GaAs). *International Journal of Innovation and Applied Studies*, Vol. 8, No. 1, pp.382-393.

8. Kabita, K.; Maibam, J.; Sharma, B.I.; Thapa, R.K.; Singh, R.K. (2014). Density Functional Theory Study of Electronic Structure, Elastic Properties and Phase Transition of Gallium Phosphide (GaP). *Advanced Science, Engineering and Medicine*, Vol. 6, No. 3, pp.354-358.
9. Kabita, K.; Maibam, J.; Sharma, B.I.; Thapa, R.K.; Singh, R.K. (2013). First Principle Calculation of Pressure-Induced Phase Transition and Band Structure of Gallium Phosphide. *Iraqi Journal of Applied Physics*, Vol. 9 No. 4, pp. 17-20.

LIST OF CONFERENCES, SEMINARS AND WORKSHOPS ATTENDED

1. Presented a paper titled "First principles study on structural, phase transition and electronic structure of Zinc Sulfide (ZnS) within LDA, GGA and mBJ potential" at XXVII IUPAP Conference on Computational Physics CCP 2015, IIT Guwahati.
2. Presented a paper titled "Theoretical study on the B3 phases of ZnSe: Structural and Electronic properties" at International E-Workshop/ Conference on Computational Condensed Matter Physics and Material Science (IWCCMP-2015), IIIITM, Gwalior.
3. Presented a paper titled "Electronic Structures of GaX (X=P, As) Under Induced Pressure: A DFT study" at the International conference on Recent trends in Applied Physical, Chemical Sciences, Mathematical/Statistical and Environmental Dynamics (PCME-2015), at JNU, New Delhi.
4. Presented a paper titled "Electronic properties of B3 phases of GaP at High Pressure: A DFT study" at the National Conference on Current Perspectives on Research on Chemical Sciences (CPRCS-2015), AUS, Silchar.
5. Presented a paper titled "Elastic Properties and Electronic Structures of Pressure induced ZnS: A DFT study" at International E-Workshop/ Conference on Computational Condensed Matter Physics and Material Science (IWCCMP-2014), IIIITM, Gwalior.
6. Presented paper titled "Ab-initio study on the electronic structure of InP" at the National seminar on Frontiers of Research in Physical Sciences, 2014, Karimganj, Assam.
7. Attended workshop on "Microwave: Basics and Applications"2014, at AUS, Silchar.
8. Attended summer school on Materials Simulation Theory and Numerics, 2014, IISER Pune.
9. Attended "Refresher Course in Theoretical Physics" 2013, at AUS, Silchar.

10. Presented paper titled “FP-LAPW investigation of the electronic structure of GaP in zinc-blende structure” 2013, at the National Seminar on Advances in Research in Physical Sciences, Cachar College, Silchar.

IOPscience iopscience.iop.org

Home Search Collections Journals About Contact us My IOPscience

First principles phase transition, elastic properties and electronic structure calculations for cadmium telluride under induced pressure: density functional theory, LDA, GGA and modified Becke–Johnson potential

This content has been downloaded from IOPscience. Please scroll down to see the full text.

2016 Mater. Res. Express 3 015901

(http://iopscience.iop.org/2053-1591/3/1/015901)

View the table of contents for this issue, or go to the journal homepage for more

Download details:

IP Address: 132.239.1.231
This content was downloaded on 18/01/2016 at 05:45

Please note that terms and conditions apply.

Materials Research Express

PAPER

First principles phase transition, elastic properties and electronic structure calculations for cadmium telluride under induced pressure: density functional theory, LDA, GGA and modified Becke–Johnson potential

RECEIVED
7 September 2015

REVISED
30 November 2015

ACCEPTED FOR PUBLICATION
8 December 2015

PUBLISHED
14 January 2016

Kh Kabita[1], **Jameson Maibam**[1], **B Indrajit Sharma**[1], **R K Brojen Singh**[2] **and R K Thapa**[3]

[1] Department of Physics, Assam University, Silchar-788011, Assam, India
[2] School of Computational and Integrative Sciences, JNU, New Delhi 110067, India
[3] Department of Physics, Mizoram University, Tanhril, Aizawl-796 009, India

E-mail: indraofficial@rediffmail.com

Keywords: DFT, phase transition, elastic properties, electronic structure

Abstract

We report first principles phase transition, elastic properties and electronic structure for cadmium telluride (CdTe) under induced pressure in the light of density functional theory using the local density approximation (LDA), generalised gradient approximation (GGA) and modified Becke–Johnson (mBJ) potential. The structural phase transition of CdTe from a zinc blende (ZB) to a rock salt (RS) structure within the LDA calculation is 2.2 GPa while that within GGA is found to be at 4 GPa pressure with a volume collapse of 20.9%. The elastic constants and parameters (Zener anisotropy factor, Shear modulus, Poisson's ratio, Young's modulus, Kleinmann parameter and Debye's temperature) of CdTe at different pressures of both the phases have been calculated. The band diagram of the CdTe ZB structure shows a direct band gap of 1.46 eV as predicted by mBJ calculation which gives better results in close agreement with experimental results as compared to LDA and GGA. An increase in the band gap of the CdTe ZB phase is predicted under induced pressure while the metallic nature is retained in the CdTe RS phase.

1. Introduction

The II-VI semiconductor compounds have been extensively studied for several decades [1–3]. The study of the high pressure properties of these compound semiconductors has been of much scientific interest in recent years as important information about the electronic and elastic properties of the material can be gained by understanding the strained effects on the bulk compounds [4]. Cadmium telluride (CdTe) is a II-VI compound semiconductor which is being studied for its application in γ-ray detectors, infrared windows, solar cells and other optoelectronic devices [5]. Its high pressure behaviour has attracted much attention in recent years. It is found to occur in zinc blende (ZB) structures and wurtzite structures under ambient conditions and transforms to a rock salt (RS) structure at high pressures [6].

Ab-initio studies of the structural, mechanical and electronic properties of a material have become more precise and systematic due to the development in computer simulations. It helps us to better understand the properties of solids which are difficult to study experimentally. Generally the theoretical investigation of the band structure and electronic properties of compound semiconductors are performed using the local density approximation (LDA), generalised gradient approximation (GGA) and GW [7, 8]. Theoretical calculation within LDA and GGA approximation underestimates the energy band gap. The most appropriate tool for studying the energy band gap is the many perturbation theory within the GW approximation [9] but it is very expensive. In 2009 an alternative method for band gap calculation was given by Tran and Blah [10] which was equally efficient and computationally cheap. The modified Becke–Johnson (mBJ)-GGA potential [11]

© 2016 IOP Publishing Ltd

minimises the limitation of LDA and GGA and performs the calculation of band gaps precisely similar to the computationally expensive GW calculations.

To date there have been detailed studies on the electronic and elastic properties of CdTe [12–14] but not much has been done at high pressures. In 1993, McMahon and his group found out that with increasing pressure, the ZB structure underwent a transition to a cinnabar structure which was stable for only a short pressure interval and later changed to an RS structure on further increasing pressure [15]. Earlier studies also confirmed the phase transition of CdTe from a ZB to an RS structure at 3.8 GPa pressure [16]. In our previous work we have reported a detailed study on the pressure induced electronic structure and elastic properties of GaP [17, 18] and GaAs [19]. The aim of the present work is to perform first principles calculations for CdTe at different pressures and study the pressure induced phase transition from the ZB to RS phase as well as the effects of pressure in the elastic properties and electronic structures.

2. Computational method

All the calculations reported in this work are performed using the full potential linearized augmented plane wave [20] method under the framework of density functional theory (DFT) [21–23] as implemented in the WIEN2K code [24]. The exchange correlation interaction effects were treated with LDA, the generalized gradient approximation of the Perdew–Burke–Ernzerhof (PBE–GGA) [25] scheme and GGA with the modified Becke–Johnson (mBJ) potential. The use of the mBJ potential along with GGA in electronic structure calculation keeps the band gap in close agreement with the experimental value. In this method, the lattice is divided into non-overlapping spheres (called an atomic or muffin tin (MT) sphere) surrounding each atomic site and an interstitial region. Inside the MT region, the potential is a product of radial function and spherical harmonics and expanded up to order $l = 10$. For the interstitial regions that are outside the MT sphere, the potentials are expanded in plane waves. In the present study the number of k-points used for the integration part for both the ZB and RS structure of CdTe is 8000 k-points with 20*20*20 k mesh which is reduced to 256 irreducible k-points inside the Brillion zone including five high symmetry points W, L, Γ, X and K. Convergence of the basis set is obtained at $R_{MT}K_{max} = 9.0$ where K_{max} gives us the plane wave cut-off. The RMT_{min} used in the calculation is 2.5. The position of the first and second atom in the ZB structure is taken to be (0, 0, 0) and (0.25, 0.25, 0.25) and in the RS structure it is (0, 0, 0) and (0.5, 0.5, 0.5) respectively. The states $4d^{10}5s^2$ and $4d^{10}5s^25p^4$ are considered as a valence electron for Cd and Te respectively. The total energy difference used for succeeding iterations is less than 0.00 001 Ryd per formula unit. The elastic constants have been determined using the stress–strain method with a volume conserving technique [26]. Only a small distortion has been considered in our calculation in order to remain within the elastic domain of the crystal.

3. Results and discussion

3.1. Structural and phase transition

Figure 1 shows the plot of total energy as a function of volume of CdTe for both the ZB and RS phase within LDA and GGA for structure optimization. From the figure, one can see that the ZB structure of CdTe has lower total energy at the equilibrium volume in both the LDA and GGA method thus indicating that the ZB structure is more stable than the RS structure. The equilibrium structural parameters of the different phases of CdTe are obtained by fitting into the Birch–Murnaghan equation [27].

The obtained structural parameters are listed in table 1 along with other theoretical and experimental data. In general the present work agrees well with other experimental and theoretical results and hence is used for further high pressure calculation.

A thermodynamically stable phase is defined as the phase with the lowest Gibb's free energy at a given pressure and temperature. In our calculation we have ignored the entropy contribution as it is basically done at zero temperature. Therefore the structural phase transition is calculated from the equal enthalpy conditions, $H = E + PV$. In figure 2, the calculated enthalpy curves of the ZB and RS phase have been plotted as a function of pressure within both (a) LDA and (b) GGA. One can see from the figures that there is a crossing over of the enthalpy at 2.2 GPa pressure with the LDA calculation and 4.0 GPa pressure with the GGA calculation. It indicates a phase transition between the two phases. The experimental data available for this phase transition of CdTe-ZB to CdTe-RS is 3.0 GPa to 3.9 GPa [36–38]. Thus we observe that the LDA method underestimates the phase transition pressure while the GGA method gives a better result than the LDA and is in close agreement with the experimentally obtained values.

Since the phase transition pressure as determined with the GGA method gives us a better result we calculate the volume collapse for GGA only. Figure 3 shows the normalised volume (Vp/Vo) as a function of pressure. It is seen that during the phase transition, the normalised volume of the ZB and RS phase is 0.90 and 0.69 respectively

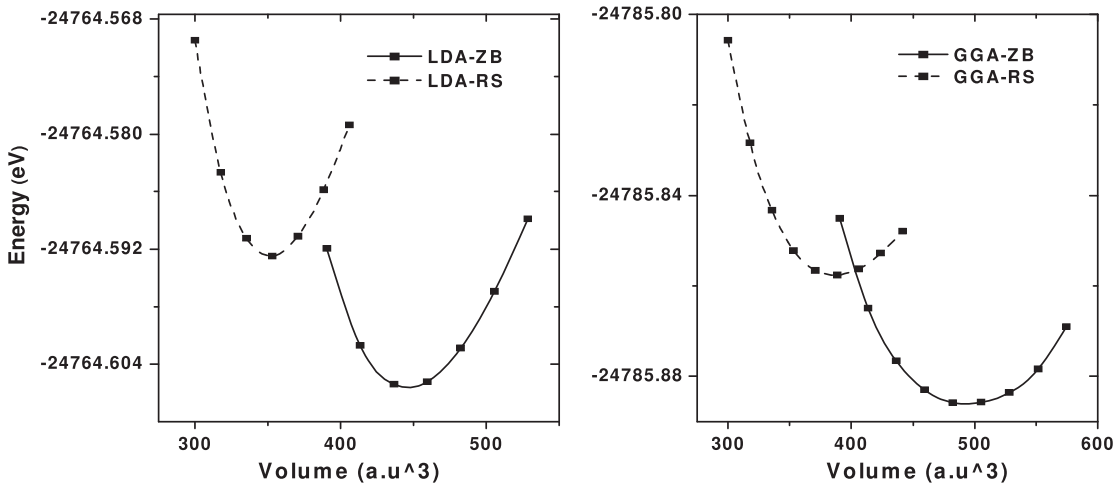

Figure 1. Total energy as a function of the volume of CdTe for ZB and RS structures within LDA and GGA.

Table 1. Experimental and calculated ground state structural parameters of CdTe.

		Zinc blende (ZB) strucutre			Rock salt (RS) structure		
		a_0 (A^0)	B_0 (GPa)	$B^/$	a_0 (A^0)	B_0 (GPa)	$B^/$
Present work	LDA	6.42	47.67	5.05	5.92	63.82	5.01
	GGA	6.65	25.28	8.35	6.11	48.24	4.99
Experimental work		6.53[a], 6.49[b]	42[g], 45[h]	6.4[g]	—	—	—
Other calculation		6.63[c], 6.62[d], 6.58[e]	33.8[c], 39.0[d], 36.6[e]	5.26[c], 5.14[c], 4.6[d]	6.11[d], 5.94[d], 5.9[f]	56.0[d], 66.4[f]	4.3[d], 5.1[i], 4.67[j]

[a] Reference [28],
[b] Reference [29],
[c] Reference [30],
[d] Reference [31],
[e] Reference [32],
[f] Reference [14],
[g] Reference [33],
[h] Reference [34],
[i] Reference [13],
[j] Reference [35].

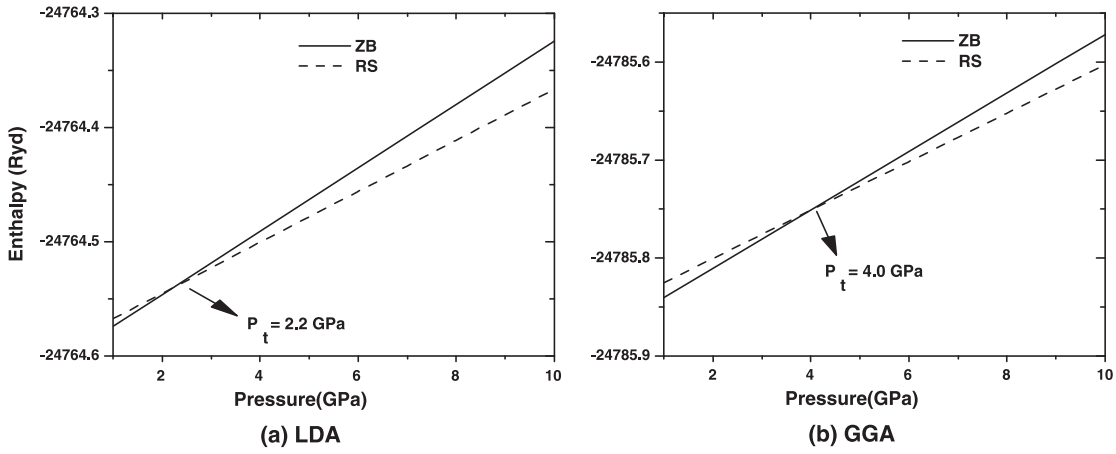

Figure 2. Enthalpy as a function of pressure for the ZB and RS phase of CdTe within (a) LDA and (b) GGA.

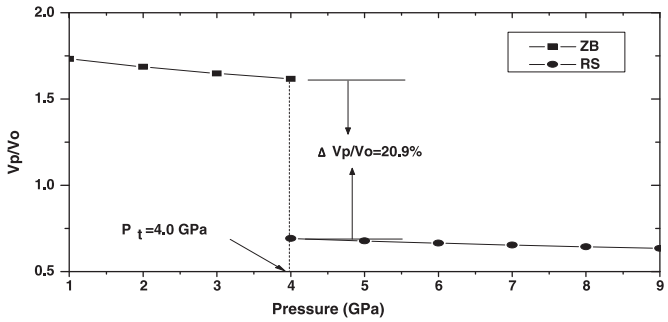

Figure 3. Normalised volume versus pressure for ZB and RS structures of CdTe within GGA.

Table 2. Phase transition pressure and volume collapse of CdTe.

	Present calculation	Expt. results	Theoretical results
Phase transition pressure (P_t) (GPa)	4.0	3.9[a], 3.8[b], 3.8[c], 3.8[d]	4.0[e], 3.9[f]
V_p/V_0	0.90	0.92[d]	0.93[b], 0.90[e]
Volume collapse (%)	20.9	—	19.0[b], 19.0[e]

[a] Reference [37],
[b] Reference [36],
[c] Reference [38],
[d] Reference [39],
[e] Reference [3],
[f] Reference [31].

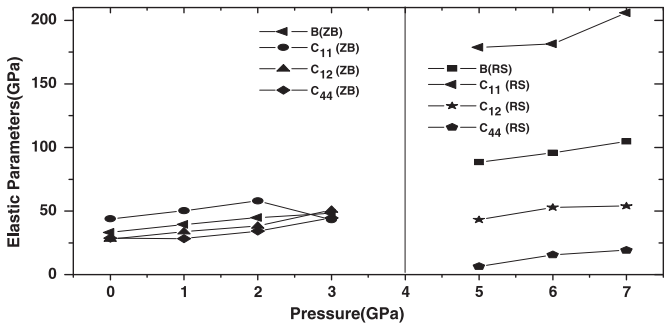

Figure 4. Elastic parameters versus pressure for the ZB and RS phase of CdTe.

with a volume reduction of 20.9% indicating that the CdTe-ZB phase is more compressible than the CdTe-RS phase. A comparison of the present results of the phase transition and volume collapse within the GGA with other experimental and theoretical results is given in table 2. It is observed that the present results of phase transition within GGA are in good agreement with other experimental and theoretical results.

3.2. Elastic properties

The elastic constants provide us with important information about the structural stability, binding characteristics and many mechanical properties of a material. For a cubic crystal the mechanical stability conditions: $(C_{11} + 2C_{12}) > 0$; C_{11}-$C_{12} > 0$; $C_{44} > 0$; $C_{11} > 0$ should be satisfied. In the present study the elastic constants are calculated within the GGA only as it has already been shown that it gives us better results than calculation within the LDA. The elastic constants of CdTe-ZB under induced pressure ranging from 0 GPa to 3 GPa pressure and for CdTe-RS at various pressures from 5 GPa to 7 GPa pressure are calculated and shown in figure 4.

In figure 4, one can clearly see that there is a linear variation in the bulk modulus as well as the elastic constants up to 2 GPa pressure in the ZB phase and 5 GPa to 7 GPa pressure in the RS phase. It is seen that at around 3 GPa pressure, the stability condition of the CdTe-ZB phase is not satisfied indicating that the structural transformation from ZB to RS starts at around 3 GPa pressure and is completed at 4 GPa pressure. Since the

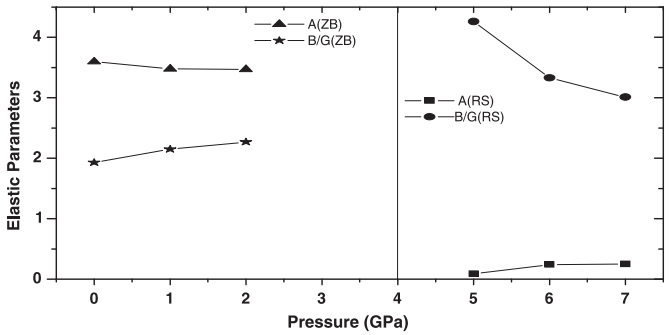

Figure 5. Elastic parameters (Zener anisotropy factor and B/G ratio) versus pressure for the ZB and RS phase of CdTe.

stability conditions are not satisfied from 3 GPa pressure and structural transition occurs at 4 GPa pressure, we perform further calculations of the elastic parameters like the Zener anisotropic factor (A), B/G ratio, Poisson's ratio (υ), Kleinmann parameter (ζ), Youngs modulus (Y), and Debye's temperature (θ_D) to determine the mechanical and thermal behaviour of CdTe in both the phases from 0 GPa to 2 GPa pressure for the CdTe-ZB phase and 5 GPa to 7 GPa pressure for the CdTe-RS phase.

The Zener anisotropy factor (A) gives us an insight into the elastic isotropy of a material. A material is said to be elastically isotropic with uniform deformation along all directions when $A = 1$. For $A > 1$, it is stiffest along <111> body diagonal and when $A < 1$, it is stiffest along <100> cube axes. In terms of elastic constants it is expressed as:

$$A = \frac{2C_{44}}{C_{11} - C_{12}} \tag{1}$$

Our calculation shows that for the CdTe-ZB phase, the value of A decreases from 3.60 to 3.46 while it increases from 0.09 to 0.25 in the RS phase with increasing pressure. It indicates that CdTe is not an elastically isotropic material in the ZB phase; it is stiffest along <111> body diagonal while it is stiffest along <100> cube axis in the RS phase. The ductility or brittleness of a material is determined by the ratio of bulk and shear modulus, B/G as proposed by Pugh [40]. If the shear modulus (G) is low we know that it has a low resistance to shear and hence is ductile, while if a material has low bulk modulus, it means the resistance fracture is low and hence is brittle. We know that the critical value which separates the ductility and brittleness of a material is 1.75. A material is said to be ductile if $B/G > 1.75$ and brittle if $B/G < 1.75$. In our calculation, we find that the B/G ratio for CdTe-ZB ranges from 1.93 to 2.15 with an increase in pressure which indicates the ductile nature at high pressure. For CdTe-RS, it is seen that after the transition pressure, the B/G ratio decreases from 4.26 to 3.01 with an increase in pressure but is greater than 1.75. Hence we can conclude that both CdTe-ZB and CdTe-RS maintain their ductile nature even at high pressures. The Zener anisotropy factor and B/G ratio as a function of pressure are shown in figure 5.

The Poisson's ratio (υ) of a material gives us information about the characteristics of bonding forces. For covalent materials, υ is 0.1, whereas for ionic materials, $\upsilon = 0.25$ [41]. It is given by the relation:

$$\upsilon = \frac{1}{2}\left(\frac{B - \left(\frac{2}{3}\right)G}{B + \left(\frac{1}{3}\right)G}\right) \tag{2}$$

where

$$G = \frac{G_V + G_R}{2} \tag{3}$$

is the isotropic shear modulus, G_v is the Voigt's shear modulus and G_R is the Reuss's shear modulus and can be expressed as:

$$G_V = \frac{C_{11} - C_{12} + 3C_{44}}{5} \tag{4}$$

and

$$\frac{5}{G_R} = \frac{4}{C_{11} - C_{12}} + \frac{3}{C_{44}} \tag{5}$$

In the present calculation, the value of υ increases from 0.27 to 0.30 in the ZB phase and decreases from 0.39 to 0.35 in the RS phase indicating higher ionic contribution in intra-atomic bonding with increasing pressure in both the phases. The lower and upper limits of υ in central force solids have been reported to be 0.25 and 0.5 respectively [42]. Thus the present result also indicates that inter atomic forces tend to be more central as pressure increases.

The relative ease of bond bending against the bond stretching is indicated by ζ (Kleimann parameter) and is calculated using the relation:

$$\zeta = \frac{C_{11} + 8C_{12}}{7C_{11} + 2C_{12}} \tag{6}$$

It also implies resistance against bond bending or bond angle distortion. In a system, minimizing bond bending leads to $\zeta = 0$ and minimizing bond stretching leads to $\zeta = 1$.

In the present study, as the pressure increases, ζ does not vary much and remains around 0.75 for CdTe-ZB and 0.41 for CdTe-RS indicating shrinkage in bond-stretching in both phases.

The Young's modulus (Y) determines the stiffness of a material and is given by

$$Y = \frac{9GB}{G + 3B} \tag{7}$$

Also, from the bulk modulus (B) and the isotropic shear modulus (G), the longitudinal elastic wave velocity (v_l) and the transverse elastic wave velocity (v_t) are calculated as follows:

$$v_l = \sqrt{\frac{3B + 4G}{3\rho}} \tag{8}$$

$$v_t = \sqrt{\frac{G}{\rho}} \tag{9}$$

Now, the average sound velocity (v_m) is given by

$$v_m = \left[\frac{1}{3}\left(\frac{2}{v_t^3} + \frac{1}{v_l^3}\right)\right]^{-(1/3)} \tag{10}$$

Using the average sound velocity υ_m, the Debye's temperature θ_D is calculated from the elastic constants data as given by:

$$\theta_D = \frac{h}{k}\left[\frac{3n}{4\pi}\left(\frac{N_A\rho}{M}\right)\right]^{1/3} v_m \tag{11}$$

where h is the Plank's constant, k is the Boltzmann constant, N_A is the Avogadro's number, n is the number of atoms per formula unit, M is the molecular mass per formula unit, $\rho\,(=M/V)$ is the density.

In the present calculation for CdTe-ZB, the value of Y increases from 44.08 GPa to 54.15 GPa while in CdTe-RS it increases from 57.65 GPa to 93.84 GPa. Hence CdTe becomes stiffer with an increase in pressure in both phases. The Debye's temperature thus calculated shows variation from 181 K to 194 K for the ZB structure while in the RS phase it is found to increase from 209 K to 247 K indicating better thermal conductivity under pressure.

3.3. Electronic structures

Under ambient pressure CdTe crystallizes in the ZB structure and the RS structure is stable at high pressures. We have therefore studied the electronic structure of CdTe at 0 GPa pressure only for the ZB phase and the electronic structure of the RS phase is studied only at high pressures. The energy band diagram of CdTe-ZB at 0 GPa pressure calculated using LDA, GGA and mBJ-GGA are shown in figure 6. From the figure one can see clearly that the conduction band minimum and the valance band maximum are located at the middle of the brillouin zone, Γ point indicating the band gap is a direct band gap. However the band gap calculated using the LDA method and GGA method in figure 6 are 0.51 eV and 0.56 eV respectively which are lower than the experimentally reported 1.44 eV [43]. Thus the LDA and GGA method underestimate the energy band gap. The mBJ-GGA calculation of the band gap in figure 6 shows 1.46 eV that reasonably agrees with the experimentally reported value of 1.44 eV with a mere difference of about 1.4%. One of the reasons for the mere difference is that the present calculation is performed in the light of DFT at absolute temperature whereas the reported

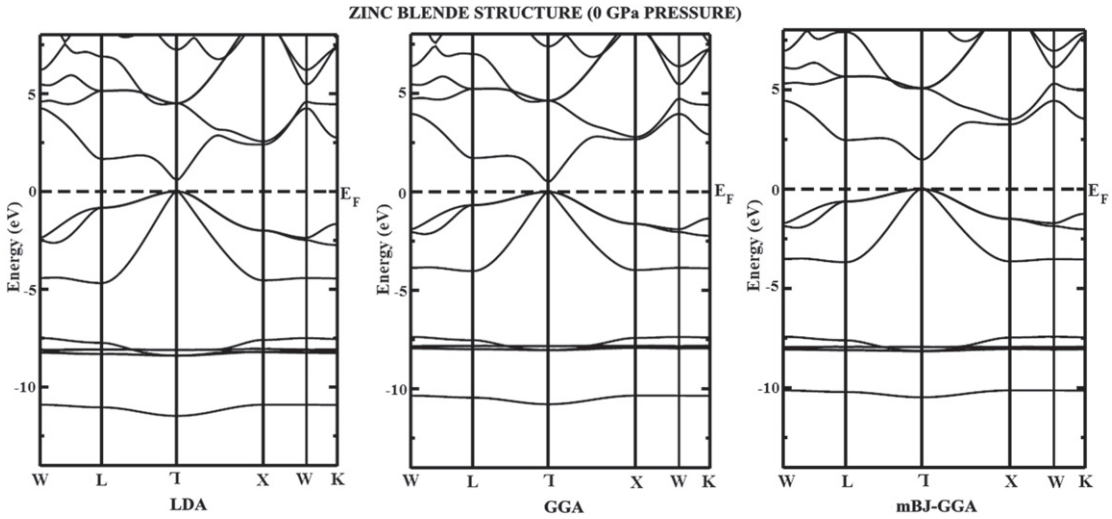

Figure 6. Band structure of CdTe-ZB at 0 GPa pressure within LDA, GGA and mBJ-GGA.

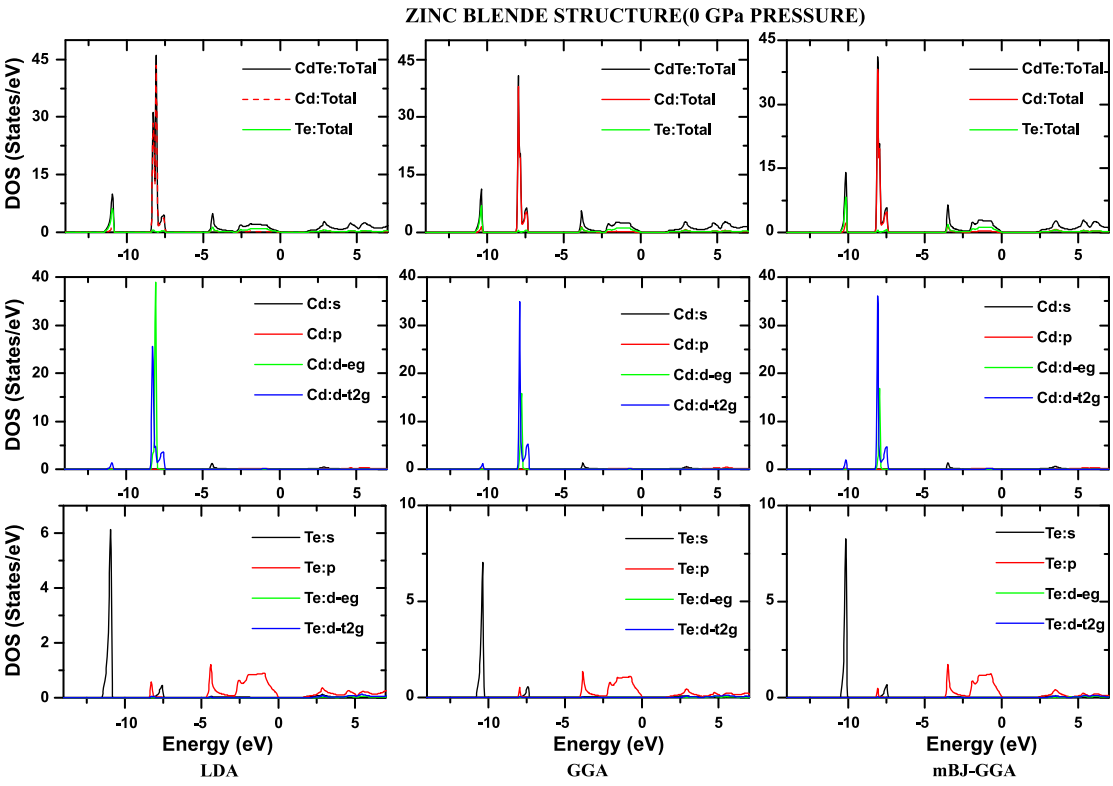

Figure 7. Total and partial DOS of CdTe-ZB at 0 GPa pressure within LDA, GGA and mBJ-GGA.

experimental value is at room temperature. Also the gap between the first and second lowest band in the band diagrams obtained using the three approximations is found to decrease following the trend LDA $>$ GGA $>$ mBJ and more importantly the gap between the lowest band and the valence band increases as LDA $<$ GGA $<$ mBJ. To better understand the electronic structure of CdTe, the total and partial DOS within the LDA, GGA and mBJ have also been studied and are shown in figure 7. Firstly, within the LDA calculation, the presence of the two lowest bands is indicated with the first lowest band mainly contributed with 6.10 eV of s-state (Te-atom) with little contribution of 1.31 eV from the d-t2g-state (Cd-atom) while the second lowest band shows a higher contribution of 39.04 eV of the d-eg- state (Cd atom) with 25.27 eV of the d-eg-state (Cd atom). One interesting fact about the contribution of the state within the LDA, GGA and mBJ is that in the first lowest band, the contribution trend of the s-state (Te atom) follows the trend LDA $<$ GGA $<$ mBJ. Similarly in

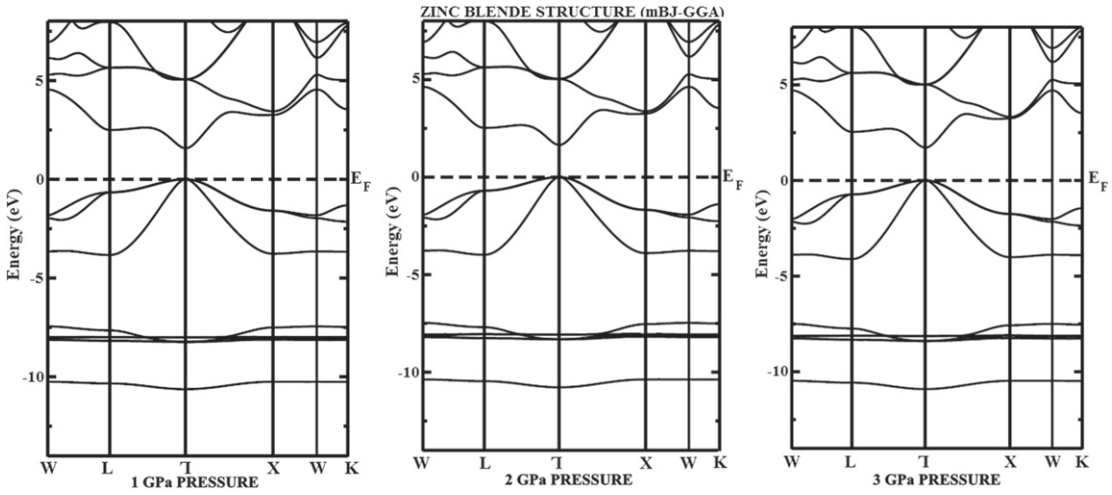

Figure 8. Energy band diagram of the CdTe ZB structure at 1 GPa, 2 GPa and 3 GPa pressure.

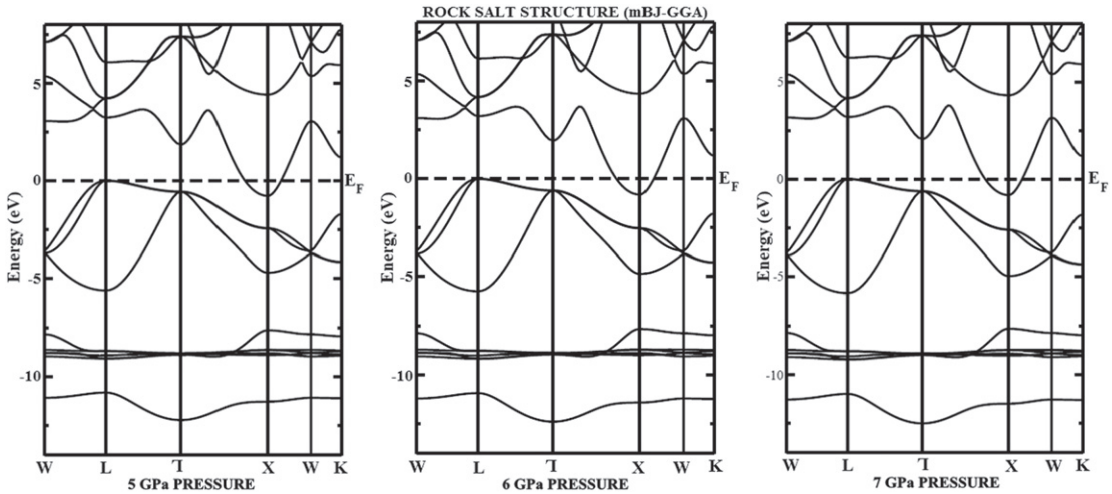

Figure 9. Energy band diagram of the CdTe RS structure at 5 GPa, 6 GPa and 7 GPa pressure.

the second lowest band the contribution trend of the d-eg state (Cd atom) is LDA $>$ GGA $>$ mBJ and for the d-t2g state (Cd atom) is LDA $<$ GGA $<$ mBJ. The valance band study of DOS within the LDA shows a contribution of 1.38 eV of the s-state (Cd atom) and 1.28 eV of the s-state (Te atom). GGA calculation shows an equal contribution of about 1.39 eV of the s-state (Cd atom) and s-state (Te atom) but within mBJ the contribution of the s-state (Te atom) is 1.78 eV while that of the s-state (Cd atom) is 1.46. Therefore the overall contribution trend of the states in the valance band within the three methods is found as LDA $<$ GGA $<$ mBJ. Thus the effective results within the mBJ calculation are due to the proper treatment of the electronic states.

The energy band diagram of CdTe-ZB at different pressures from 1 GPa pressure to 3 GPa is shown in figures 8(a)–(c) and from 5 GPa pressure to 7 GPa of CdTe-RS is also shown in figures 9(a)–(c). The band diagram under induced pressure of CdTe-ZB in figure 8 shows that as the pressure increases to 1 GPa, 2 GPa and 3 GPa, the energy gap between Γ and X increases to 2.42 eV $<$ 2.45 eV $<$ 2 .47 eV while the gap between Γ and L decreases from 3.21 eV $>$ 3.18 eV $>$ 3.16 eV respectively towards the Fermi level. On the other hand the band diagram under pressure 5 GPa, 6 GPa, 7 GPa of CdTe-RS in figures 9(a)–(c) clearly indicates the conduction band crosses towards the valance band confirming the transition from the direct band gap nature to metallic at higher pressure.

For detailed analysis on the band structure of CdTe, the total DOS plots for both the ZB and RS structures are also studied at different pressures. Figures 10 and 11 show the total DOS plots of CdTe-ZB at 1 GPa, 2 GPa and 3 GPa pressure and CdTe-RS at 5 GPa, 6 GPa and 7 GPa pressure. In figure 10 the contribution of the Te atom and Cd atom in the lowest band and the contribution of the Cd atom in the valance band decreases with

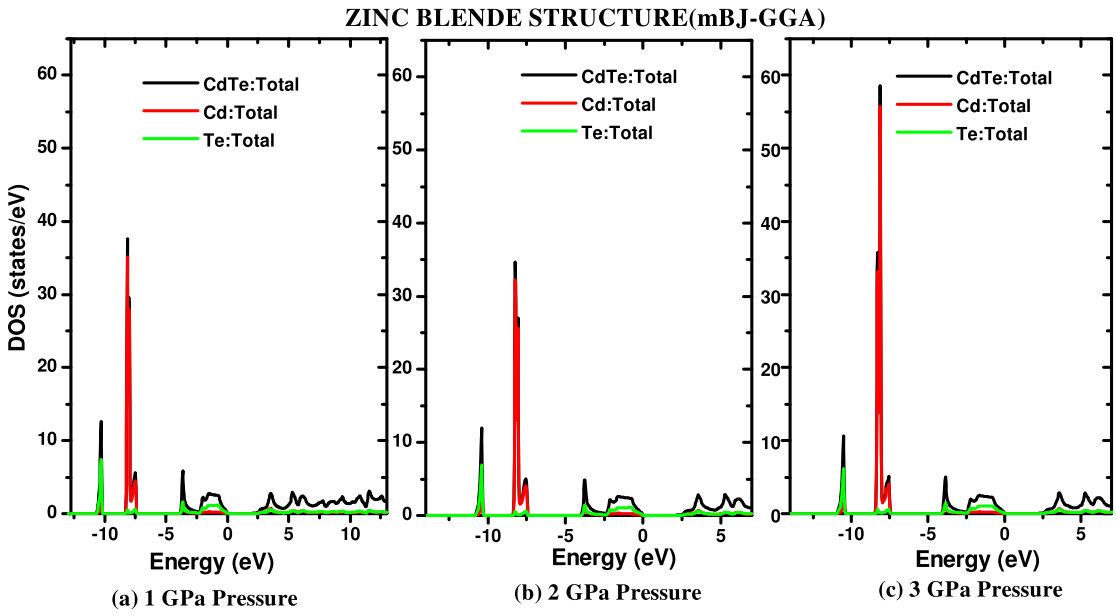

Figure 10. Total DOS of the CdTe-ZB structure at (a) 1 GPa pressure, (b) 2 GPa pressure and (c) 3 GPa pressure.

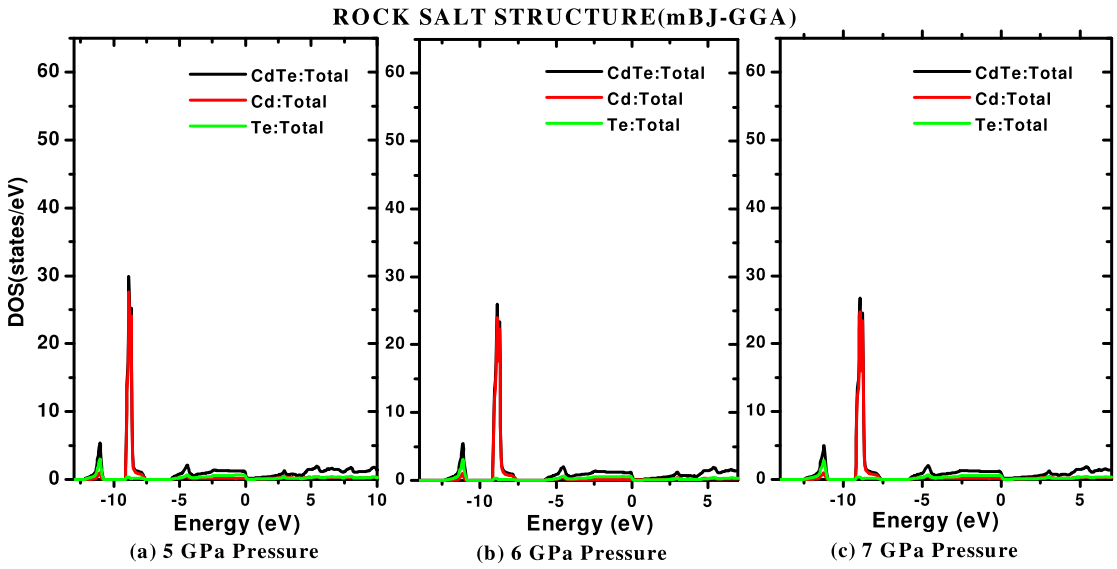

Figure 11. Total DOS of the CdTe-RS structure at (a) 5 GPa pressure, (b) 6 GPa pressure and (c) 7 GPa pressure.

pressure. But at 3 GPa, pressure around the structural transition starts and the contribution of the Cd atom in the lowest band suddenly increases. However in the DOS of CdTe-RS as shown in figure 11, it is clear that there is crossing over of the conduction band in the valance band indicating a metallic character.

Thus to conclude, the variation of the direct energy band gap of CdTe-ZB with pressure is shown in figure 12. It is clearly seen that as the pressure increases the band gap of CdTe-ZB increases linearly. This may be due to the fact that with an increase in pressure the unit cell in the lattice is compressed leading to smaller normalised volume and larger binding energy which would therefore result in an increasing band gap with increasing pressure. However in the case of CdTe-RS there is no prominent change in the metallic nature of the band structure with increasing pressure. Thus we conclude that the variation in pressure does not much affect the band gap of CdTe-RS and only affects the CdTe-ZB structure.

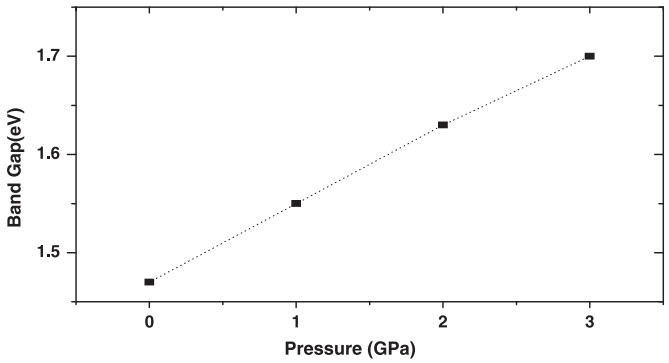

Figure 12. Variation of the direct band gap of CdTe-ZB with pressure.

4. Summary and conclusions

The structural properties of CdTe in both the ZB and RS phases are studied within the LDA and GGA. The structural phase transition of CdTe from the ZB structure to the RS structure within the LDA is found to occur at 2.2 GPa pressure while calculation within the GGA shows a phase transition at 4 GPa pressure with a volume collapse of 20.9%. The GGA calculation shows close agreement with other experimental and theoretical results. The elastic constants for both the structures are calculated at different pressures and found to show a linear increase with pressure. The elastic parameters such as the Zener anisotropy factor, Shear modulus, Poisson's ratio, Young's modulus, Kleinmann parameter and Debye's temperature are also calculated and it is found that both the ZB and RS phase maintain their ductile nature even at high pressures. Shrinkage in bond-stretching and the stiffness of CdTe are observed in both the phases with an increase in pressure while the ZB phase shows a poor thermal conductivity at high pressures. The band diagram of CdTe-ZB at 0 GPa pressure within the LDA, GGA underestimate the band gap while the mBJ method shows a direct band gap of 1.46 eV and is found to be in close agreement with the experimental value. The direct band gaps of CdTe-ZB show a linear increase while the metallic nature is found to be retained in CdTe-RS under induced pressure. Thus we conclude that the mBJ-GGA is an efficient theoretical technique for the calculation of band structures and will be a successful tool for the engineering of compound semiconductors. The present study will stimulate experimental studies of high pressures and shed new light on high pressure applications of optoelectronic devices.

References

[1] Mujica A, Rubio A, Munoz A and Needs R J 2003 *Rev. Mod. Phys.* **75** 863
[2] Shimojo F *et al* 2004 *Phys. Rev.* B **70** 184111
[3] Miao M S and Lambrecht W R L 2005 *Phys. Rev. Lett.* **94** 225501
[4] Nelmes R J and McMahon M I 1998 *Semicond. Semimetals* **54** 145
[5] Wei S and Zhang S B 2000 *Phys. Rev.* B **62** 6944
[6] Deligoz E, Colakoglu K and Ciftci Y 2006 *Physica* B **373** 124
[7] Aulbur W G, Städele M and Görling A 2000 *Phys. Rev.* B **62** 7121
[8] Shishkin M, Marsman M and Kresse G 2007 *Phys. Rev. Lett.* **99** 246403
[9] Aryasetiawan F and Gunnarsson O 1998 *Rep. Prog. Phys.* **61** 237
[10] Tran F and Blaha P 2009 *Phys. Rev. Lett.* **102** 226401
[11] Perdew J P, Burke S and Ernzerhof M 1996 *Phys. Rev. Let.* **77** 3865
[12] McMahon M I, Nelmes R J, Wright N G and Allan D R 1993 *Phys. Rev.* B **48** 16246
[13] Benkhettou N, Rached D and Rabah M 2006 *Czech. J. Phys.* **56** 409
[14] Sharma E, Singh A and Sakalle U K 2012 *Int. J. of Engg. Sci. & Mgmt.* (*IJESM*) **2** 186
[15] Nelmes R J, McMahon M I, Wright N G and Allan D R 1993 *Phys. Rev.* B **48** 1314
[16] Edwards L and Drickamer H G 1961 *Phys. Rev.* **122** 1149
[17] Kabita K, Maibam J, Indrajit Sharma B, Thapa Singh R K and Brojen R K 2014 *Adv. Sci. Engg. Med.* **6** 354
[18] Kabita K, Maibam J, Indrajit Sharma B, Thapa Singh R K and Brojen R K 2014 *Iraqi J Appl. Phys.* **9** 17
[19] Kabita K, Maibam J, Indrajit Sharma B, Thapa Singh R K and Brojen R K 2014 *Int. J. Innovation and Appl. Stds.* **8** 382
[20] Wimmer E, Krakauer H, Weinert M and Freeman A J 1981 *Phys. Rev.* B **24** 864
[21] Hohenberg P and Kohn W 1964 *Phys. Rev. 3B* **136** 864
[22] Kohn W and Sham L J 1965 *Phys. Rev. 4A* **140** 1133
[23] Cottenier S 2002 *Density Functional Theory and the Family of (L)APW-methods: a step-by-step Introduction* (Belgium: Insti-tuut voor Kern-en Stralingsfysica, K U Leuven)
[24] Blaha P, Schwarz K, Madsen G K H, Kvasnicka D and Luitz J 2001 *WIEN2k An Augmented Plane Wave + Local Orbitals Program for Calculating Crystal Properties* (Austria: Karlheinz Schwarz, Techn. Universitat Wien)
[25] Becke D and Johnson E R 2006 *J. Chem. Phys.* **124** 221101
[26] Birch F 1947 *Phys. Rev.* **71** 809

[27] Birch F J 1938 *J. Appl. Phys.* **9** 279
[28] Lalitha S, Karazhanov S Z, Ravindran P, Senthilarasu S, Sathyamoorthy R and Janabergenov J 2006 *Physica* B **387** 227
[29] Polit J *et al* 2006 *J. Appl. Phys.* **100** 013521
[30] Ouendadji S, Ghemid S, Meradji H and Hassan F E H 2011 *Comput. Mater. Sci.* **50** 1460
[31] Zerroug S, Sahraoui F A and Bouarissa N 2007 *Eur. Phys. J.* B **57** 9
[32] Al-Douri Y, Reshak A H, Baaziz H, Charifi Z, Khenata R, Ahmad S and Hashim U 2010 *Sol. Energy* **84** 1979
[33] Strössner K, Ves S, Dieterich W, Gebhardt W and Cardona M 1985 *Solid State Commun.* **56** 563
[34] Smith T F and White G K 1975 *J. Phys. C Solid state Phys.* **8** 2031
[35] Van Camp P E and Van Doren V E 1994 *Solid State Commun.* **91** 607
[36] Mei J R and Lemos V 1984 *Solid State Commun.* **52** 785
[37] Nelmes R J, McMahon M I, Wright N G and Allan D R 1995 *Phys. Rev.* B **51** 15723
[38] Al'fer S A and Skums V F 2001 *Inorg. Mater.* **37** 1237
[39] Borg Y I and Smith D K 1967 *J. Phys. Chem. Sol.* **28** 49
[40] Pugh S F 1954 *Phil. Mag.* **45** 823
[41] Bannikov V 2, Shein I R and Ivanovskii A L 2007 *Phys. Status. Solidi. Rapid. Res. Lett.* **3** 89
[42] Fu H *et al* 2008 *Comput. Mater. Sci.* **44** 774
[43] Kittel C 1986 *Introduction to Solid State Physics* 6th edn (New York: John Wiley) p185

Volume 94

2016

An NRC Research Press Journal

Une revue de NRC Research Press

www.nrcresearchpress.com

Canadian Journal of Physics

Revue canadienne de physique

In cooperation with the Canadian Association of Physicists

Avec le concours de l'Association canadienne des physiciens et physiciennes

NRC Research Press

NRC Research Press

ARTICLE

A detailed first principle study on the structural, elastic, and electronic properties of indium arsenide (InAs) under induced pressure

Kh. Kabita, M. Jameson, B.I. Sharma, R.K. Brojen, and R.K. Thapa

Can. J. Phys. Downloaded from www.nrcresearchpress.com by CSP Customer Service on 03/24/16
For personal use only.

Abstract: An ab initio calculation of the structural, elastic, and electronic properties of indium arsenide (InAs) under induced pressure is investigated using density functional theory with modified Becke–Johnson potential within the generalised gradient approximation of the Perdew–Burke–Ernzerhof scheme. The lattice parameters are found to be in good agreement with experimental and other theoretical data. The pressure-induced structural phase transition of InAs zinc blende to rock salt structure is found to occur at 4.7 GPa pressure with a 17.2% of volume collapse. The elastic properties of both the zinc blende and rock salt structures at different pressures are studied. The electronic band structures at different pressures for both the structures are investigated using the total and partial density of states. The energy band gap of the InAs zinc blende phase is increased with increasing pressure while in rock salt the phase the conduction band crosses towards the valence band and thus shows metallic behaviour.

Key words: density functional theory (DFT), modified Becke–Johnson (mBJ) potential, density of states (DOS), energy band diagram, elastic properties, phase transition.

Résumé : Nous présentons un calcul ab initio des propriétés structurelles, élastiques et électroniques de l'arséniure d'indium (InAs) sous pression, à l'aide de la théorie de la fonctionnelle de densité avec un potentiel modifié de Becke–Johnson, à l'intérieur de l'approximation du gradient généralisé du schéma de Perdew–Burke–Ernzerhof. Nous trouvons que les paramètres du réseau sont en bon accord avec les données expérimentales et d'autres résultats théoriques. Nous trouvons que la transition de phase de InAs induite par la pression, de la phase blende de zinc à sel gemme se produit à 4.7 GPa, avec diminution de volume de 17.2 %. Nous étudions les propriétés élastiques des structures blende de zinc et sel gemme en utilisant les densités d'état, totale et partielle. La bande en énergie interdite du blende de zinc croît avec l'augmentation de pression, alors que dans la phase sel gemme la bande de conduction traverse vers la bande de valence et montre ainsi de meilleures propriétés métalliques. [Traduit par la Rédaction]

Mots-clés : théorie de la fonctionnelle de densité, diagramme de la bande d'énergie, densité d'états, propriétés élastiques, transition de phase.

PACS Nos.: 71.15.Mb, 71.20.-b;71.20.Nr.

1. Introduction

The technological importance of group III–V compound semiconductors has increased over the past years because of its electronic and mechanical properties and has received considerable interest from experimentalist and theorists [1–3]. To understand, the structural phase transition of a material and the influence of band structure parameters on the electronic properties of semiconductors, their study under induced pressure is found to be an effective tool. Also, the study of elastic constants at different pressures plays an important role in mechanical stability, strength, phase transition, and a material response to various conditions [4, 5]. One of the interesting phenomena that may occur under applied pressure is a sudden change in the arrangement of the atoms (i.e., structural phase transition). Indium arsenide is an important group III–V compound semiconductor having high electron mobility and narrow energy band gap. It is widely used in construction of infrared detectors and diode lasers [6]. It crystallizes in cubic zinc blende (ZB) structure under ambient conditions. At high pressure it is found to undergo structural phase transition to rock salt (RS) structure. The pressure-induced phase transition to metallic state was first reported by Minomura and Drickamer [7] at 8.46 GPa pressure from high pressure resistivity measurements. Pitt and Vyas [8] in 1973 reported the phase transition from the ZB to RS through resistivity measurements. In 2014, Wang et al. [9] also studied its electronic transport properties using the non-equilibrium Green's function combined with density functional theory. Although there have been extensive studies on structural, mechanical, and electronic properties of InAs, the experimental and theoretical study of these properties under high pressure is still very scarce. In our previous study we extensively studied the pressure-induced structural, mechanical, and electronic properties of GaP [10, 11] and GaAs [12]. The main aim of this work is to present a detailed study of the behaviour of the elastic and electronic properties of InAs in ZB and RS phases under pressure.

2. Computational methods

All theoretical calculations of InAs are performed based on the WIEN2K code [13] using the full potential linearized augmented plane wave (FP-LAPW) [14] method with modified Becke–Johnson potential [15] under the framework of density functional theory

Received 29 April 2015. Accepted 2 November 2015.

Kh. Kabita, M. Jameson, and B.I. Sharma. Department of Physics, Assam University, Silchar-788011, Assam, India.
R.K. Brojen. School of Computational and Integrative Sciences, JNU, New Delhi 110067, India.
R.K. Thapa. Department of Physics, Mizoram University, Tanhril, Aizawl-796 009, India.
Corresponding author: B.I. Sharma (email: indraofficial@rediffmail.com).

Can. J. Phys. Downloaded from www.nrcresearchpress.com by CSP Customer Service on 03/24/16
For personal use only.

[16–18]. The generalized gradient approximation of the Perdew–Burke–Ernzerhof scheme [19] is used for treating the exchange correlation interaction effects. In this method, the lattice is divided into non-overlapping spheres (called atomic or muffin tin sphere) surrounding each atomic site and an interstitial region. Inside the muffin tin region, the potential is a product of radial function and spherical harmonics and is expanded up to order $l = 10$. For the interstitial regions that are outside the muffin tin spheres, the potentials are expanded in plane waves. The number of k-points used for the integration part is 8000k-points, which is reduced to 256 irreducible k-points inside the Brillion zone, including five high symmetry points W, L, Γ, X, and K. Convergence of the basis set is obtained at $R_{MT}K_{max} = 9.0$ where K_{max} gives us the plane wave cut-off. The elastic constants have been determined using the stress–strain method with volume conserving technique [20]. In our calculation only a small distortion has been considered to remain within the elastic domain of the crystal.

3. Results and discussion

3.1. Structural properties

The stability structure of InAs is obtained from the ground state structures of ZB and RS structures of InAs. The energy as a function of the primitive cell volume of ZB and RS phases is shown in Fig. 1. From Fig. 1, one can clearly see that the InAs-ZB structure is more stable than the RS structure. The equilibrium lattice parameters of InAs crystal in ZB and RS structures are obtained by fitting the resultant curve to the Birch–Murnaghan equation [21]. The calculated structural parameters are compared with other results [22–27] and are given in Table 1, and the results are found to be in good agreement with other results and hence are used for further calculations.

3.2. Phase transition and elastic properties

The pressure-induced phase transition of InAs-ZB to InAs-RS phase at zero temperature is investigated from the equal enthalpy conditions, $H = E + PV$. Figure 2 shows the enthalpy as a function of pressure of both the InAs-ZB and InAs-RS structures. It is clearly seen that the phase transition of InAs-ZB to InAs-RS is found to occur at 4.7 GPa pressure. The normalised volumes (V_p/V_o) of the crystals in ZB and RS phases are found to be 0.924 and 0.752, respectively, during the phase transition with a volume collapse of 17.2% indicating that the ZB phase is more compressible than the RS phase, as given in Fig. 3. Our calculated results of phase transition and volume collapse are compared with other experimental and theoretical results [8, 26–29] and are shown in Table 2. The present calculation of phase transition is found to be small as compared to the reported experimental results. The reasoning for the difference may be because the present calculation is done at absolute zero temperature.

The elastic constants of a material give us important information about the nature of the force operating in the solids and are the basic parameters that are used for studying the elastic properties of a material. Because the phase transition pressure is 4.7 GPa, elastic constants are calculated for the lattice corresponding to pressure ranging from 0 to 4 GPa of the ZB phase and 5 to 9 GPa of the RS phase. The results for our calculation are shown in Fig. 4. Our obtained results are found to satisfy the mechanical stability conditions: $(C_{11} + 2C_{12}) > 0$; $C_{11}C_{12} > 0$; $C_{44} > 0$; $C_{11} > 0$ of ZB and RS structures. Also in Fig. 4, one can clearly see that there is a linear variation of elastic constants with pressure up to 4 GPa of ZB phase and 5 to 9 GPa of RS phase, which indicates the stability of the ZB and RS phases before and after the transition pressure 4.7 GPa.

Fig. 1. Total energy as a function of primitive cell volume of InAs in ZB and RS phases.

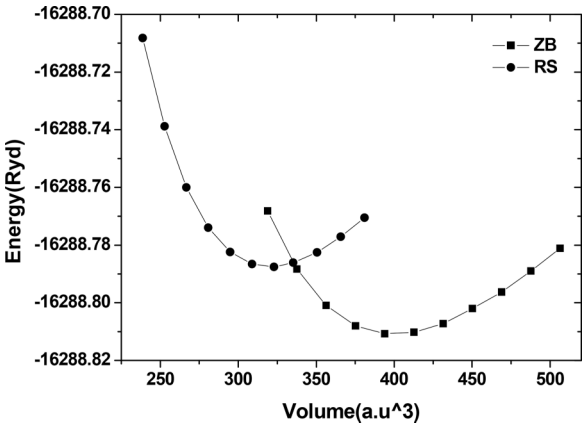

Table 1. Lattice constant, a_0 (Å); bulk modulus, B (GPa); and pressure derivative of bulk modulus, B' of ZB and RS structure of InAs at zero pressure.

Structure		a_0 (Å)	B_0 (GPa)	B'_0
ZB	Present work	6.18	49.48	4.78
	Expt. results	6.058[a]	59.2±5[e]	6.8±2[e]
	Theo. results	6.10[b], 6.08[c]	55.51[c], 50.4[d]	—
RS	Present work	5.74	62.98	4.84
	Expt. results	5.5005[e], 5.514[f]	40.6±14[e]	7.3±1[e]
	Theo. results	5.65[c]	—	—

[a][21].
[b][22].
[c][23].
[d][24].
[e][25].
[f][26].

Fig. 2. Enthalpy variation of InAs in ZB and RS structure as a function of pressure.

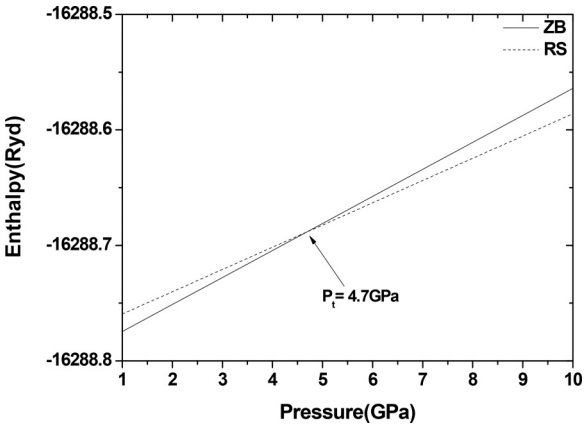

In light of these observations, the elastic parameters, such as Zener anisotropic factor (A), Poisson's ratio (υ), Kleinmann parameter (ζ), Young's modulus (Y), and Debye's temperature (θ_D), are calculated for both the InAs-ZB and InAs-RS phases to determine the mechanical and thermal behaviour at high pressure from the relation given by Mayer et al. [30].

The Zener anisotropy factor of a material determines the isotropy of that material. A material is said to be elastically isotropic with uniform deformation along all directions when $A = 1$. For

Can. J. Phys. Downloaded from www.nrcresearchpress.com by CSP Customer Service on 03/24/16
For personal use only.

Fig. 3. Phase transition between ZB and RS structure of InAs at 4.7 GPa pressure.

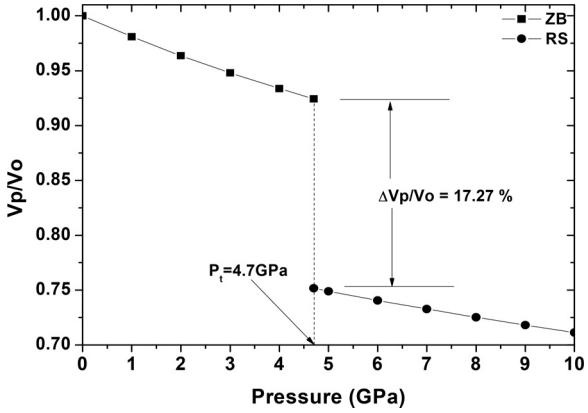

Table 2. Phase transition pressure P_t (GPa) and volume collapse of InAs.

	Present calculation	Expt. results	Theo. results
Transition pressure, P_t (GPa)	4.7	7[a], 6.9±0.2[c]	3.9[d], 4.0[e]
Volume collapse (%)	17.2	17.0±0.2[a], 18.8[b]	17.0[f]

[a][25].
[b][26].
[c][8].
[d][28].
[e][29].

Fig. 4. Elastic constants (C_{11}, C_{12}, C_{44}) as a function of pressure of InAs-ZB and InAs-RS phases.

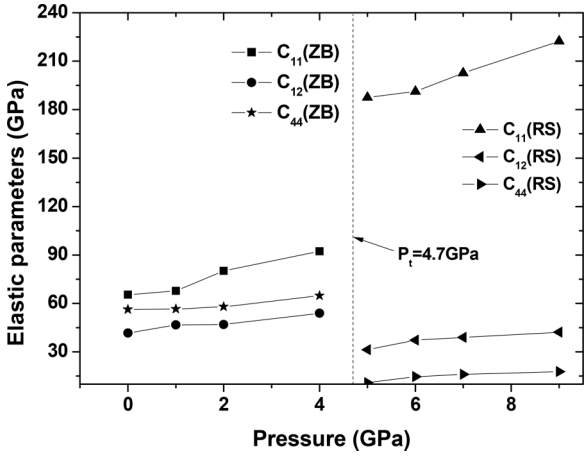

$A > 1$, it is stiffest along ⟨111⟩ body diagonal and when $A < 1$, it is stiffest along ⟨100⟩ cube axes.

In terms of elastic constants it is expressed as

$$A = \frac{2C_{44}}{C_{11} - C_{12}} \tag{1}$$

In our calculation, the value of A decreases from 5.35 to 3.37 in the ZB phase while in the RS phase it increases from 0.18 to 0.2 with pressure. Thus we find that A is stiffest along ⟨111⟩ body diagonal in the ZB phase and after transition to RS phase it becomes stiffest along ⟨100⟩ cube axes. Poisson's ratio (υ) gives us

Fig. 5. Elastic parameters (Zener anisotropy factor, Poisson's ratio, Kleinmann parameter, and B/G ratio) as a function of pressure of InAs in (*a*) ZB phase and (*b*) RS phase.

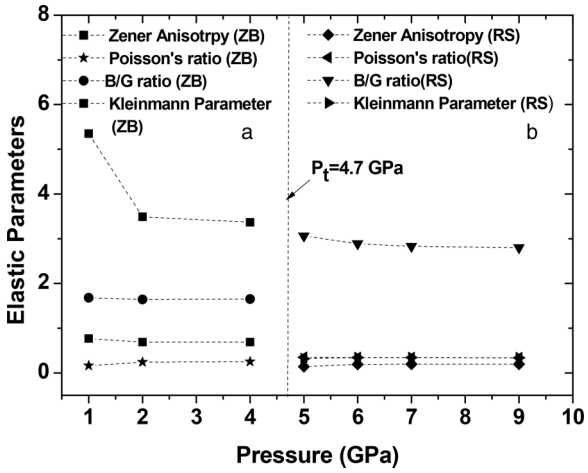

Fig. 6. Elastic parameters (Debye's temperature and Young's modulus) as a function of pressure of InAs in (*a*) ZB phase and (*b*) RS phase.

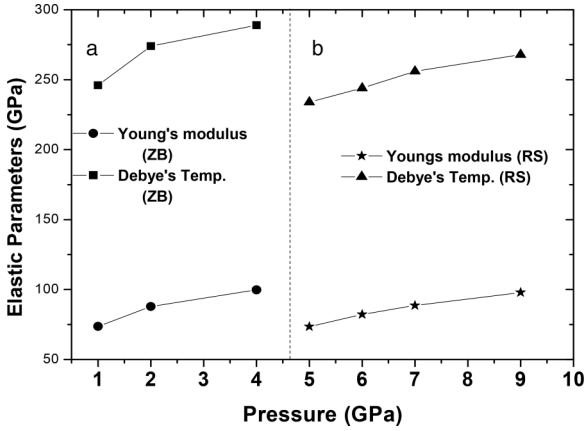

information about the characteristics of bonding forces. It is given by the relation

$$\upsilon = \frac{1}{2}\left[\frac{B - (2/3)G}{B + (1/3)G}\right] \tag{2}$$

where

$$G = \frac{G_V + G_R}{2} \tag{3}$$

is the isotropic shear modulus, G_V is Voigt's shear modulus, and G_R is the Reuss's shear modulus and can be expressed as

$$G_V = \frac{C_{11} - C_{12} + 3C_{44}}{5} \tag{4}$$

and

$$\frac{5}{G_R} = \frac{4}{(C_{11} - C_{12})} + \frac{3}{C_{44}} \tag{5}$$

Fig. 7. Energy band diagram of InAs at zero pressure in (*a*) ZB structure and (*b*) RS structure.

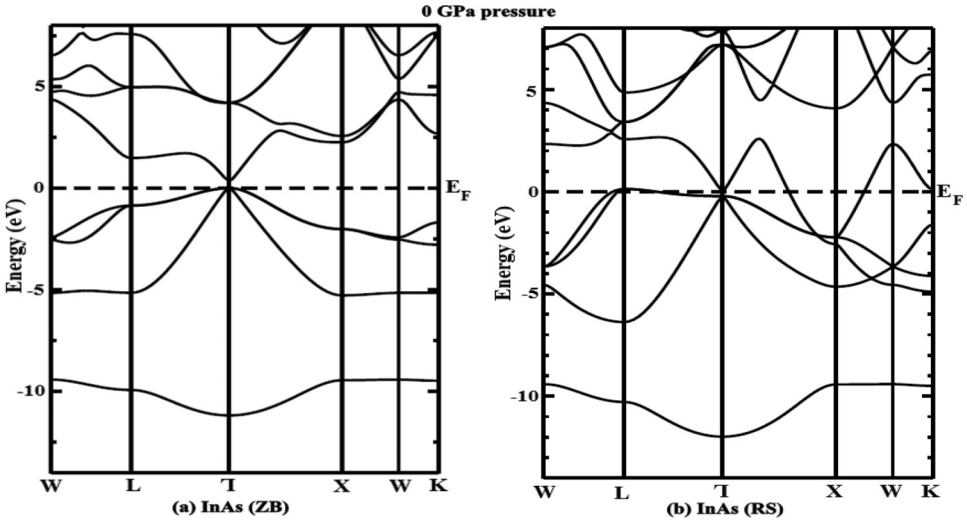

Fig. 8. DOS of InAs: (*a*) total DOS of InAs-ZB; (*b*) In (indium atom) partial DOS in InAs-ZB; (*c*) As (arsenic atom) partial DOS in InAs-ZB; (*d*) total DOS of InAs-RS; (*e*) In (indium atom) partial DOS in InAs-RS; and (*f*) As (arsenic atom) partial DOS in InAs-RS.

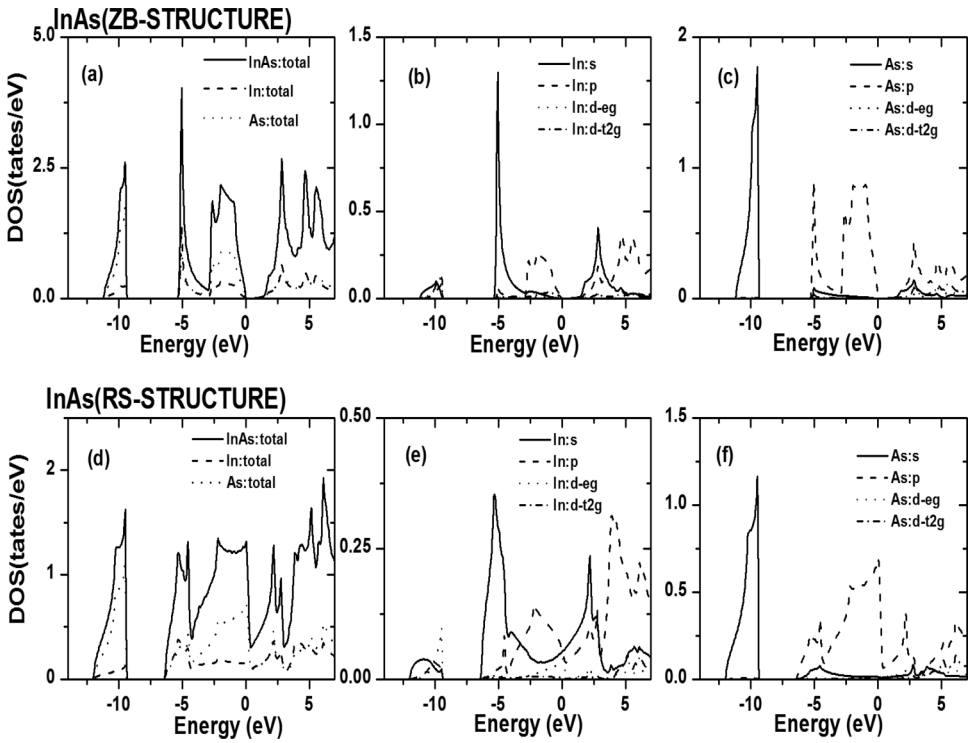

For covalent materials, the value of Poisson's ratio (υ) is 0.1, whereas for ionic materials $\upsilon = 0.25$ [31]. The lower and upper limits of υ in central force solids have been reported to be 0.25 and 0.5, respectively [32]. Our results for Poisson's ratio show that as pressure increases, the value of υ increases from 0.16 to 0.25 in the ZB phase while it remains around 0.34 in the RS phase indicating that with increasing pressure the ionic contribution to the interatomic bonding becomes dominant. It also indicates that with increasing pressure interatomic forces tend to be more central.

The relative ease of bond bending against the bond stretching is indicated by ζ (Kleimann parameter) and is calculated using the relation

$$\zeta = \frac{C_{11} + 8C_{12}}{7C_{11} + 2C_{12}} \tag{6}$$

It also implies resistance against bond bending or bond angle distortion. In a system, minimizing bond bending leads to $\zeta = 0$ and minimizing bond stretching leads to $\zeta = 1$.

In the present study, ζ of the ZB phase is found to vary from 0.77 to 0.69 with pressure while in the RS phase it is found to increase from 0.31 to 0.34 showing shrinkage in bond stretching in the ZB phase and shrinkage in bond bending in the RS phase.

Can. J. Phys. Downloaded from www.nrcresearchpress.com by CSP Customer Service on 03/24/16
For personal use only.

Fig. 9. Energy band diagram of InAs-ZB structure: (*a*) 1 GPa pressure; (*b*) 2 GPa pressure; (*c*) 3 GPa pressure; and (*d*) 4 GPa pressure.

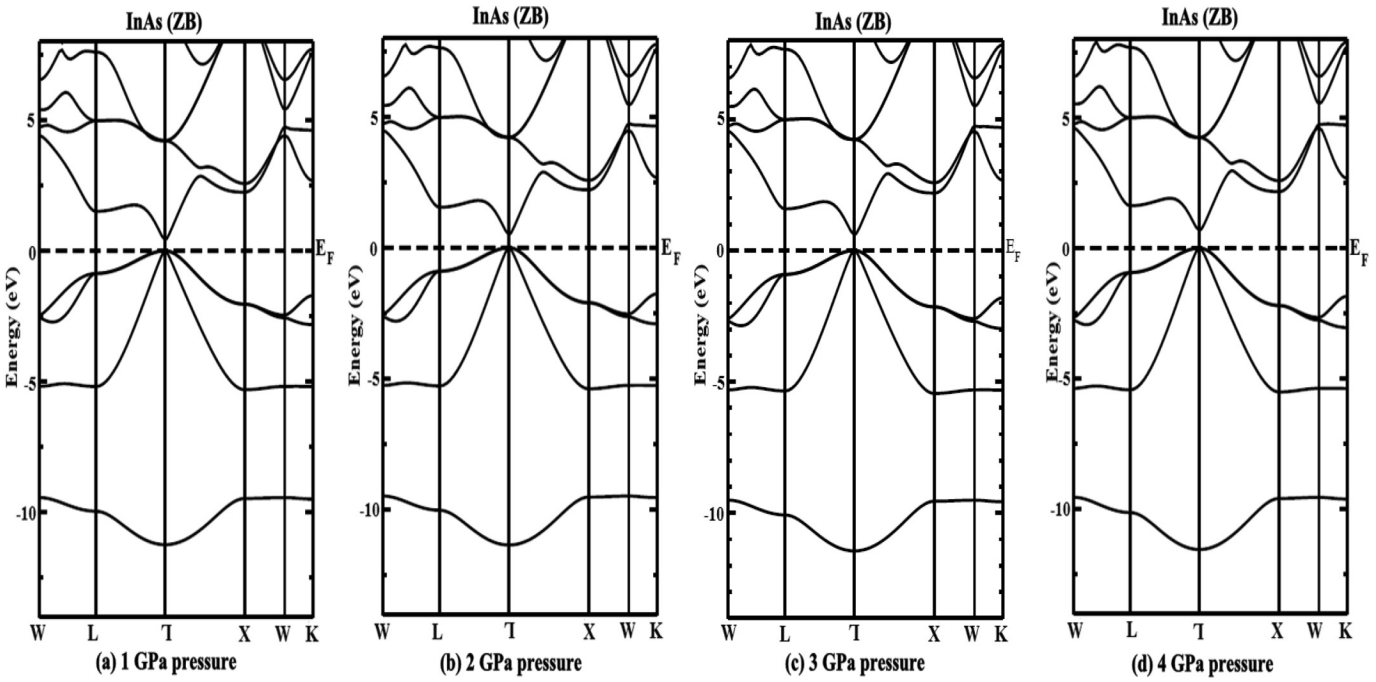

The ductile and brittle behaviour of a material can be understood from the ratio of the bulk and shear moduli (B/G) [33]. If the shear modulus (G) is low we know that the material has a low resistance to shear and hence is ductile, while if a material has low bulk modulus, it means the resistance to fracture is low and hence the material is brittle. We know that the critical value, which separates the ductility and brittleness of a material, is 1.75. A material is said to be ductile if $B/G > 1.75$ and brittle if $B/G < 1.75$. In our calculation, the B/G ratio of InAs-ZB remains around 0.64 with increase in pressure, which shows that InAs-ZB retains its brittle nature even at high pressure, but in the case of InAs-RS it is greater than 1.75 and decreases with increasing pressure. Hence we conclude that the ZB phase of InAs is brittle in nature and becomes ductile after it undergoes a structural phase transition to the RS phase. The elastic parameters as a function of pressure of both the InAs-ZB and InAs-RS are given in Fig. 5.

The stiffness of a material is given by Y (Young's modulus)

$$Y = \frac{9GB}{G + 3B} \tag{7}$$

Also, from the bulk modulus (B) and the isotropic shear modulus (G), the longitudinal elastic wave velocity (v_l) and the transverse elastic wave velocity (v_t) are calculated as follows:

$$v_l = \sqrt{\frac{3B + 4G}{3\rho}} \tag{8}$$

$$v_t = \sqrt{\frac{G}{\rho}} \tag{9}$$

Now, the average sound velocity (v_m) is given by

$$v_m = \left[\frac{1}{3}\left(\frac{2}{v_t^3} + \frac{1}{v_l^3}\right)\right]^{(-1/3)} \tag{10}$$

Fig. 10. Variation of band gap with pressure of InAs-ZB structure.

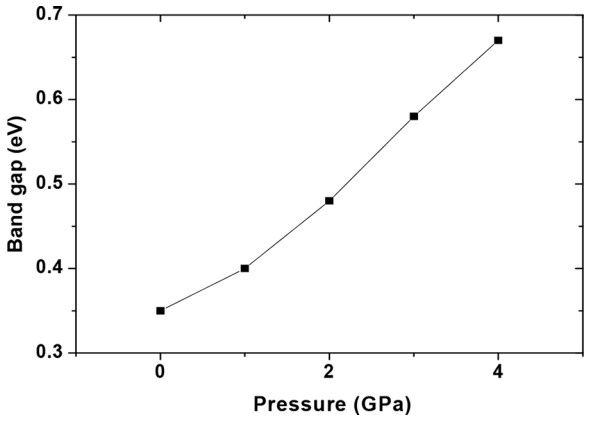

Using the average sound velocity, v_m, the Debye temperature θ_D is calculated from the elastic constants data as given by

$$\theta_D = \frac{h}{k}\left[\frac{3n}{4\pi}\left(\frac{N_A\rho}{M}\right)\right]^{1/3} v_m \tag{11}$$

where h is Plank's constant, k is the Boltzmann's constant, N_A is Avogadro's number, n is the number of atoms per formula unit, M is the molecular mass per formula unit, and ρ (= M/V) is the density.

Our calculated results of Young's modulus and Debye's temperature are given in Fig. 6. We find a linear increase in Y from 73.62 to 99.72 GPa in the InAs-ZB phase with increasing pressure while in the InAs-RS phase the value of Y increases from 73.53 to 97.84 GPa. Hence InAs becomes more rigid with increasing pressure. The value of Debye's temperature is also found to increase from 246 to 290 K for the InAs-ZB phase and 234 to 268 K in InAs-RS, indicating a stiffer lattice and better thermal conductivity in both phases.

Can. J. Phys. Downloaded from www.nrcresearchpress.com by CSP Customer Service on 03/24/16
For personal use only.

Fig. 11. Energy band diagram of InAs-RS structure: (*a*) 5 GPa pressure; (*b*) 6 GPa pressure; (*c*) 7 GPa pressure; and (*d*) 9 GPa pressure.

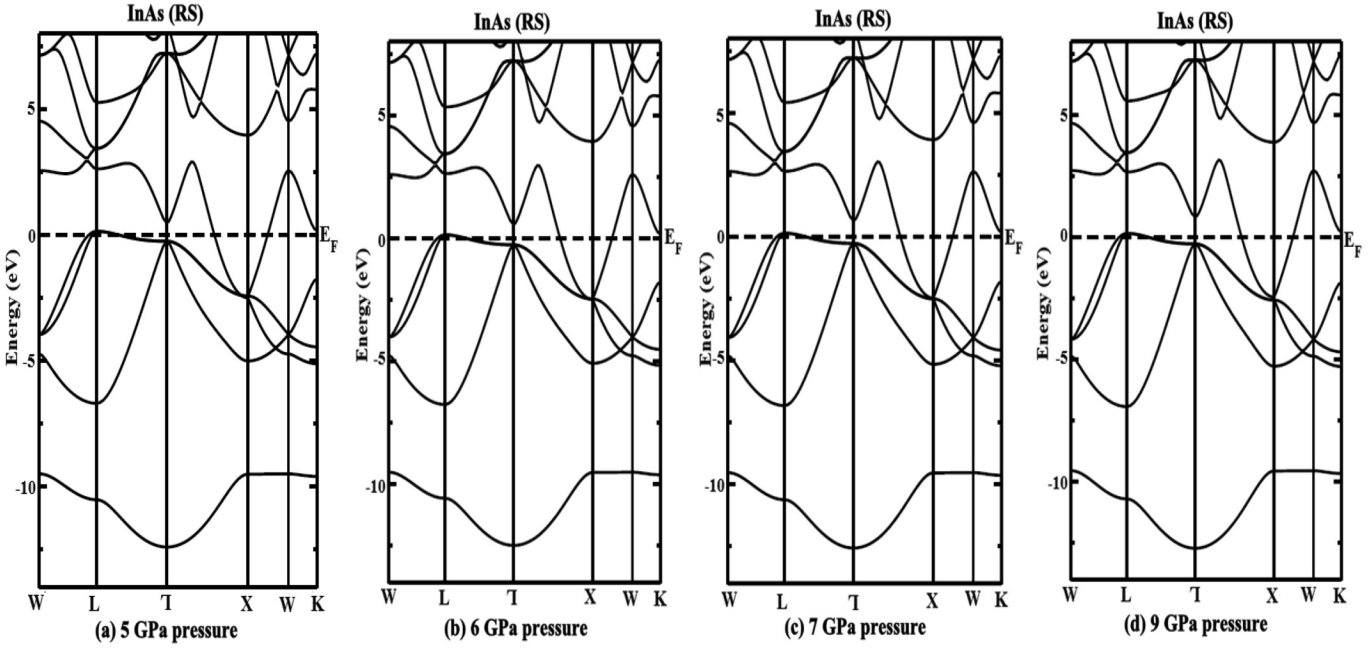

Fig. 12. Total DOS of InAs-ZB under pressure: (*a*) 1 GPa pressure; (*b*) 2 GPa pressure; (*c*) 3 GPa pressure; and (*d*) 4 GPa pressure.

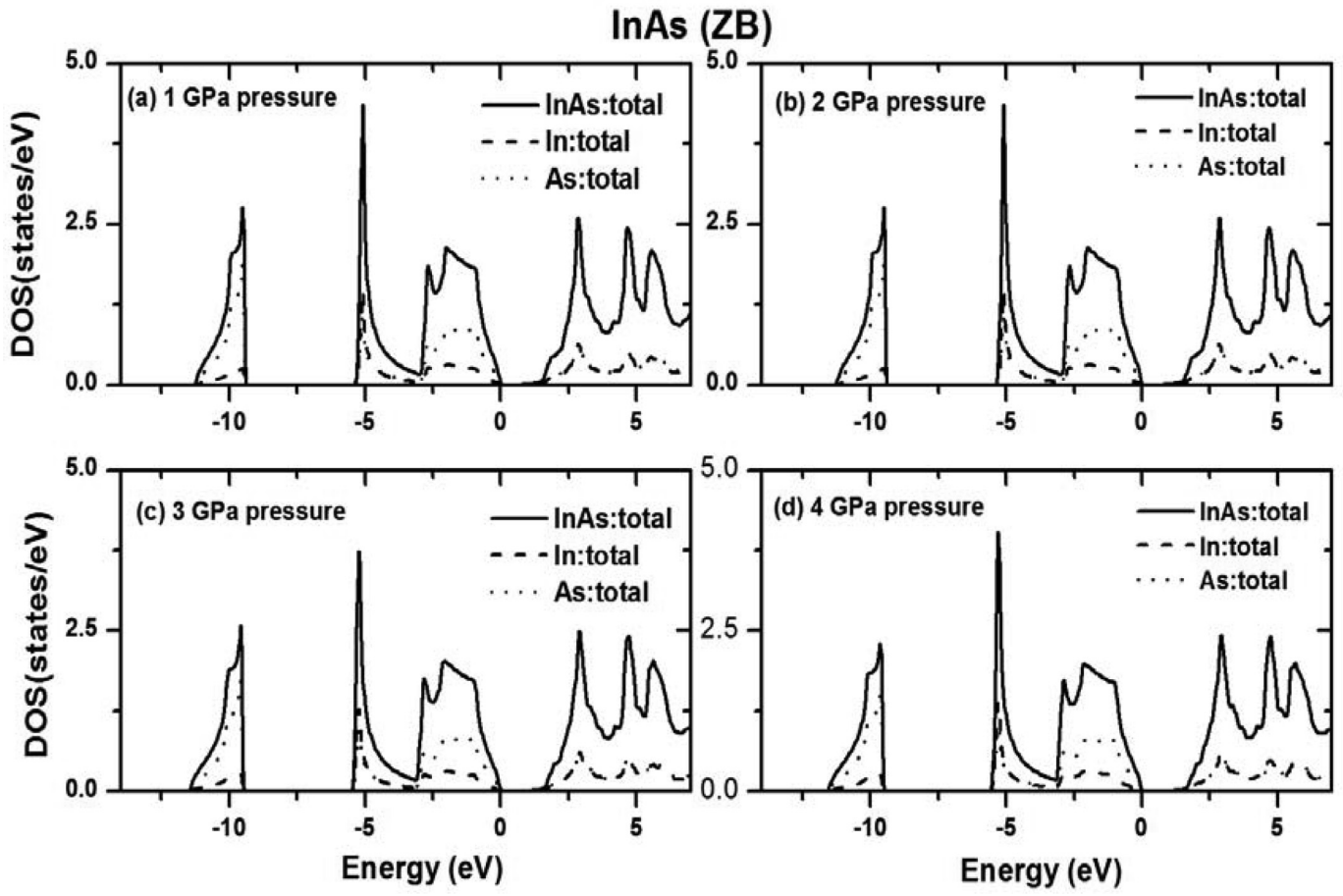

Can. J. Phys. Downloaded from www.nrcresearchpress.com by CSP Customer Service on 03/24/16
For personal use only.

Fig. 13. Total DOS of InAs-RS under pressure: (*a*) 5 GPa pressure; (*b*) 6 GPa pressure; (*c*) 7 GPa pressure; and (*d*) 9 GPa pressure.

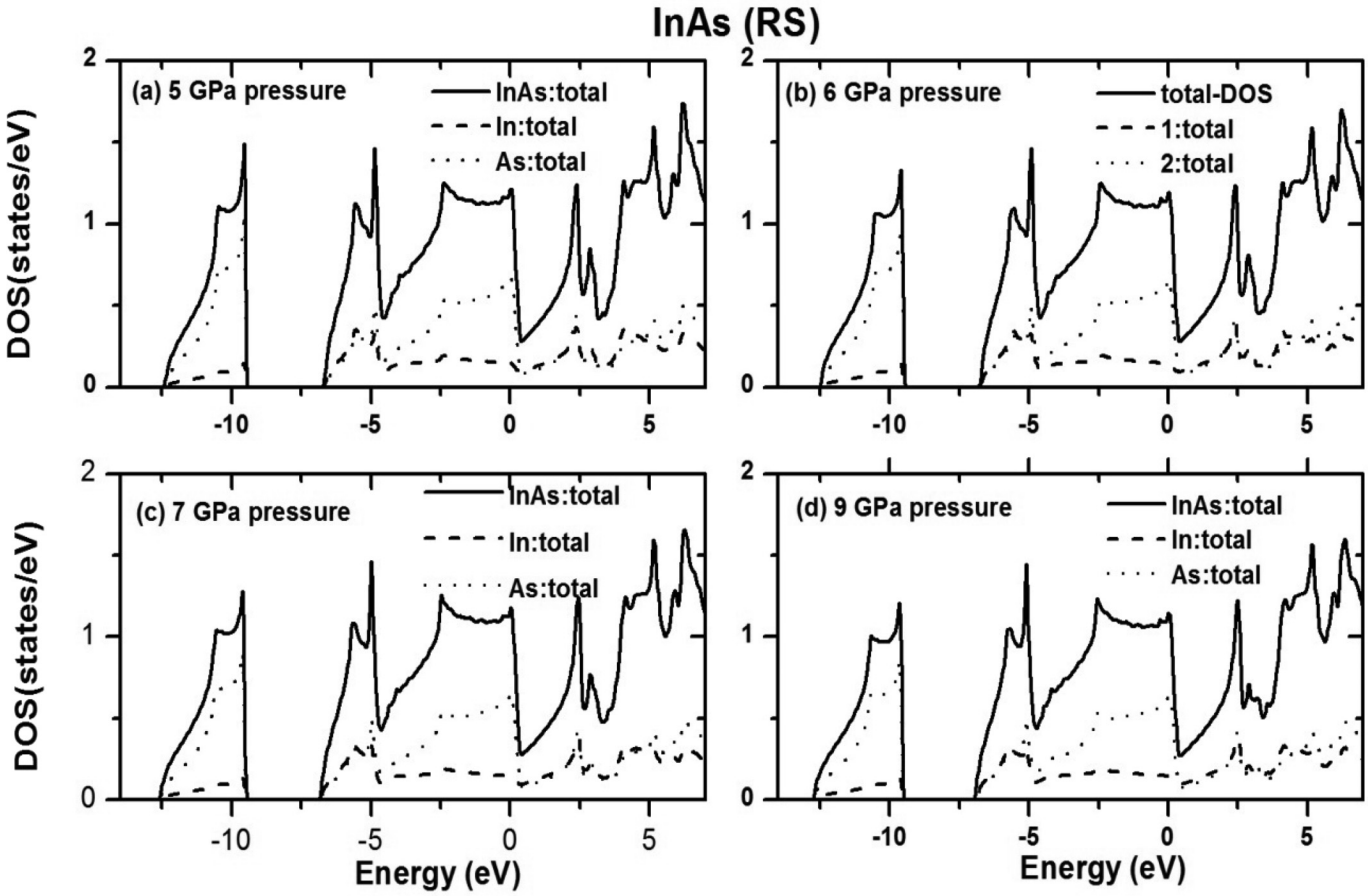

Can. J. Phys. Downloaded from www.nrcresearchpress.com by CSP Customer Service on 03/24/16
For personal use only.

3.3. Electronic structure

Figures 7*a* and 7*b* show the energy band diagrams of InAs-ZB and InAs-RS, respectively, at zero pressure. In Fig. 7*a*, it is observed that the conduction band minimum and the valance band maximum are located at the middle of the Brillioun zone, Γ point. Therefore InAs-ZB structure is a direct band gap semiconductor with an energy band gap of 0.35 eV, which is in good agreement with the experimental value of 0.43 eV [34]. The energy band diagram of InAs-RS as given in Fig. 7*b* shows a prominent difference in the band diagram as compared to that of InAs-ZB. It is interesting to note that there is a crossover of the conduction band towards the valence band, thus indicating the metallic nature of InAs-RS structure. In other words, InAs crystallized in RS structure has a tendency to exhibit metallic nature under high induced pressure above 4.7 GPa. The total and partial DOS plots of InAs-ZB and InAs-RS are shown in Figs. 8*a*–8*c* and 8*d*–8*f*, respectively. From the DOS plots of InAs-ZB, one can see that the lowest band is mainly contributed by the As-s state. The valance band is found to be mainly contributed by the In-s state with significant contribution from the As-p state and In-p state with little contribution from the In-d state. A strong hybridisation is found to occur between the In and As atoms. In the same pattern, the DOS plots of InAs-RS indicate that the lowest band is mainly dominated by the As-s state and the valance band is mainly contributed by As-p and In-p orbitals.

The energy band diagram of InAs-ZB structure under induced pressures 1, 2, 3, and 4 GPa are shown in Figs. 9*a*, 9*b*, 9*c*, and 9*d*, respectively. From these figures, one can observe that there is increase in the band gap with increasing pressure. Figure 10 shows the variation in band gap of InAs-ZB with increasing pressure. This variation could be explained based on DOS diagrams under pressure; the energy eigenvalue corresponding to s, p, and d orbital lies in the higher region with increasing pressure. In the same way, energy band diagrams of InAs-RS structure under induced pressures 5, 6, 7, and 9 GPa are shown in Figs. 11*a*, 11*b*, 11*c*, and 11*d*, respectively. Interestingly, it is seen that there is still crossover of the conduction band towards the valance band under pressure and thus the metallic nature remains. The total density of states of InAs-ZB and InAs-RS under induced pressures are shown in Figs. 12*a*–12*d* and Figs. 13*a*–13*d*, respectively. In Fig. 12, if one sees it systematically, it is found that the band separation near the Fermi line increases with increasing pressure. This is consistent with the observation for band gap in band structure. Similarly in Fig. 13, one observes the continuation of band across the Fermi line indicating metallic character, which is the prominent observation in the band structure of InAs-RS structure. One of the reasons for the metallic nature is band broadening with increase in pressure and the overlap of filled valance band and conduction band.

4. Conclusion

The phase transition under induced pressure of InAs–ZB to RS structure occurs at 4.7 GPa pressure with a volume collapse of 17.2% indicating that the ZB phase is more compressible than the RS phase. The elastic constants of both the phases are found to satisfy the stability conditions and undergo a linear variation with increase in pressure. The elastic parameters are also calculated for both ZB and RS phases. With increase in pressure, InAs-ZB is stiffest along ⟨111⟩ body diagonal while it becomes stiffest along ⟨100⟩ cube axes in InAs-RS. The ionic contribution to interatomic bond-

ing is also dominant as the pressure increases. The ZB phase of InAs is found to be brittle in nature and becomes ductile after it undergoes a structural phase transition to RS phase. It is also found that with increasing pressure both InAs-ZB and InAs-RS showed stiffer lattice and better thermal conductivity. The InAs-ZB phase is found to be a direct band gap semiconductor with an energy band gap of 0.35 eV while the InAs-RS phase exhibits metallic properties. The band gap under induced pressure of InAS-ZB is found to increase, while in the case of InAs-RS there is crossover of atomic orbitals across the Fermi level and hence it exhibits a metallic nature. The total DOS of the InAs-ZB phase shows that the band gap increases because of the energy eigenvalue corresponding to s, p, and d orbitals lies in the higher region with increasing pressure while in the case of the InAs-RS phase there is a broadening of conduction band width with increase in pressure resulting in crossover of conduction orbital towards the valence band. The prominent contribution in the total DOS near the Fermi level of InAs comes from the atomic In-s orbital, As-p, and In-p orbitals in both the phases.

References

1. A. Rashid, H. Javad, A. Hadi, A. Maqsood, and Fazal-e-Aleem. Comput. Mater. Sci. **39**, 580 (2006). doi:10.1016/j.commatsci.2006.08.014.
2. S. Anantathanasarn, Y. Barbarin, N.I. Cade, P.J. van Veldhoven, E.A.J.M. Bente, Y.S. Oei, H. Kamada, M.K. Smit, and R. Nötzel. Mater. Sci. Eng. B, **147**, 124 (2008). doi:10.1016/j.mseb.2007.08.027.
3. J.M Besson, J.P. Itié, A. Polian, G. Weil, J.L. Mansot, and J. Gonzales. Phys. Rev. B, **44**, 4214 (1991). doi:10.1103/PhysRevB.44.4214.
4. S.Q. Wang and H.Q. Ye. Phys. Stat. Sol. (b), **240**, 45 (2003). doi:10.1002/pssb.200301861.
5. A. Mujica, A. Rubio, A. Muñoz, and R.J. Needs. Rev. Mod. Phys. **75**, 863 (2003). doi:10.1103/RevModPhys.75.863.
6. D.R. Lide. 1998. Handbook of chemistry and physics. CRC Press, Boca Raton, Fla. 87th ed.
7. S. Minomura and H.G. Drickamer. J. Phys. Chem. Solids, **23**, 451 (1962). doi:10.1016/0022-3697(62)90085-9.
8. G.D Pitt and M.K.R. Vyas. J. Phys. C: Solid State Phys. **6**, 274 (1973). doi:10.1088/0022-3719/6/2/009.
9. Q. Wang, J. Zhang, R. Li, Y. Xu, X. Miao, and D. Zhang. J. Appl. Phys. **115**, 233712 (2014). doi:10.1063/1.4885039.
10. Kh. Kabita, M. Jameson, B. Indrajit Sharma, R.K. Thapa, and R.K. Brojen Singh. Adv. Sci. Eng. Med. **6**, 354 (2014). doi:10.1166/asem.2014.1483.
11. Kh. Kabita, M. Jameson, B. Indrajit Sharma, R.K. Thapa, and R.K. Brojen Singh. Iraqi J. Appl. Phys. **9**, 17 (2014).
12. Kh. Kabita, J. Maibam, B. Indrajit Sharma, R K. Brojen Singh, and R.K. Thapa. Int. J. Innovation Appl. Stud. **8**, 382 (2014).
13. P. Blaha, K. Schwarz, G.K.H. Madsen, D. Kvasnicka, and J. Luitz. 2001. WIEN2k an augmented plane wave + local orbitals program for calculating crystal properties. Karlheinz Schwarz, Techn. Universitat Wien, Austria.
14. E. Wimmer, H. Krakauer, M. Weinert, and A.J. Freeman. Phys. Rev. B, **24**, 864 (1981). doi:10.1103/PhysRevB.24.864.
15. A.D. Becke and E.R. Johnson. J. Chem. Phys. **124**, 221101 (2006). doi:10.1063/1.2213970. PMID:16784253.
16. P. Hohenberg and W. Kohn. Phys. Rev. **136**, B864 (1964). doi:10.1103/PhysRev.136.B864.
17. W. Kohn and L.J. Sham. Phys. Rev. **140**, A1133 (1965). doi:10.1103/PhysRev.140.A1133.
18. S. Cottenier. 2002. Density functional theory and the family of LAPW-methods: a step- by-step Introduction. Insti-tuut voor Kern-en Stralingsfysica, K.U.Leuven, Belgium.
19. J.P. Perdew, K. Burke, and M. Ernzerhof. Phys. Rev. Lett. **77**, 3865 (1996). doi:10.1103/PhysRevLett.77.3865.
20. F. Birch. Phys. Rev. **71**, 809 (1947). doi:10.1103/PhysRev.71.809.
21. F. Birch. J. Appl. Phys. **9**, 279 (1938). doi:10.1063/1.1710417.
22. J. Jeong, T.E. Schlesinger, and A.G. Milnes. J. Cryst. Growth, **87**, 265 (1988). doi:10.1016/0022-0248(88)90174-1.
23. N.E. Christensen, S. Satpathy, and Z. Pawlowska. Phys. Rev. B, **36**, 1032 (1987). doi:10.1103/PhysRevB.36.1032.
24. L. Pedesseau, J. Even, A. Bondi, et al. J. Phys. D: Appl. Phys. **41**, 165505(1-8) (2008). doi:10.1088/0022-3727/41/16/165505.
25. S.G. Shen. J. Phys. Condens. Matter, **6**, 8733 (1994). doi:10.1088/0953-8984/6/42/006.
26. Y.K. Vohra, S.T. Weir, and A.L. Ruoff. Phys. Rev. B, **31**, 7344 (1985). doi:10.1103/PhysRevB.31.734.
27. J.C. Jamieson. Science, **139**, 845 (1963). doi:10.1126/science.139.3557.845. PMID:17798195.
28. M.I. McMahon and R.J. Nelmes. Phys. Status Solidi (b), **198**, 389 (1996). doi:10.1002/pssb.2221980151.
29. A. Mujica, R.J. Needs, and A. Muñoz. Phys. Status Solidi (b), **198**, 461 (1996). doi:10.1002/pssb.2221980160.
30. B. Mayer, H. Anton, E. Bott, M. Methfessel, J. Sticht, J. Harris, and P.C. Schmidt. Intermetallics, **11**, 23 (2003). doi:10.1016/S0966-9795(02)00127-9.
31. V.V. Bannikov, I.R. Shein, and A.L. Ivanovskii. Phys. Status Solidi RRL, **1**, A89 (2007). doi:10.1002/pssr.200600116.
32. H. Fu, D. Li, F. Peng, T. Gao, and X.L. Cheng. Comput. Mater Sci. **44**, 774 (2008). doi:10.1016/j.commatsci.2008.05.026.
33. S.F. Pugh. Philos. Mag. **45**, 823 (1954). doi:10.1080/14786440808520496.
34. C. Kittel. 1986. Introduction to solid state physics. John Wiley, New York. 6th ed. pp. 185.

Can. J. Phys. Downloaded from www.nrcresearchpress.com by CSP Customer Service on 03/24/16
For personal use only.

Copyright © 2015 American Scientific Publishers
All rights reserved
Printed in the United States of America

Advanced Science Letters
Vol. 21, 2906-2910, 2015

Elastic Properties and Electronic Structures of Pressure Induced Zinc Sulphide (ZnS): A Density Functional Theory Study

Kh. Kabita[1], Jameson Maibam[1], B. Indrajit Sharma[1]*, R.K. Thapa[2] and R. K. Brojen Singh[3]

[1]*Department of Physics, Assam University, Silchar-788011, Assam, India.*
[2]*Department of Physics, Mizoram University, Tanhril, Aizawl-796 009*
[3] *School of Computational and Integrative Sciences, JNU, New Delhi 110067, India.*

A self-consistent ab-initio investigation on the pressure induced elastic properties and electronic structure of ZnS in zinc-blende (ZB) and rock-salt (RS) structure is performed using the full potential linearized augmented plane wave (FP-LAPW) method with modified Becke-Johnson (mBJ) potential under the framework of Density Functional Theory (DFT). A phase transition from the four-fold ZB structure to six-fold RS structure is found occurring at 17.6 GPa pressure with a volume collapse of 12.8%. The obtained results are compared and found to be in consistent with other experimental and theoretical results. The elastic constants and elastic parameters are calculated at different pressures. We find a linear dependence between the elastic constants and pressure in both ZB and RS structure except in C_{44} of the RS structure. The energy band diagrams of both the structures under induced pressure are also studied. The ZB structure is found to be a direct band gap semiconductor while the RS structure is found to be an indirect band gap semiconductor.

Keywords: Density Functional Theory (DFT), Density of states (DOS), Energy band structure, Elastic properties, Phase transition.

1. INTRODUCTION

In recent years, the interest in study of II-VI compound semiconductors has considerably increased because of its developments in the field of optoelectronics and scientific applications. A number of theoretical and experimental studies have been performed for better understanding of the structural and electronic properties of the II-VI compounds [1, 2, 3]. ZnS is a II-VI compound semiconductor having wide band gap which is of great importance due to its potential applications in many optoelectronic devices such as light emitting diodes (LED) and laser diodes (LD) [4, 5]. It is found to crystallize in zinc-blende (ZB) and wurzite (WZ) structure under ambient pressure conditions. In various studies, a phase transition from four-fold co-ordinated zinc-blende (ZB) to six-fold co-ordinated rock-salt (RS) has been reported at elevated pressure [6, 7, 8].

The developments in the computer simulations have resulted in the ab-initio study of the structural, mechanical and electronic properties more systematic and precise. It helps us in better understanding and estimation of the properties of solids under induced pressure which are difficult to study experimentally. The band gap and the elastic constants play a fundamental role in understanding the electrical, optical and mechanical properties of a material. Therefore the study of the band gap and elastic constant at various pressures are important for proper understanding of these properties. Even though there have been many studies on the phase transition and electronic structure of ZnS, there has been very few study on the pressure-induced elastic properties and band structure of ZnS. In our previous studies we have presented a detailed study on the structural, electronic and elastic properties of GaP [9, 10] under induced pressure. The present

*Author to whom correspondence should be addressed.

 1936-6612/2015/21/2906/005 doi: 10.1166/asl.2015.6347

paper is a continuation of our first principle study of the compound semiconductors and a detailed study of the electronic structures of ZnS in both the ZB and RS phases under induced-pressure has been presented. The paper has been organised as follows. After this introduction, the methods used in our calculation are described in section 2. In section 3 the results of our study are given and discussed in detailed. The conclusion of our study is given in section 4.

2. COMPUTATIONAL METHOD

The first principle study of ZnS calculation is performed using the first principle full potential linearised augmented plane wave (FP-LAPW) [11] method within the generalised gradient approximation (GGA) of Perdew-Burke-Ernzerhof (PBE-GGA) [12] with modified Becke-Johnson (mBJ) [13] potential under the framework of density functional theory (DFT) [14,15,16]. This method is used as it is one of the most accurate methods in electronic structure calculation of crystals. In this method, the lattice is divided into non-overlapping atomic spheres surrounding each atomic sites and an interstitial region [17]. Inside the muffin tin (MT) region, the potential is a product of radial function and spherical harmonics and expanded up to order l = 10. For the interstitial regions that are outside the muffin tin spheres, the potentials are expanded in plane waves. 8000 k-points are used for the integration part which reduces to 256 irreducible k-points inside the Brillouin zone. Convergence is obtained at $R_{MT}K_{max}$ = 9.0 where R_{MT} is the atomic sphere radii and K_{max} gives the plane wave cut-off. All calculations are performed with the equilibrium lattice constants which are determined from the plot of the total energy against the unit cell volume by fitting to the Birch-Murnaghan equation of states [18]. The overall calculation is done with WIEN2K [19].

3. RESULTS AND DISCUSSION

3.1. Phase Transition and Elastic Properties

The phase transition of a material plays an important role in understanding the structural, mechanical and physical properties of a material under pressure. For determination of the zero temperature pressure induced phase transition of ZnS-ZB phase to ZnS-RS phase the usual condition of equal enthalpies i.e. H=E+PV is used. The transition pressure from the ZB phase to the RS phase is calculated at the precise point where the enthalpies of the two phases are equal. The enthalpy as a function of energy is shown in figure 1. The phase transition from ZB to RS structure is found to occur at 17.6 GPa pressure which agrees well with the experimental value of 18.1 GPa pressure [20] and other theoretical results of 17.5 GPa and 17.4 GPa pressures [21, 22] respectively. There is a volume collapse of 12.8% at the transition pressure indicating ZB phase is more compressible than the RS phase.

Elasticity describes the response of a compound to a very small loading which causes reversible deformation. The anisotropic features, binding characteristics and structural stability of a material can be determined from study of the pressure dependence of elastic constants. For a cubic crystal, the mechanical stability conditions are: $(C_{11}+2C_{12}) > 0$; $C_{11}C_{12} > 0$; $C_{44} > 0$; $C_{11} > 0$. The elastic constants with increase in pressure for both the structures are shown in figure 2. It is found that the mechanical stability conditions are satisfied when the pressure is below the transition pressure in the ZB phase and above the transition pressure in the RS structure.

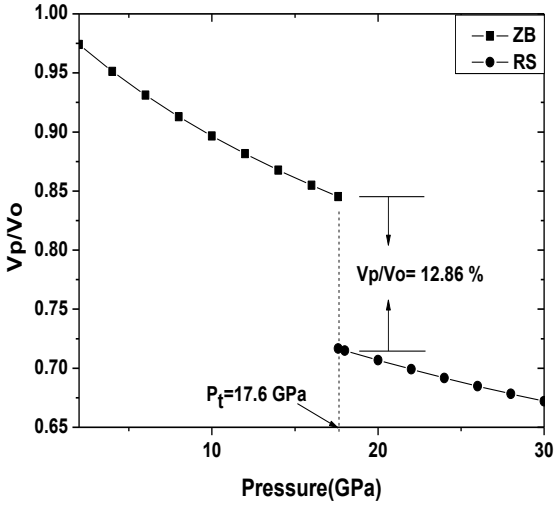

Figure 1. Phase transition of ZnS in zinc blende structure to rock salt structure.

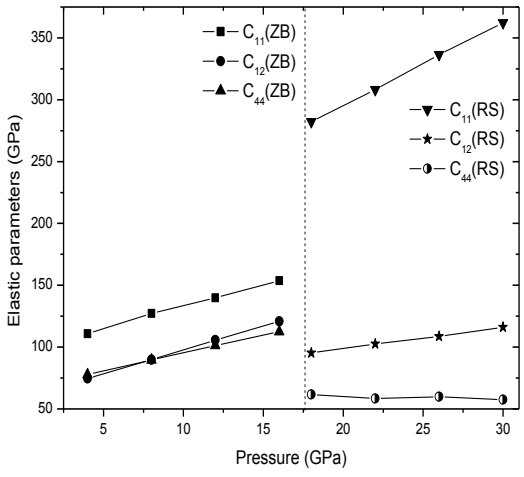

Figure 2. Elastic constants (C_{11}, C_{12}, C_{44}) as a function of pressure for ZnS-ZB and ZnS-RS structure.

A linear relationship between the elastic constants (C_{11}, C_{12}, C_{44}) and pressure can be seen in both the phases

except for C_{44} in RS structure. Also C_{11} is found to be more sensitive to change in pressure than C_{12} and C_{44}.

In the light of these observations, the elastic parameters, Zener anisotropic factor (A), Poisson's ratio (υ), Kleinmann parameter (ζ), Youngs modulus (Y), and Debye's temperature (θ_D) are calculated to determine the mechanical and thermal behaviour ZnS in both the structures. Figure 3(a), 3(b), 4(a) and 4(b) shows the calculated elastic parameters of ZnS with variation in pressure from 0 to 16 GPa pressure for ZB phase and from 18 GPa to 30 GPa pressure for RS phase. Poisson's ratio (υ) gives us information about the characteristics of bonding forces. The value of poisson's ratio (υ) is 0.1 for covalent materials, whereas for ionic materials, υ = 0.25 [23]. In our calculation, the value of υ varies from 0.28 to 0.32 in the ZB phase and from 0.29 to 0.32 in the RS phase indicating higher ionic contribution in intra-atomic bonding with increasing pressure. The lower and upper limits for υ in central force solids have been reported to be 0.25 and 0.5 respectively [24]. Thus our values also indicates that, inter atomic forces tends to be more central as pressure increases. The relative ease of bond bending against the bond stretching is indicated by ζ (Kleimann parameter). It also implies resistance against bond bending or bond angle distortion. In a system, minimizing bond bending leads to ζ = 0 and minimizing bond stretching leads to ζ =1. In the present study, as the pressure increases, ζ for the ZB phase is found to vary from 0.76 to 0.85 and 0.47 to 0.48 for the RS phase, indicating shrinkage in bond-stretching.

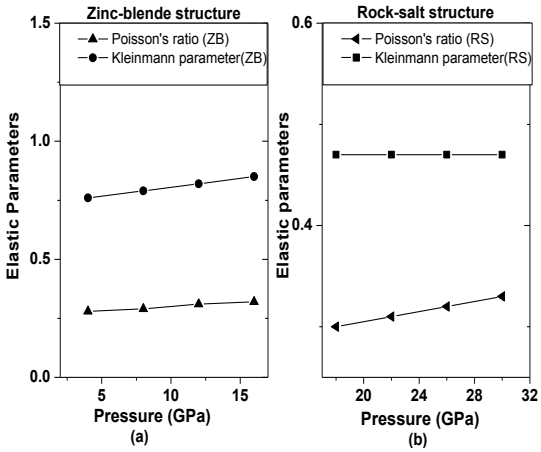

Figure 3. Elastic parameters (Poisson's ratio and Kleinmann parameter) as a function of pressure for ZnS in (a) ZB phase and (b) RS phase.

The stiffness of a material is given by Y (Young's modulus). A linear increase in Y with increase in pressure is found in both phases of ZnS and hence ZnS becomes more rigid with increase in pressure. The value of Debye's temperature is also found to vary from 401K to 437K for the ZB phase and from 493K to 509K for the RS phase indicating stiffer lattice and better thermal conductivity.

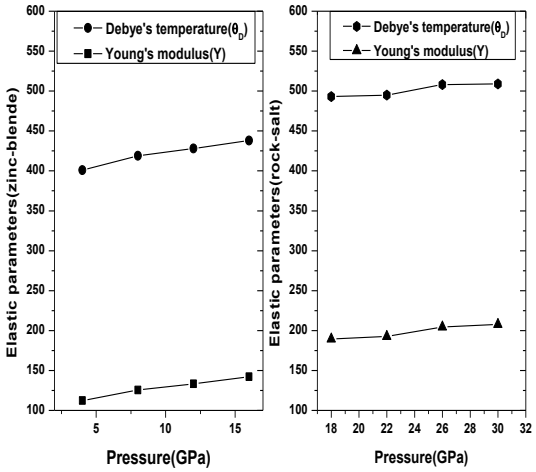

Figure 4. Elastic parameters (Debye's temperature and Young's modulus) as a function of pressure for ZnS in (a) ZB phase and (b) RS phase.

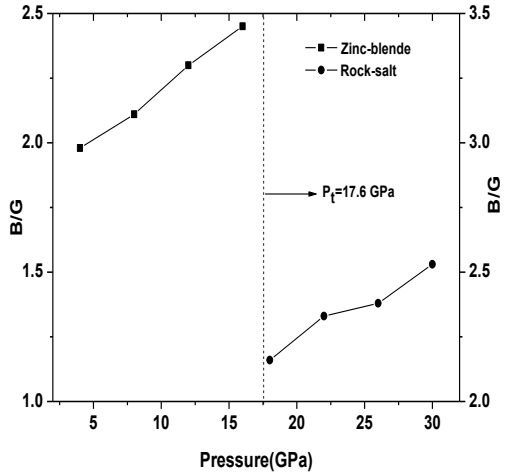

Figure 5. B/G ratio as a function of pressure for ZB and RS phase

The ductility or brittleness of a material is determined by the ratio between the bulk and shear modulus, B/G as proposed by Pugh [25]. A material is found to be brittle if B/G < 1.75 and ductile if B/G > 1.75. The B/G ratio of our present study varies from 1.91 to 2.45 for ZB phase and 2.16 to 2.53 for RS phase with increase in pressure as shown in figure 5. Therefore ZnS structure is found to be ductile and even with increase in pressure ductility is retained.

3.2. Electronic Properties

The energy band diagram of ZnS- ZB structure at 0 GPa pressure has been presented in many studies and found to be a direct band gap semiconductor. In our study we have found out the energy band gap of ZnS at different pressures. The variation in the energy band gap with pressure is shown in figure 6. Figure 7(a), 7(b), 7(c) and

7(d) shows the energy band diagram of ZnS- ZB structure at different pressures. The direct band gap of ZnS-structure is found to increase with pressure which is due to the fact that the energy eigenvalues corresponding to s, p, and d orbital's lies in the higher region with increasing pressure.

The energy band diagram of ZnS-RS structure at different pressures are shown in figure 8(a), 8(b), 8(c) and 8(d). The ZnS-RS structure is found to be an indirect band gap semiconductor. In this case, variations of band gap under pressures are not observed prominently. Thus we conclude that the band gap of RS structure of ZnS is not much affected by pressure.

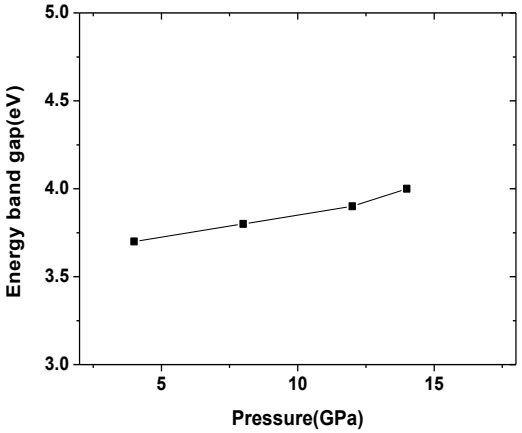

Figure 6. Variation of energy band gap of ZnS-ZB structure with pressure.

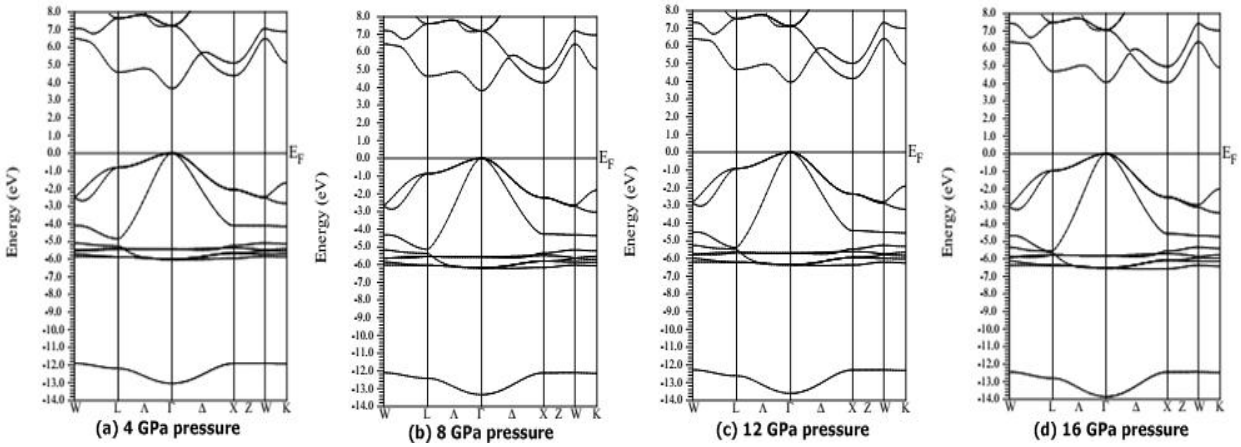

Figure 7. Energy band diagram of ZnS-ZB-structure at (a) 4 GPa pressure, (b) 8 GPa pressure, (c) 12 GPa pressure and (d) 16 GPa pressure.

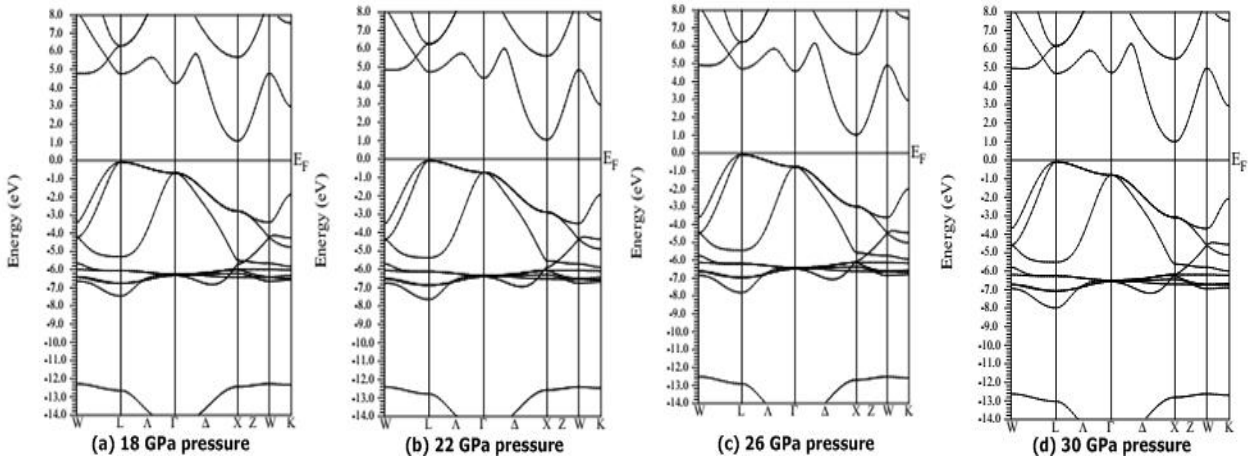

Figure 8. Energy band diagram of ZnS-RS-structure at (a) 18 GPa pressure, (b) 22 GPa pressure, (c) 26 GPa pressure and (d) 30 GPa pressure.

4. CONCLUSIONS

The phase transition of ZnS-zinc blende phase to rock salt phase is found to occur at 17.6 GPa pressure with a volume collapse of 12.86% indicating that zinc blende structure is more compressible than the rock salt structure. The values of elastic constants for both the structures are satisfied for mechanical stability conditions. A linear relationship between the elastic constants and induced pressures is observed in both the phases. In the electronic structure, the zinc blende structure of ZnS is found to be a direct band gap semiconductor with a band gap of 3.49 eV at ambient pressure and increases with pressure whereas rock salt structure is found as indirect band gap having not much variation in band gap with pressure.

REFERENCES

1. C.S. Wang and B.M. Klein, *Phys. Rev. B* **24,** 3393-3416 (1981).
2. Y. N. Xu and W. Y. Ching, *Phys. Rev. B* **48**, 4335-4351 (1993).
3. P. Schrer, P. Kruger and J. Pollmann, *Phys. Rev. B* **47,** 6971-6980 (1993).
4. E. Bellotti, K. F. Brennan, R. Wang and P. P. Ruden, *J. Appl. Phys.* **82,** 2961-2964 (1997).
5. S. Q. Wang, Appl. *Phys. Lett.* **88**, 061902(1)-061902(3) (2006).
6. S. Desgreniers, L. Beaulieu, and I. Lepage, *Phys. Rev. B* **61**, 8726 –8733 (2000).
7. S. K. Gupta, S. Kumar and S. Auluck, *Opt. Commun.* **284 (1),** 20-26 2011.
8. Z. Li, B. Lui, S. Yu, J. Wang, Q. Li, B. Zou, T. Cui, Z. Liu, Z. Chen and J. Lui J. *Phys. Chem. C* **115** 357-361 (2011).
9. Kh. Kabita, Maibam Jameson, B. Indrajit Sharma, R. K. Thapa Singh and R. K. Brojen *Adv. Sci. Eng. Med.* **6** 354-358 (2014)
10. Kh. Kabita, Maibam Jameson, B. Indrajit Sharma, R. K. Thapa Singh, R. K. Brojen *Iraqi J Appl. Phys.* **9** 17-20 (2014).
11. E. Wimmer, H. Krakauer, M. Weinert and A. J. Freeman, *Phys. Rev. B* **24,** 864-875 (1981).
12. J. P. Perdew, K. Burke and M. Ernzerhof *Phys. Rev. Lett.* **77,** 3865-3868 (1996).
13. A. D. Becke and E. R. Johnson, *J. Chem. Phys.* **124,** 221101-221104 (2006).
14. P. Hohenberg and W. Kohn, *Phy. Rev.3B* **136,** 864-871 (1964).
15. W. Kohn and L. J. Sham, *Phys. Rev. 4A* **140,** 1133-1138 (1965).
16. S. Cottenier, *"Density Functional Theory and the family of (L)APW-methods: a step-by-step Introduction"* Belgium, Insti-tuut voor Kern-en Stralingsfysica, K.U.Leuven ISBN 90-807215-1-4. (2002).
17. O. K. Andersen *Phys. Rev. B.* **12,** 3060-3083 (1975).
18. F. Birch, *Phys. Rev.* **71,** 809-824 (1947).
19. P. Blaha, K. Schwarz, G. K. H. Madsen, D. Kvasnicka and J. Luitz, *"An anaugmented plane wave + local orbitals program for calculating crystal properties*",*Wien2k. Techn. Universitat* (Wien, Austria) ISBN 3-9501031-1-2. (2001)
20. A. Nazzal and A. Qteish, *Phys. Rev. B* **53** 8262-8266 (1996).
21. R. Chen, X. F. Li, L. C. Cai and J. Zhu, *Solid State Comm.* 139 246-249 (2006).
22. C.E. Hu, L.L. Sun, Z.Y. Zeng and X.R. Chen, *Chin. Phys. Letters* **25**, 675-678 (2008).
23. V. V. Bannikov, I. R. Shein and A. L. Ivanovskii *Phys. Status. Solidi. Rapid. Res. Lett.* **3** 89-100 (2007)
24. H. Fu, D. Li, F Peng et al. *Comput. Mater. Sci.* **44** 774-778 (2008)
25. S. F. Pugh *Phil. Mag.* **45** 823-843 (1954).

Received: 8 April 2015. Accepted: 22 May 2015.

First principle study on pressure-induced electronic structure and elastic properties of indium phosphide (InP)

K. Kabita, J. Maibam, B. I. Sharma, R. K. Thapa & R. K. Brojen Singh

Indian Journal of Physics

ISSN 0973-1458
Volume 89
Number 12

Indian J Phys (2015) 89:1265-1271
DOI 10.1007/s12648-015-0701-0

Springer

Your article is protected by copyright and all rights are held exclusively by Indian Association for the Cultivation of Science. This e-offprint is for personal use only and shall not be self-archived in electronic repositories. If you wish to self-archive your article, please use the accepted manuscript version for posting on your own website. You may further deposit the accepted manuscript version in any repository, provided it is only made publicly available 12 months after official publication or later and provided acknowledgement is given to the original source of publication and a link is inserted to the published article on Springer's website. The link must be accompanied by the following text: "The final publication is available at link.springer.com".

Author's personal copy

Indian J Phys (December 2015) 89(12):1265–1271
DOI 10.1007/s12648-015-0701-0

ORIGINAL PAPER

First principle study on pressure-induced electronic structure and elastic properties of indium phosphide (InP)

K Kabita[1], J Maibam[1], B I Sharma[1]*, R K Thapa[2] and R K Brojen Singh[3]

[1]Department of Physics, Assam University, Silchar 788011, Assam, India

[2]Department of Physics, Mizoram University, Tanhril, Aizawl 796 009, India

[3]School of Computational and Integrative Sciences, JNU, New Delhi 110067, India

Received: 22 January 2015 / Accepted: 02 April 2015 / Published online: 26 May 2015

Abstract: The structural, elastic and electronic properties of indium phosphide in zinc-blende and rock-salt structure under various pressures are studied using the first principle calculation based on the density functional theory with modified Becke–Johnson potential. The pressure-induced structural phase transition from zinc blende to rock salt is observed at 9.3 GPa pressure with 16.4 % volume collapse, indicating that zinc-blende structure is more compressible as compared to rock-salt structure. The elastic constants and elastic parameters such as Zener anisotropic factor, Kleinmann parameter, Poisson's ratio, isotropic shear modulus, Young's modulus and Debye's temperature under different pressures are obtained and show a linear relation with pressure. The electronic band structures at different pressures are investigated using the total and partial density of states. The calculated results are found to be in good agreement with other theoretical and experimental results.

Keywords: Density functional theory; Energy band diagram; Elastic properties; Phase transition

PACS Nos.: 71.15.Mb; 71.20.−b; 71.20.Nr

1. Introduction

The study of compound semiconductors exhibiting new crystal phases under pressure has led to an increase interest in the study of high-pressure behaviour of III–V compound semiconductors [1, 2]. The studies of structural properties, phase diagram and high-pressure phases of III–V compounds have aroused considerable scientific interest in the past decades due to its technological importance. In recent years many theoretical and experimental studies on the electronic and structural properties as well as the phase transition of group III–V compound semiconductors have been undertaken [3–7]. Indium phosphide (InP) is an important III–V compound semiconductor, which has been intensively studied for their technological importance and has become a very promising material for opto-electronic devices, solar cells, high-performance computing and communications [8–10]. The study of the effect of pressure in materials has recently become of much interest in solid-state physics. The energy band gap and elastic constants of a semiconductor play crucial role in the study of material properties. Therefore, in order to gain better understanding of material properties, the studies of the changes in the energy band gap and elastic constants of semiconductor compounds under externally induced pressure are very important.

In the literature, the semiconductor-to-metallic phase transition from zinc-blende (ZB) to rock-salt (RS) structure of InP is found to occur between 8.5 and 13.3 GPa pressures [11–14]. The phase stability of group III phosphide has been studied by Arbouche et al. [15], who have found the phase transition of InP occurring at about 7.35 GPa pressure. Branicio et al. [16] have studied the high-pressure phases of InP and found the phase transition from ZB to RS occurring at 10.2 GPa pressure. Although there have been many studies on the structural and electronic properties of InP, the high-pressure study on the electronic structures and elastic properties of InP is still very rare. The experimental study of these quantities at high pressure is very

*Corresponding author, E-mail: indraofficial@rediffmail.com

© 2015 IACS

Author's personal copy

difficult and therefore, many theoretical calculations are usually used. GW [17] is a method, which is commonly used for the calculation of the electronic structures but also very expensive in terms of computational cost and time of calculation. For calculation of systems, which are not complex systems of heavy atom, LDA and GGA methods are good enough for the electronic structure calculations but results in underestimation of the band gaps. In our previous studies, we have extensively studied the pressure-induced phase transition, structural, electronic and elastic properties of GaP [18, 19]. In the present paper, we have performed the pressure-induced phase transition from the fourfold coordinated ZB structure to sixfold coordinated RS structure of InP using the full potential linearized augmented plane wave (FP-LAPW) method with modified Becke–Johnson (mBJ) potential under the framework of density functional theory (DFT) with main emphasis on the study of the variation in elastic constants, elastic parameters, band gap and density of states (DOS) with increasing pressure.

2. Theoretical and computational method

The calculations of InP are performed using the FP-LAPW [20] method with mBJ potential [21] under the framework of DFT [22–24]. The exchange–correlation interaction effects are treated within the generalized gradient approximation of Perdew–Burke–Ernzerhof (PBE-GGA) scheme [25] as implemented in the WIEN2k code [26]. In this method, the lattice is divided into non-overlapping spheres (called atomic or muffin tin sphere) surrounding each atomic sites and an interstitial region. Inside the muffin tin (MT) region, the potential is a product of radial function and spherical harmonics and expanded up to order of $l = 10$. For the interstitial regions that are outside the muffin tin spheres, the potentials are expanded in plane waves. The number of k-points used for the integration part is 8000, which is reduced to 256 irreducible k-points inside the Brillouin zone including five high-symmetry points W, L, Γ, X and K. Convergence of the basis set is obtained at $R_{MT}K_{max} = 9.0$, where K_{max} gives us the plane-wave cut-off. The elastic constants have been determined using the stress–strain method with volume-conserving technique [27]. In our calculations, only small lattice distortions have been considered in order to remain within the elastic domain of the crystal.

3. Results and discussion

3.1. Structural properties

The static equilibrium properties of the crystal structure of ZB and RS of InP are obtained by minimization of the total energy with respect to the unit cell volumes per molecule and fitting it to the Birch–Murnaghan equation [28]. The calculated structural parameters are compared with other results and are given in Table 1. Our results are found to be in good agreement with other experimental results of Paul [29] with lattice constant 5.9 Å and 5.87 Å by Madelung [30] along with the theoretical results of Mujica and Needs [31] with lattice constant of 5.94 Å, bulk modulus of 68 GPa and 4.9 derivative of bulk modulus. There are also other references reporting lattice constants as 5.87 Å, 5.95 Å, bulk modulus as 65.5, 72, 68, 71, 60 GPa and derivative of bulk modulus as 4.59, 4.67, 4.41 [32–38]. For the InP-RS structure, there are not much available data on the structural parameters. Hence, the results of our structural data for both the ZB and RS structure are used for further elastic and electronic structure calculations.

Table 1 Lattice constant 'a(Å)', bulk modulus 'B(GPa)' and pressure derivative of bulk modulus (B′) of ZB and RS structure of InP at zero pressure

	a(Å)	B(GPa)	B′
ZB structure			
Present work	5.97	60.5	4.64
Expt. results	5.90[a], 5.87[b]	65.5[d], 72[e]	4.59[c],
Theoretical results	5.94[b], 5.95[c]	68[b], 71[f], 60 [g]	4.9[b], 4.41 [g], 4.67 [h]
RS structure			
Present work	5.54	74.78	4.76
Expt. results	5.71[b], 5.24[b]		
Theoretical results			

[a] Ref [30], [b] Ref [32], [c] Ref [33], [d] Ref [34], [e] Ref [38], [f] Ref [39], [g] Ref [37], [h] Ref [36]

3.2. Phase transition and elastic properties

The usual conditions for equal enthalpy, i.e. the pressure at which, the enthalpy $H = E + PV$ is same for both the structures, are used to obtain the zero-temperature pressure-induced phase transition. The ZB–RS phase transition of InP is found to occur at 9.3 GPa pressure with a volume collapse of 16.4 %, indicating that the ZB phase is more compressible than the RS phase. Our calculated results of phase transition are compared with other experimental results of 9.5 GPa by Menoni et al. [14], 9.8 GPa pressure by Mc Mahon [39] and 10.3 GPa transition pressure and 14.9 volume collapse by Madelung [30] and theoretical results of transition pressure as 7.3, 7.5, 8.5, 10.2, 11.0 GPa and volume collapse as 18, 15, 17 % by different group of researchers [15, 16, 40–43] as shown in Table 2. We find

Author's personal copy

Table 2 Phase transition pressure 'P_t(GPa)' and volume collapse of InP

	Present calculation	Expt. results	Theoretical results
Transition pressure (P_t) (GPa)	9 .3	9.5[a], 10.3 ± 0.2[b], 9.8[c]	7.3[d], 7.5[e], 8.5[f], 11.0 [g]
Volume collapse (%)	16.45	14.9[b]	18[f], 15 [g], 17 [h]

[a] Ref [14], [b] Ref [32], [c] Ref [40], [d] Ref [15], [e] Ref [41], [f] Ref [42], [g] Ref [43], [h] Ref [44]

that our results are closer to the experimental data than other theoretical results. Hence, the DFT calculation using the mBJ potential gives us more accurate results than other theoretical studies.

The elastic constant plays an important role in the study of the relationship between crystal structure and bonding. The mechanical stability condition of a crystal at high pressure can be understood from the pressure dependence of the elastic constants. For a cubic crystal, the Born mechanical stability conditions are as follows: $(C_{11} + 2C_{12}) > 0$; $C_{11}C_{12} > 0$; $C_{44} > 0$; $C_{11} > 0$. In the present study, the elastic constants (C_{11}, C_{12}, C_{44}) are computed using the volume-conserving technique [27] for a lattice volume corresponding to pressure ranging from 0 to 8 GPa pressure for the ZB and 10 GPa pressure to 16 GPa pressure for RS phase and found to satisfy the stability conditions. The Zener anisotropic factor (A), Poisson's ratio (υ), Kleinmann parameter (ζ), Young's modulus (Y) and Debye's temperature (θ_D) are important elastic parameters, which determine the mechanical and thermal behaviour of a material. In our study we have calculated these parameters for both the structures using the relation given by Mayer et al. [44]. The elastic isotropy of a material is determined by the Zener anisotropic factor (A). For $A = 1$, the material is elastically isotropic and deform uniformly along all directions of the body. If $A > 1$, it is stiffest along <111> body diagonals and when $A < 1$, it is stiffest along <100> cube axes. It is expressed as:

$$A = \frac{2C_{44}}{C_{11} - C_{12}} \tag{1}$$

Kleinmann parameter (ζ) describes the relative position of the cation and anion sub-lattices and is given by the relation:

$$\zeta = \frac{C_{11} + 8C_{12}}{7C_{11} + 2C_{12}} \tag{2}$$

The Poisson's ratio (υ) provides a sharp criterion for differentiating the brittleness and ductility in solids. It gives us the stability of crystal against shear and is calculated using the relation,

$$\upsilon = \frac{1}{2}\left(\frac{B - (2/3)G}{B + (1/3)G}\right) \tag{3}$$

where B is the Bulk modulus and G is the isotropic shear modulus given by

$$G = \frac{G_V + G_R}{2} \tag{4}$$

where G_v is the Voigt's shear modulus corresponding to the upper bound of G values and G_R is the Reuss's shear modulus corresponding to the lower bound of G values. G_v and G_R can be expressed as:

$$G_V = \frac{C_{11} - C_{12} + 3C_{44}}{5} \tag{5}$$

$$G_R = \frac{5(C_{11} - C_{12})C_{44}}{4C_{44} + 3(C_{11} - C_{12})} \tag{6}$$

The Young's modulus is determined to measure the stiffness of the solid and is given by:

$$Y = \frac{9GB}{G + 3B} \tag{7}$$

Debye's temperature gives us explicit information about lattice vibrations and is also an important parameter determining the thermal characteristics of a material. It is calculated using the average sound velocity (υ_m) given by the relation [45]:

$$\theta_D = \frac{h}{k}\left[\frac{3n}{4\pi}\left(\frac{N_A\rho}{M}\right)\right]^{1/3}\upsilon_m \tag{8}$$

where h is the Plank's constant, k is the Boltzmann constant, N_A is the Avogadro's number, n is the number of atoms per formula unit, M is the molecular mass per formula unit, ρ is the density and υ_m is given by [46]:

$$\upsilon_m = \left[\frac{1}{3}\left(\frac{2}{\upsilon_t^3} + \frac{1}{\upsilon_l^3}\right)\right]^{-(1/3)} \tag{9}$$

where υ_t and υ_l are the transverse and longitudinal velocities, respectively, which are obtained from Navier's equation as [47]:

$$\upsilon_l = \sqrt{\frac{3B + 4G}{3\rho}} \tag{10}$$

$$\upsilon_t = \sqrt{\frac{G}{\rho}} \tag{11}$$

The calculated elastic parameters of InP with variation of pressure from 0 GPa pressure up to 8 GPa of ZB phase and

Author's personal copy

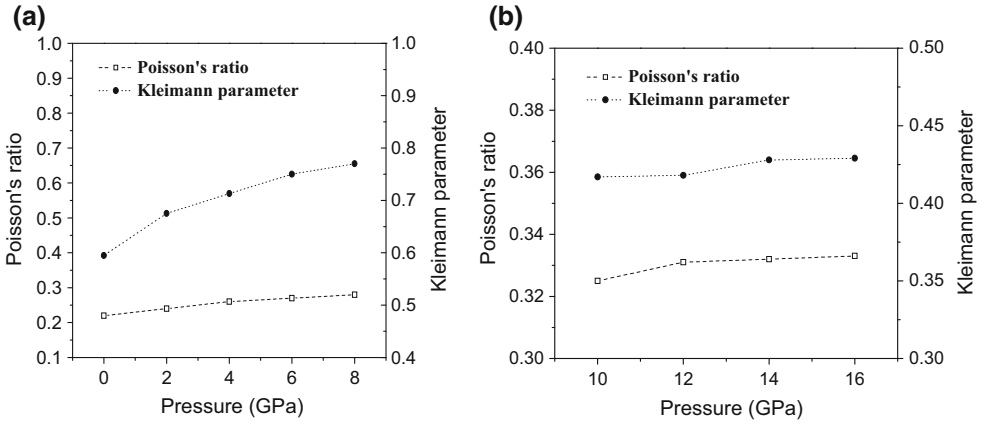

Fig. 1 Elastic parameters (Poisson's ratio and Kleinmann parameter) as a function of pressure of InP in: (**a**) ZB phase and (**b**) RS phase

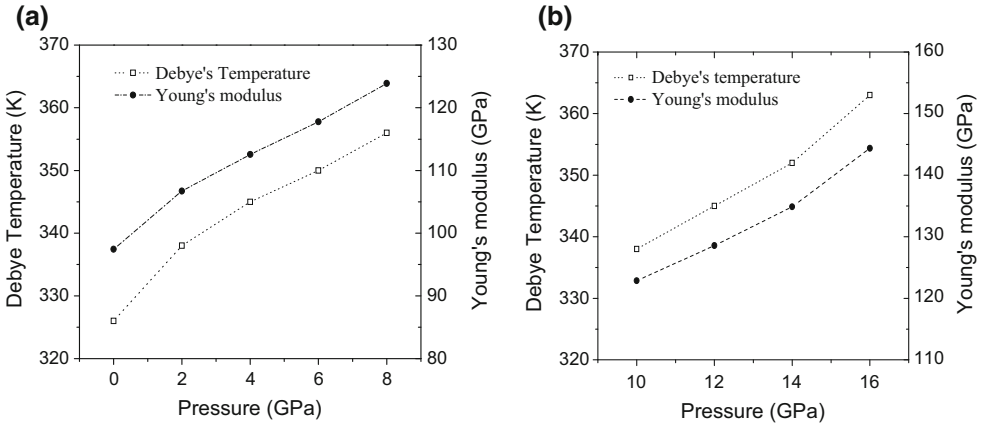

Fig. 2 Elastic parameters (Debye's temperature and Young's modulus) as a function of pressure of InP in: (**a**) ZB phase and (**b**) RS phase

from 10 to 16 GPa pressure of RS phase are shown in Figs. 1(a), 1(b) and 2(a), 2(b). A consistent pattern of linear increase in elastic parameters with increase in pressure can be observed from these figures. The parameter A (Zener anisotropic factor) shows a variation from 3.16 to 4.77 and 0.35 to 0.36 with increase in pressure of ZB and RS phase, respectively, showing the degree of elastic anisotropy. The degree of directionality of the covalent bonds is given by the Poisson's ratio (υ). For covalent materials, $\upsilon = 0.1$, whereas for ionic materials, $\upsilon = 0.25$ [48]. Our calculations show that with increase in pressure, the value of υ varies from 0.22 to 0.28 of the ZB phase and from 0.32 to 0.33 of the RS phase, showing that with increase in pressure, the ionic contribution to inter-atomic bonding becomes dominant. It has been reported [49] that for central force solids the lower and upper limits for υ are 0.25 and 0.5, respectively. Our values also indicate that as pressure increases, inter-atomic forces tend to be more central. ζ (Kleinmann parameter) quantifies internal strain and thus indicates the relative ease of bond bending against the bond stretching. It also implies resistance against bond bending or bond angle distortion. In a system, minimizing bond bending leads to $\zeta = 0$ and minimizing bond stretching leads to $\zeta = 1$. In the present study, as the pressure increases, ζ of the ZB phase is found to vary from 0.59 to 0.77 and 0.41 to 0.42 of the RS phase, indicating the shrinkage in bond stretching. The larger the value of Y (Young's modulus), the stiffer is the material. Our results show a linear increase in Y with increase in pressure and hence, InP becomes more rigid with increase in pressure in both the phases. With increase in pressure, the value of Debye's temperature is also found to vary from 326 to 357 K of the ZB phase and from 338 to 363 K of the RS phase, indicating stiffer lattice and better thermal conductivity. The empirical malleability measure of a material is determined by the value of B/G ratio [50]. A material is found to be brittle if $B/G < 1.75$ and ductile if $B/G > 1.75$. The B/G ratio of present study varies from 1.52 to 1.94 of ZB phase and 2.5 to 2.6 of RS phase with increase in pressure as shown in Fig. 3. Therefore, InP structure is found to be brittle and with increase in pressure it tends to become ductile.

3.3. Electronic structures and density of states

The energy band diagram of the ZB structure of InP at 0 GPa pressure has been reported in many papers and found to be a direct band gap semiconductor [5, 7, 16]. The

Author's personal copy

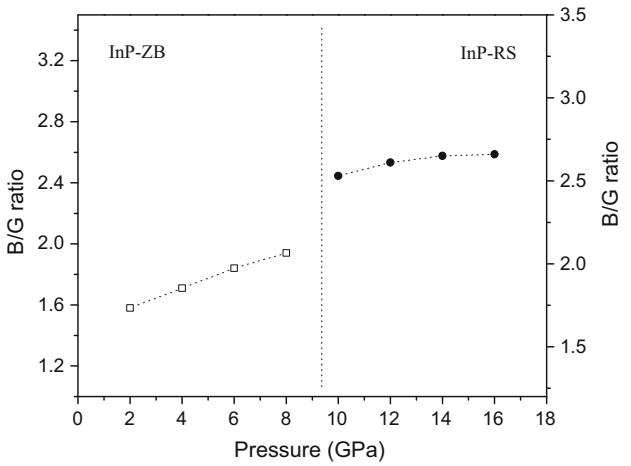

Fig. 3 B/G ratio as a function of pressure of InP-ZB and InP-RS phase

results of our energy band diagram show a direct energy band gap of 1.31 eV, which is in good agreement with the experimental value of 1.42 eV [38] and better than other LDA results of 0.62 eV and GGA results of 0.85 eV [38], and in case of InP-RS structure metallic nature is found to occur. The partial DOS plots of InP-ZB are shown in Fig. 4(a), 4(b) and for InP-RS structure in Fig. 4(c), 4(d) respectively. In the partial DOS plot of InP-ZB the three prominent peaks could be seen in valence band. The first peak from the left is dominated by the *P–p* state with a significant contribution from the In-d state. The second peak is mainly dominated by the In-s state with significant contribution from the *P–p* state and small contribution from the In-p state and In-d state. In case of the RS structure, the first peak is mainly dominated by the *P-s* state with little contribution from the In-*d* state and In-*p* state and the second peak is found to be mainly contributed by the *P–p* state with a mere contribution from the In-*s* state. We therefore find that the highest contribution towards the total density of states near the Fermi level of the ZB structure is In-s state and of RS structure is the *P–p* state. In our study the energy band gaps of InP at various pressures have also been calculated. Figure 5(a)–5(d) show the energy band diagrams of InP-ZB structure at different pressures. The variation in energy band gap of InP-ZB with increase in pressure is also shown in Fig. 6. We find that there is a linear increase in the band gap of InP-ZB as the pressure increases, which may due to

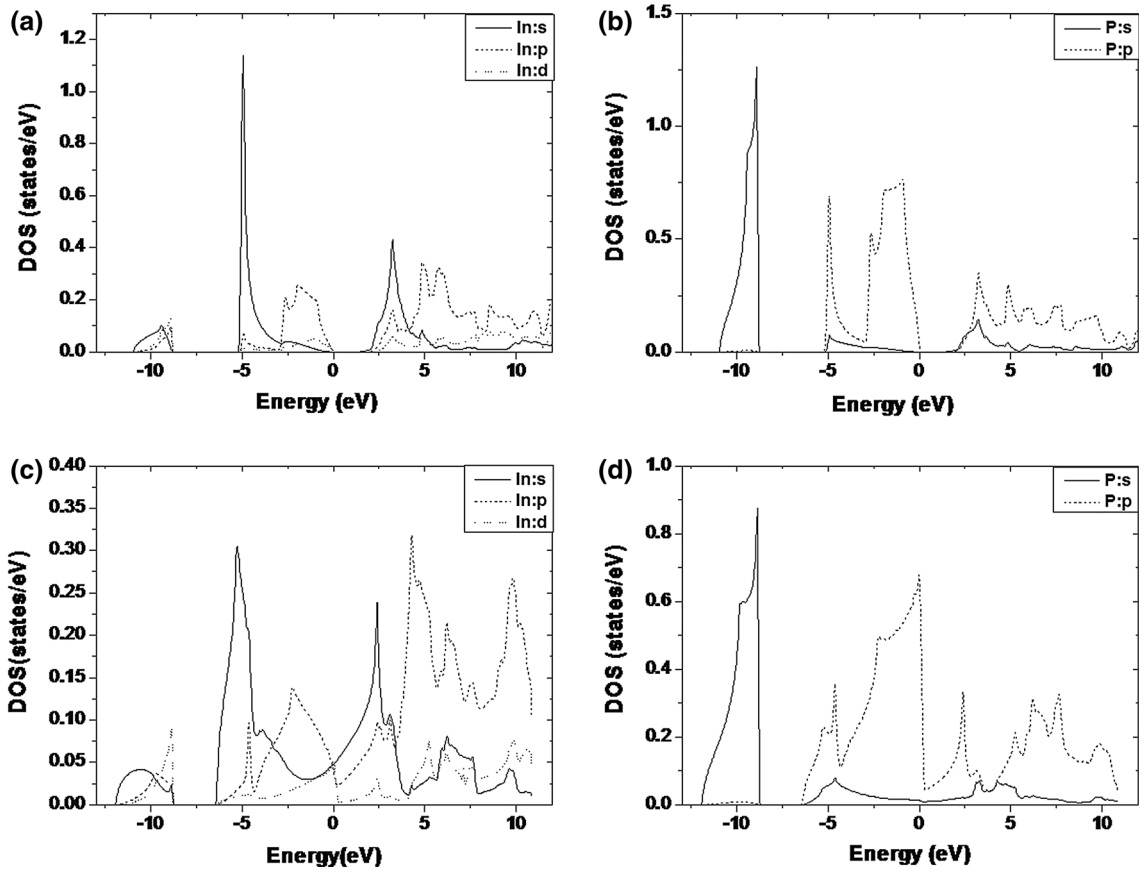

Fig. 4 DOS of InP: (**a**) In partial DOS of InP-ZB (**b**) P partial DOS of InP-ZB (**c**) In partial DOS of InP-RS (**d**) P partial DOS of InP-RS

Author's personal copy

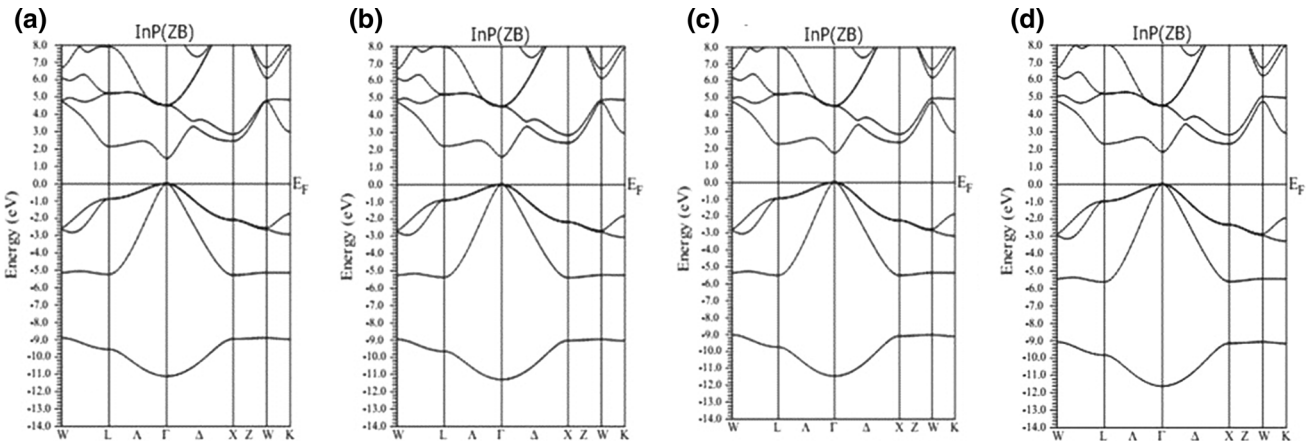

Fig. 5 Energy band diagram of InP-ZB structure: (**a**) 2 GPa pressure, (**b**) 4 GPa pressure, (**c**) 6 GPa pressure and (**d**) 8 GPa pressure

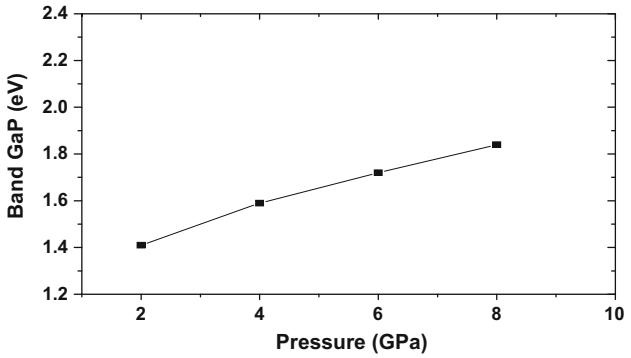

Fig. 6 Pressure versus band gap of InP-ZB structure at different pressures

presence of the energy eigenvalues corresponding to *s*, *p* and *d* orbitals in the higher region with increasing pressure. In Fig. 7(a)–7(d), the energy band diagrams under various pressures of the RS structure are presented and observed that the crossing over of conduction band towards the valence band does not change and hence, the metallic nature is retained even at higher pressures. Our result concludes that the energy band gap of the RS phase of InP is not much affected by the variation in pressure.

4. Conclusions

The structural properties of both InP-ZB and InP-RS are studied and found to be in good agreement with other experimental and theoretical results. The phase transition from the ZB structure to RS structure of InP is found to occur at 9.3 GPa pressure with a volume collapse of 16.45 %, indicating that InP-ZB structure is more compressible than the InP-RS structure. The elastic constants of InP at various pressures of both the structures are obtained and the corresponding elastic parameters are calculated. In both the ZB and RS structures, the values of elastic

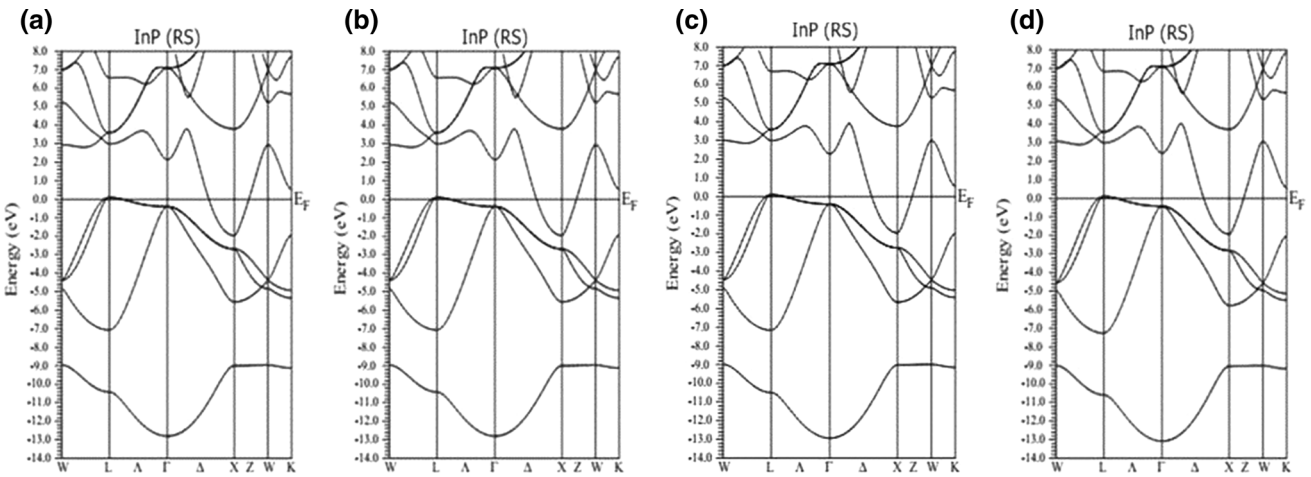

Fig. 7 Energy band diagram of InP-RS structure: (**a**) 2 GPa pressure, (**b**) 4 GPa pressure, (**c**) 6 GPa pressure and (**d**) 8 GPa pressure

Author's personal copy

constants as well as the elastic parameters are found to have a linear relation with increase in pressure. The Poisson's ratio calculation shows dominance in the ionic contribution to the inter-atomic bonding with increase in pressure. Shrinkage in bond stretching with increase in pressure is also found from the study of Kleinmann parameter. The study of the Debye's temperature shows stiffer lattice and better thermal conductivity with pressure. The InP-ZB structure is found to be a direct band gap semiconductor with an energy band gap of 1.31 eV, while the InP-RS structure is found to be metallic. The total density of states of InP is obtained and we find that in the ZB structure, In-*s* state has the highest contribution towards the total density of states near the Fermi level, whereas in RS structure, *P–p* state has the highest contribution. It is found that in the InP-ZB structure the band gap increases with increasing pressure, whereas in the InP-RS structure there is no much variation in band gap with increase in pressure. Hence, our results conclude that there are substantial changes in the elastic parameters of both InP-ZB and InP-RS structures and energy band gap of InP-ZB phase, but no prominent change is observed in the electronic structure of InP-RS phase with variation in pressure.

References

[1] Y K Vohra, S T Weir and A L Ruoff *Phys. Rev. B* **31** 7344 (1981)
[2] S Schilling and R N Shelton *Phys. of Solids Under Pressure* (New York: North-Holland) (1981)
[3] J M Besson, J P Itie, A Polian, G Weil, J L Mansot and J Gonzales *Phys. Rev. B* **44** 4214 (1991)
[4] M Jameson, B Indrajit Sharma, R Bhattacharjee, R K Thapa and R K Brojen *Physica B* **406** 4041 (2011)
[5] A Mujica, A Rubio, A Munoz and R J Needs *Rev. Mod. Phys.* **75** 912 (2003)
[6] J Sjakste, N Vast and V Tyuterev *Phys. Rev. Lett*. **99** 236405 (2007)
[7] E S Kadantsev arXiv:1005.0615vl [*cond-mat.mtrl-sci*] (2010)
[8] L Sukit, P Reunchan, A Janotti and G V W Chris *Phys. Rev. B* **77** 195209 (2008)
[9] L Lin, G T Woods and T A Callcott *Phys. Rev. B* **63** 235107 (2001)
[10] J G Díaz, G W Bryant, W Jaskólski and M Zielinski *Phys. Rev. B* **75** 245433 (2007)
[11] S Minomura and H G Drickamer *J. Phys. Chem. Solids* **23** 451 (1962)
[12] J C Jamieson *Science* **139** 845 (1963)
[13] T Soma, J Satoh and H Matsuo *Solid State Commun*. **42** 889 (1982)
[14] C S Menoni and I L Spain *Phys. Rev. B* **35** 7520 (1987)
[15] O Arbouche, B Belgoumene, B Soudinia, Y Azzaz, H Bendaoud and K Amara *Comput. Mater. Sci.* **47** 685 (2010)
[16] P S Branicio, J P Rino and F Shimojo *Appl. Phys. Lett*. **88** 161919 (2006)
[17] G Onida, L Reining and A Rubio *Rev. Mod. Phys*. **74** 601 (2012)
[18] K. Kabita, M Jameson, B Indrajit Sharma, R K Thapa Singh and R K Brojen *Adv. Sci. Eng. Med.* **6** 354 (2014)
[19] K. Kabita, M Jameson, B Indrajit Sharma, R K Thapa Singh and R K Brojen *Iraqi. J. Appl. Phys.* **9** 17 (2014)
[20] E Wimmer, H Krakauer, M Weinert and A J Freeman *Phys. Rev. B* **24** 864 (1981)
[21] A D Becke and E R Johnson *J. Chem. Phys*. **124** 221101 (2006)
[22] P Hohenberg and W Kohn *Phys. Rev*. **136** 864 (1964)
[23] W Kohn and L J Sham *Phys. Rev.* **140** 1133 (1965)
[24] S Cottenier *Density Functional Theory and the family of (L)APW-methods: a step-by-step Introduction* (Belgium: Instituut voor Kern-en Stralingsfysica, K. U. Leuven) ISBN 90-807215-1-4 (2002)
[25] J P Perdew, S Burke and M Ernzerhof *Phys. Rev. Lett.* **77** 3865 (1996)
[26] P Blaha, K Schwarz, G K H Madsen, D Kvasnicka and J Luitz WIEN2k *An Augmented Plane Wave + Local Orbitals Program for Calculating Crystal Properties* (Austria: Karlheinz Schwarz, Techn. Universitat Wien) ISBN 3-9501031-1-2 (2001)
[27] F Birch *Phys. Rev.* **71** 809 (1947)
[28] F Birch, *J. Appl. Phys*. **9** 279 (1938)
[29] W Paul *J. App. Phys.* **32** 2082 (1961)
[30] O Madelung *Semiconductors Physics of Group IV elements and III-V compounds* Landolt-Bornstein, New Series, Group III vol. 17 part A (Berlin: Springer-Verlag) (1982)
[31] A Mujica and R J Needs *Phys. Rev. B* **55** 9659 (1997)
[32] S Kalvoda, B Paulus, P Flude and H Stoll *Phys. Rev. B* **7** 4027 (1997)
[33] A Seidl, A Gorling, P Vogl, J A Majewski and M Levy *Phys. Rev. B* **53** 3764 (1996)
[34] D Nichols, D Rimia and R Sladek *Solid State Commun.* **36** 667 (1980)
[35] R Trommer, H Muller, M Cardona and P Vogl *Phys. Rev. B* **21** 4878 (1980)
[36] M Yousaf, M A Saeed, R Ahmed, MM Alsardia, A R M Isa and A Shaari *Commun. Theor. Phys*. **58** 777 (2012)
[37] R W G Wyckoff, *Crystal Structures* 2nd edn. (Malabar: Krieger) (1986)
[38] R Ahmed, F Aleem, S J Hashemifar and H Ak-barzadeh *Phys. B* **403** 1876 (2008)
[39] M I Mc Mahon, R J Nelmes, N G Wright and D R Allan *Proceedings of the Joint Conference on the AIRATP/APS On High-Pressure Science and Technology*, June 28–July 2 (eds.) S C Schmit, J W Shaner, G A Samara and M Ross (Colorado: ColoradoSprings) p 629 (1993)
[40] I Lukacevic, D Kirin, P K Jha and S K Gupta *Phys. Status Solidi B* **247** 273 (2010)
[41] H Chenghua, F Wang and Z Zheng *J. Mater. Res*. **27**, 1105 (2012)
[42] R K Singh and S Singh *Phys. Rev. B* **39** 671 (1989)
[43] S B Zhang and M L Cohen *Phys. Rev. B* **35** 7604 (1987)
[44] B Mayer et al. *Intermetallics* **11** 23 (2003)
[45] L Johnston, G Keeler, R Rollins and S Spicklemire *The Consortium for Upper-Level Physics Software*, (New York: John Wiley) (1996)
[46] I Anderson *J. Phys. Chem. Solids* **24** 909 (1963)
[47] E Schreiber, O L Anderson and N Soga *Elastic constants and their measurements.* (New York: McGraw-Hill) (1973)
[48] V V Bannikov, I R Shein and A L Ivanovskii *Phys. Status. Solidi. Rapid. Res. Lett.* **3** 89 (2007)
[49] H Fu et al. *Comput. Mater. Sci.* **44** 774 (2008)
[50] S F Pugh *Phil. Mag.* **45** 833 (1954)

Journal of Basic and Applied Engineering Research
Print ISSN: 2350-0077; Online ISSN: 2350-0255; Volume 2, Number 13; April-June, 2015 pp. 1064-1067
© Krishi Sanskriti Publications
http://www.krishisanskriti.org/jbaer.html

Electronic Structures of GaX(X=P, As) under Induced Pressure: A First Principle Study

Kh. Kabita[1] and B. Indrajit Sharma[2]*

1,2*Department of Physics, Assam University, Silchar-788011, Assam,* ***India***
E-mal: [2]indraofficial@rediffmail.com

Abstract—*A first principle study on the electronic structures of GaX (X=P, As) under induced pressure is performed using the modified-becke Johnson potential under the framework of Density Functional Theory. In the present calculation, GaP undergoes a phase transition from B3 to B1 phase at 21.9 GPa pressure with a volume collapse of 14.11% while GaAs undergoes a transition from B3 to B1 phase at 10.7 GPa pressure with a volume collapse of 14.2% indicating that B3 phase of both the compounds is more compressible than the B1 phase. The energy band diagram of GaP-B3 phase and GaAs-B3 phase show an indirect band gap of 2.33eV and a direct band gap of 1.3eV respectively while B1 phase for both the compounds show metallic nature which is in good agreement with other theoretical and experimental studies. Under induced pressure the indirect band gap of GaP-B3 phase and direct band gap of GaAs-B3 phase increases while in the B1 phase, the metallic nature of GaP and GaAs is retained and does not vary with pressure.*

1. INTRODUCTION

The development in the field of optoelectronic devices and scientific applications of III-V compound semiconductors has led to its extensive study in recent years [1-3]. GaX (X=P, As) is a III-V compound semiconductor which is being considered of great technological importance due to its potential application in many optoelectronic devices such as light emitting diodes (LED) and laser diodes (LD)[4,5]. The study of the electronic and structural properties helps us in characterizing, understanding and predicting the mechanical properties of a material. Therefore the variation in the energy band gap under induced pressure help us for better understanding of these properties under extreme conditions of pressure.

In literature it has been reported that GaP and GaAs crystallizes in zinc-blende (B3) structure under ambient pressure conditions. In various studies it is reported that when pressure is applied the volume decreases and a structural phase transition to rock salt (B1) structure is found to occur [6-8].

The ab-inito study of the structural and electronic properties of a material has become more systematic and precise with the developments in the computer simulation. It helps us in better understanding and estimation of the properties of a material under induced pressure which are difficult to study experimentally. Even though there have been many studies on the phase transition and electronic properties of GaP and GaAs, there have been few studies on the effect of pressure on the electronic structure of these compounds. The present paper is mainly focused on the study of the variation in the energy band gap under induced pressure in both B3 and B1 phases using the WIEN2K code based on DFT. The paper has been organized as follows. After this introduction, the methods used in our calculation are described in section 2. In section 3 the results of our study are given and discussed in detailed. The conclusion of our study is given in section 4.

2. COMPUTATIONAL METHODS

The first principle study of GaX(X=P,As) calculation is performed using the first principle full potential linearized augmented plane wave (FP-LAPW) [9] method within the generalized gradient approximation (GGA) of Perdew-Burke-Ernzerhof (PBE-GGA) [10] with modified Becke-Johnson (mBJ) [11] potential under the framework of density functional theory (DFT) [12-14]. This method is used as it is one of the most accurate methods in electronic structure calculation of crystals. In this method, the lattice is divided into non-overlapping atomic spheres surrounding each atomic sites and an interstitial region [15]. Inside the muffin tin (MT) region, the potential is a product of radial function and spherical harmonics and expanded up to order l = 10. For the interstitial regions that are outside the muffin tin spheres, the potentials are expanded in plane waves. 8000 k-points are used for the integration part which reduces to 256 irreducible k-points inside the Brillouin zone. Convergence is obtained at $R_{MT}K_{max}$ = 9.0 where R_{MT} is the atomic sphere radii and K_{max} gives the plane wave cut-off. The position of the first and second atom of the B3 and B1 structures of GaP is taken to be (0,0,0), (0.25,0.25,0.25) and (0,0,0), (0.5,0.5,0.5) respectively. $3d^{10}4s^24p^1$, $3s^23p^3$ and $3d^{10}4s^24p^3$ states are respectively considered as the valence electrons for Ga, P and As respectively. All calculations are performed with the equilibrium lattice constants which are determined from the plot of the total energy against the unit cell volume by fitting to the Birch-Murnaghan equation of states [16]. The overall calculation is done with WIEN2K [17].

3. RESULTS AND DISCUSSION

The ground state lattice parameter for GaP and GaAs in both B3 and B1 phase are obtained by the structure optimization. A series of different lattice constant are used to calculate the total energy and the corresponding primitive cell volume. The energy versus unit cell volume curves for both GaP and GaAs are shown in Fig. 1(a) and Fig. 1(b). We can clearly see that in both the figures the B3 phase is more stable than the B1 phase which is in good agreement with other theoretical and experimental results.

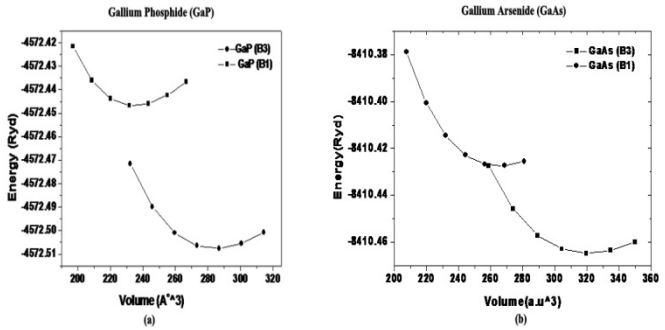

Fig. 1: Total energy verses unit cell volume for B3 and B1 phases of (a) GaP and (b) GaAs.

The phase transition is important for understanding the structural, mechanical and physical properties of a material under pressure. The phase transformation of four-fold coordinated structure (B3) of GaX (X=P, As) to a more denser six fold coordinated structure (B1) under pressure is calculated using the condition of equal enthalpies i.e. the H=E+PV. The structural phase transition from B3 to B1 phase for GaP and GaAs are shown in Fig. 2(a) and Fig. 2(b).

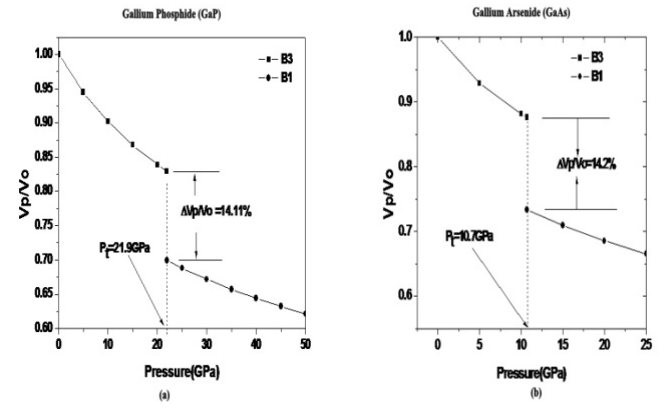

Fig. 2: Phase transition from B3 to B1 phase for (a) GaP and (b) GaAs.

We find that the structural phase transition for GaP-B3 to GaP-B1 occurs at 21.9 GPa pressure with a volume collapse of 14.11% while GaAs undergoes a structural phase transition from B3 to B1 phase at 10.7 GPa pressure with a volume collapse of 14.2% indicating that in both GaP and GaAs, the B3 phase is more compressible than the B1 phase. The energy band diagram of GaP and GaAs has already been reported in many theoretical and experimental studies [18-20]. In the present study we find that GaP-B3 phase is an indirect band gap semiconductor with a band gap of 2.3eV while GaP-B1 phase is metallic. Also GaAs-B3 phase is a direct band gap semiconductor with a band gap of 1.3eV while GaAs-B1 phase shows metallic nature. Therefore we find that our results for both B1 and B3 phases of GaP and GaAs are in close agreement with previous reported data. We have also calculated the energy band gap of GaX(X=P, As) at different pressures for both B1 phase and B3 phase.

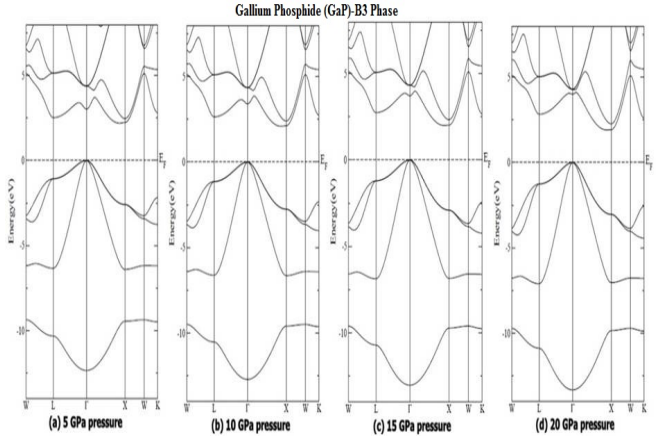

Fig. 3: Energy band diagram of B3-phase of GaAs in (a) 5 GPa pressure (b) 10 GPa pressure (c) 15 GPa pressure and (d) 20 GPa pressure.

Fig. 3(a), 3(b), 3(c) and 3(d) shows the energy band diagram of B3 phase of GaP at different pressures. One interesting thing that we find from the band structure diagrams in Fig. 4 is that as the pressure increases to 5 GPa, 10 GPa 15 GPa and 20 GPa, the gap between the Γ-L increases while the gap between Γ-X decreases towards the fermi level indicating possibilities of crossing over of the conduction band towards the valance band. The variation in the energy band gap with pressure for B3 phase of GaP is also shown in Fig. 6 for clear analysis of the changes between Γ-X and Γ-L with pressure. The energy band diagram of B1 phase of GaP at different pressures after the phase transition is also shown in Fig. 5(a), 5(b), 5(c) and 5(d). From the Fig. we can clearly see crossing over of the conduction band towards the valance band hence confirming the transition from direct band gap nature to metallic at higher pressure.

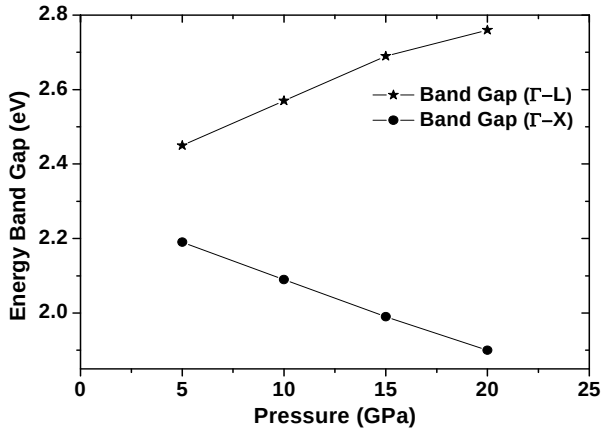

Fig. 4: Variation of Energy band gaps of GaP-B3 phase with pressure.

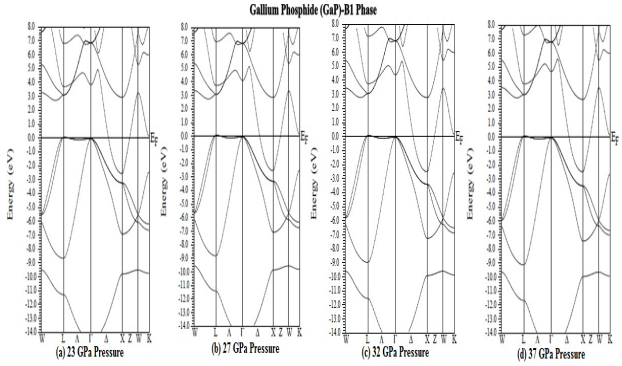

Fig. 5: Energy band diagram of B1-phase of GaP in (a) 23 GPa pressure (b) 27 GPa pressure (c) 32 GPa pressure and (d) 37 GPa pressure.

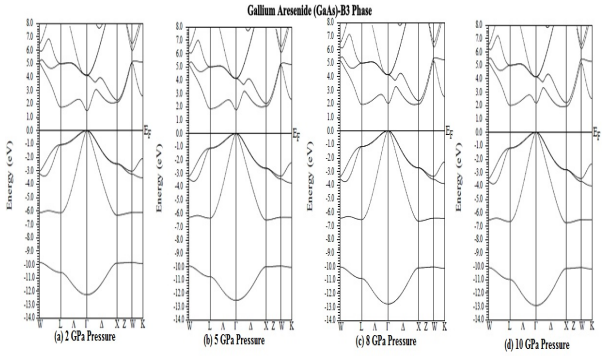

Fig. 6: Energy band diagram of B3-phase of GaAs in (a) 2 GPa pressure (b) 5 GPa pressure (c) 8 GPa pressure and (d) 10 GPa pressure.

In Fig. 6(a), 6(b), 6(c) and 6(d), the energy band diagrams of GaAs-B3 phase at different pressures are given. From the figures we find that the gap between the Γ point increases as the pressure increases but if we closely study the energy band diagram we find that the gap at the X point decreases which indicates possibility of crossing over at higher pressure as in case of GaP. The variation of gap at the Γ point and X point with increase in pressure is given in Fig. 7.

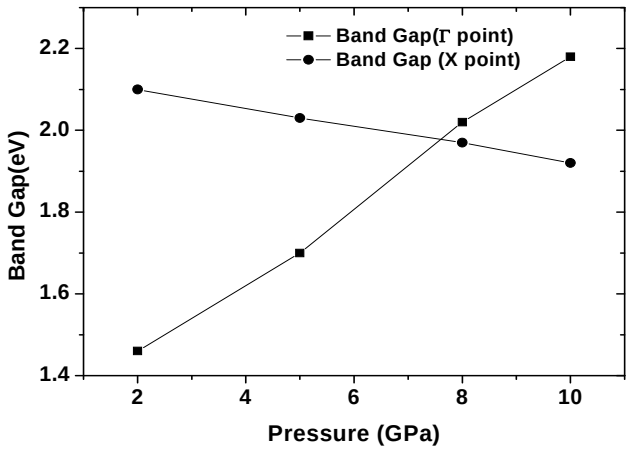

Fig. 7: Variation of Energy band gaps of GaAs-B3 phase with pressure.

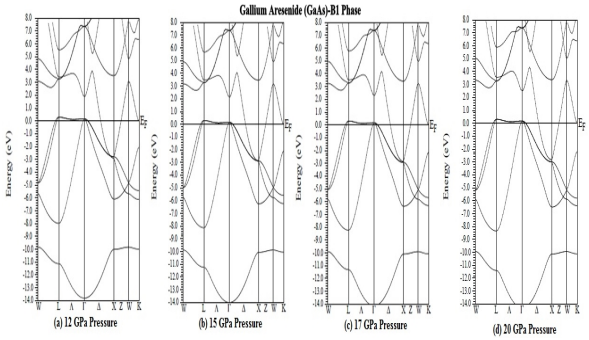

Fig. 8: Energy band diagram of B1-phase of GaAs in (a) 12 GPa pressure (b) 15 GPa pressure (c) 17 GPa pressure and (d) 20 GPa pressure.

Fig. 8(a), 8(b), 8(c) and 8(d) shows the energy band diagram of the B1 phase of GaAs. From the Fig. we find that the metallic nature is retained even at high pressure without much variation. Hence we conclude that the energy band gap of both GaP and GaAs in B3 phase is affected by pressure while the energy band gaps of B1 phase is not much affected by pressure.

4. CONCLUSIONS

The structural properties of GaX (X=P, As) in both B3 and B1 structure are studied and B3 phase is found to be more stable than the B1 phase. A structural phase transition from B3 to B1 is found to occur at 21.9 GPa pressure with a volume collapse

of 14.11% in GaP while GaAs undergoes a structural transition from B3 to B1 phase at 10.7 GPa pressure with a volume collapse of 14.2% indicating that B3 phase of both the compounds is more compressible than the B1 phase. The energy band diagram shows that GaP-B3 is an indirect band gap semiconductor with a band gap of 2.3 eV while GaAs-B3 is a direct band gap semiconductor with a band gap of 1.3 eV. The B1 phase of both the compounds is also found to be metallic which are found to be in good agreement with other experimental and theoretical studies. The energy band gaps for GaP-B3 phase between the Γ-L points, increased while the gap between the Γ-X points decreased under induced pressure. Also GaAs-B3 phase showed an increase in gap at the Γ point and decrease at X point under induced pressure. However the metallic behavior of GaP-B1 and GaAs-B1 phase do not show any change under induced pressure. Thus we conclude that the B3 phase of both GaP and GaAs are affected by pressure while the B1 phase is not affected by pressure.

REFERENCES

[1] Bouhemadou, A., Khenata, R., Kharoubi, M., Seddik, T., Reshak, A. H., and Al-Douri, Y., *Comp. Mater. Sci.*, 45, 2009, pp. 474-479.

[2] Arbouche, O., Belgoum`ene, B., Soudini, B., Azzaz, Y., Bendaoud, H., and Amara, K., *Comp. Mater. Sci*., 47, 2010, pp. 685-692.

[3] Sukit, L., Reunchan, P., Janotti, A., and Chris, G. V. W., *Phys. Rev. B*, 77, 2008, 195209-1952015.

[4] Jiao, Z. Y., Ma, S. H., and Guo, Y. L., *Comp. Theor. Chem*., 970, 2011, 79-87.

[5] Smith, F. W., Le, H. Q., Diadiuk, V., Hollis, M. A. Calawa, A. R., Gupta, S., Frankel, M., Dykaar, D. R., Mourou, G. A., and Hsiang, T. Y., *Appl. Phys. Lett.*, 54, 1989, 890-892.

[6] Durandurdu, M., and Darbold, D. A., *Phys. Rev* B, 66, 2002, 045209(1)-045209(5).

[7] Al-Douri, Y., Mecabih, S., Benosman, N., and Aourag, H., *Physica B*, 325, 2003, pp. 362-371.

[8] Mujica, A., and Needs, R. J., *J. Phys. Condens. Matter*, 8, 1996, L237-L243.

[9] Wimmer, E., Krakauer, H., Weinert, M., and Freeman, A. J., *Phys. Rev. B* 24**,** 1981, pp. 864-875

[10] Perdew, J. P., Burke, K., and Ernzerhof, M., *Phys. Rev. Lett*. 77, 1996, pp. 3865-3868.

[11] Becke, A. D., and Johnson, E. R., *J. Chem. Phys.* 124, 2006, pp. 221101-221104.

[12] Hohenberg , P., and Kohn, W., *Phy. Rev.3B*, 136, 1964, pp. 864-871.

[13] Kohn, W., and Sham, L. J., *Phys. Rev. 4A* 140, 1965, pp. 1133-1138.

[14] Cottenier, S., *"Density Functional Theory and the family of (L)APW-methods: a step-by-step Introduction"* Belgium, Instituut voor Kern-en Stralingsfysica, K.U.Leuven ISBN 90-807215-1-4, 2002.

[15] Andersen, O. K., *Phys. Rev. B*. 12, 1975, pp. 3060-3083.

[16] Birch, F., *Phys. Rev.* 71, 1947, pp. 809-824.

[17] Blaha, P., K. Schwarz, Madsen, G. K. H., Kvasnicka, D., and Luitz, J., *"An anaugmented plane wave + local orbitals program for calculating crystal properties*",*Wien2k. Techn. Universitat* (Wien, Austria) ISBN 3-9501031-1-2. 2001.

[18] Al-Douri, Y., Ali Hussain, R., *Applied Phys.A*, 2011, pp. 1159-1167.

[19] C. Kittel, Introduction to Solid State Physics 6th Ed. (New York: John Wiley) 1986, pp.185.

[20] Madelung, O., *Landolt-Börnstein, Semiconductor, Physics of II-IV and I-VII Compounds, Semimagnetic Semiconductors, New Series, Group III,* V. 17 (Springer: Berlin

STRUCTURAL PHASE TRANSITION OF INDIUM ARSENIDE UNDER INDUCED PRESSURE: A DENSITY FUNCTIONAL THEORY STUDY

Kh. Kabita[1], B. Indrajit Sharma*[1], Jameson Maibam[1], R. K. Brojen Singh[2] and R.K. Thapa[3]
[1]*Department of Physics, Assam University, Silchar-788011, Assam, India.*
[2] *School of Computational and Integrative Sciences, JNU, New Delhi 110067, India.*
[3]*Department of Physics, Mizoram University, Tanhril, Aizawl-796 00, India.*
*For correspondence. (indraofficial@rediffmail.com)

Abstract: We have carried out the first-principles calculations to show phase transition of binary compound semiconductor Indium Arsenide under induced pressure in the light of density functional theory with the generalised gradient approximation of Perdew-Burke-Ernzerhof as exchange correlation potential. The calculated lattice parameters are found to be in good agreement with other theoretical and experimental data. The pressure induced phase transition from zinc-blende to rock salt structure is found to occur at 4.7 GPa pressure with a 17.27% of volume collapse.

Keywords: Density Functional Theory (DFT); energy band diagram; elastic properties; phase transition

PACS: 71.15.Mb, 71.20.-b, 71.20.Nr

1. Introduction:

The technological importance of group III-V compound semiconductors have increased over the past years due to its electronic and mechanical properties and have received considerable interest from experimentalist and theorists. To understand, the structural phase transition of a material and the influence of band structure parameters on the electronic properties of semi-conductors, the study under induced pressure is found to be an effective tool. Also the study of elastic constants at different pressure plays an important role in mechanical stability, strength, phase transition and a material response to various conditions. One of the interesting phenomena that may occur under applied pressure is a sudden change in the arrangement of the atoms i.e. structural phase transition. Indium Arsenide (InAs) is an important group III-V compound semiconductor having high electron mobility and narrow energy band gap. It is widely used in construction of infrared detectors and diode lasers [1]. It crystallizes in cubic zinc-blende (ZB) structure under ambient conditions. At high pressure it is found to undergo structural phase transition to rock-salt (RS) structure. The pressure-induced phase transition to metallic state was first reported by Minomura and Drickamer at 8.46 GPa pressure from high pressure resistivity measurements [2]. Pitt and Vyas reported the phase transition from the Zinc-blende (ZB) to Rock-salt (RS) through resistivity measurements [3]. Although there have been extensive studies on structural, mechanical and electronic properties of InAs, the experimental and theoretical study of these properties under high pressure is still very scarce. The main aim of this work is to present a detailed study of the structural changes of InAs in ZB to RS phase under induced pressure. The paper is organised as follows. The theoretical and computational method is described in section 2. In section 3, the results and discussion of our study is given and our conclusions are summarized in section 4.

2. Theoretical and Computational Method:

All theoretical calculations of InAs is performed based on the WIEN2K code [4] using the full potential linearized augmented plane wave (FP-LAPW) [5] method with modified Becke-Johnson (mBJ) potential [6] under the framework of Density Functional Theory (DFT) [7,8,9]. The generalized gradient approximation (GGA) of Perdew-Burke-Ernzerhof scheme is used for treating the exchange correlation interaction effects [10]. In this method, the lattice is divided into non-overlapping spheres (called atomic or muffin tin sphere) surrounding each atomic sites and an interstitial region. Inside the muffin tin (MT) region, the potential is a product of radial function and spherical harmonics and expanded up to order l = 10. For the interstitial regions that are outside the muffin tin spheres, the potentials are expanded in plane waves. The number of k-points used

for the integration part is 8000 k-points which is reduced to 256 irreducible k-points inside the Brillion zone including five high symmetry points W, L, Γ, X and K. Convergence of the basis set is obtained at $R_{MT}K_{max}$ = 9.0 where K_{max} gives us the plane wave cut-off.

3. Results and Discussion:

The energy as a function of the primitive cell volume for ZB and RS phase is shown in figure 1. From the figure, one can clearly see that the InAs-ZB structure is more stable than the RS structure. The equilibrium lattice parameters of the InAs crystal in zinc-blende and rock-salt structure is obtained by fitting the resultant curve to the Birch-Murnaghan equation [11]. The calculated structural parameters are compared with other results [12,13,14,15,16] and are given in table 1. Our results are found to be in good agreement with other results and hence are used for further calculations.

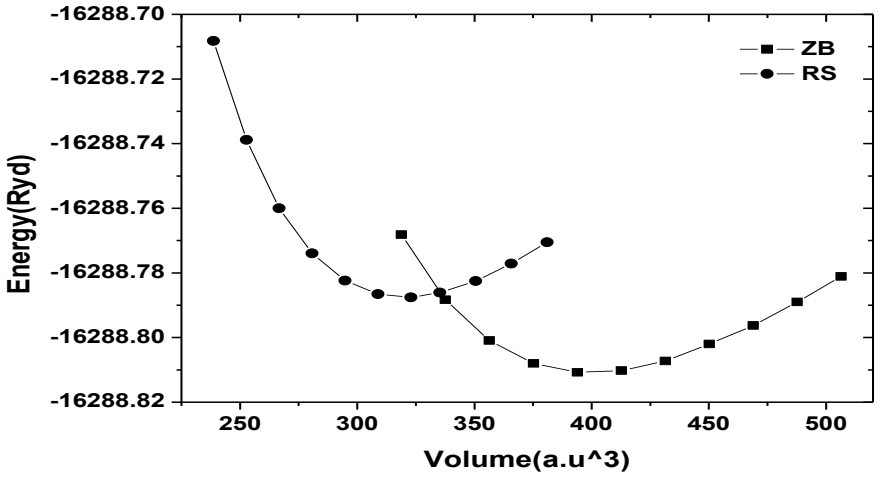

Figure 1. Total energy as a function of primitive cell volume of InAs in ZB and RS phases.

Table 1. Lattice constants, bulk modulus and pressure derivative of bulk modulus of InAs-ZB and InAs-RS at zero pressure.

Structure		a(A^0)	B(GPa)	B/
ZB	Present work	6.188	49.48	4.78
	References	6.058[a], 6.10[b], 6.08[c]	55.51[c], 59.2±5[d]	6.8±2[d]
RS	Present work	5.748	62.98,	4.84
	References	5.65[c], 5.5005[d], 5.514[e]	40.6±14[d]	7.3±1[d]

Ref.12[a], Ref.13[b], , Ref.14[c] , Ref.15[d] , Ref.16[e]

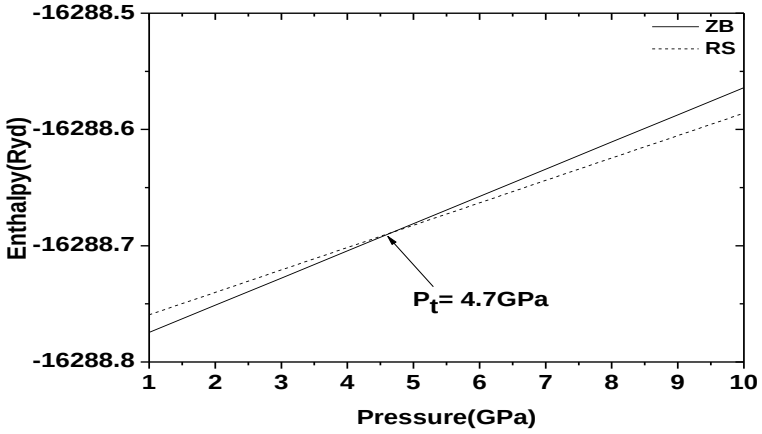

Figure 2. Enthalpy variation of InAs in ZB and RS structures as a function of pressure.

The pressure induced phase transition of InAs-ZB to InAs-RS phase is investigated from a series of ground state optimisation at various pressures. After optimisation, the enthalpy, H = E + PV is used to obtain the pressure induced phase transition. Figure 2 shows the enthalpy as a function of pressure of both the InAs-ZB and InAs-RS structure. It is clearly seen that the phase transition of InAs-ZB structure to InAs-RS structure is found to occur at 4.7 GPa pressure.

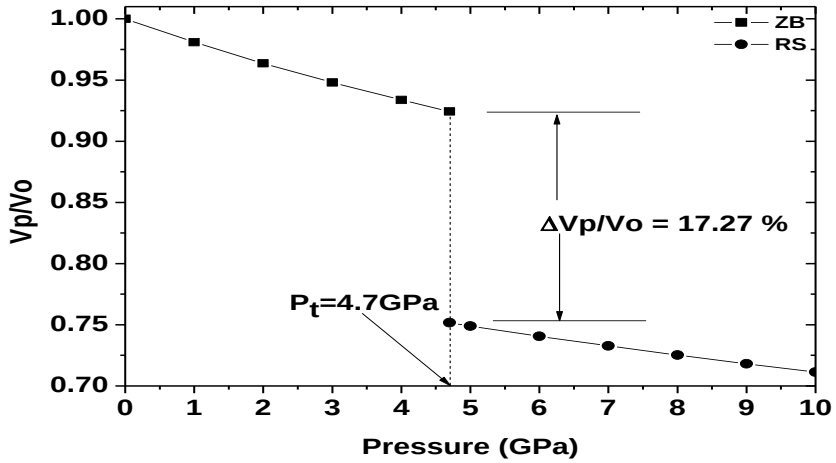

Figure 3. Phase transition between ZB and RS structure of InAs at 4.7 GPa pressure.

Table 2. Phase transition pressure and volume collapse comparisons with other experimental and theoretical data:

	Present calculation	Expt. results	Theoretical results
Transition pressure (P_t) (GPa)	4.7	7[a] , 6.9±0.2[c]	3.9[d], 4.0[e], 6.0[f],
Volume collapse (%)	17.2	17.0±0.2[a], 18.8[b]	17.0[g], 24.0[h]

Ref.15[a], Ref.16[b], Ref.17[c], Ref.18[d], Ref.19[e], Ref.20[g], Ref.21[h]

The normalised volume (V_p/V_o) of the crystal in ZB phase and RS phase is also found to be 0.924 and 0.752 respectively during the phase transition with a volume collapse of 17.2% indicating that ZB phase is more compressible than the RS phase as given in figure 3. Our calculated results of phase transition and volume collapse are compared with other experimental and theoretical results [17,18,19,20,21] and are shown in table 2. We find that our results are closer to the experimental data than other theoretical results.

4. Conclusions:

The calculated optimised structural parameter of Indium Arsenide in both zinc-blende and rock salt structure phase are compared with other theoretical end experimental results and are found to be in good agreement. The phase transition of InAs-ZB structure to InAs-RS structure under induced pressure is found to occur at 4.7 GPa pressure. The normalized volume of the crystal in ZB phase and RS phase is also found to be 0.924 and 0.752 respectively during the phase transition with a volume collapse of 17.2% indicating that ZB phase is more compressible than the RS phase.

References:

[1] D. R. Lide, Handbook of Chemistry and Physics (87 ed.), Boca Raton, CRC Press, pp 4–61, 1998.
[2] S. Minomura, H. G. Drickamer, J. Phys. Chem Solids, 23, 451, 1962.
[3] G. D. Pitt and M. K. R. Vyas, J. Phys. C: Solid State Phys., 6, 274, 1973.
[4] P. Blaha, K. Schwarz, G. K. H. Madsen, D. Kvasnicka and J. Luitz, WIEN2k An Augmented Plane Wave + Local Orbitals Program for Calculating Crystal Properties (Austria : Karlheinz Schwarz, Techn. Universitat Wien), ISBN3- 9501031-1-2, 2001.
[5] E. Wimmer, H. Krakauer, M. Weinert and A. J. Freeman, Phys. Rev. B, 24, 864, 1981.
[6] A. D. Becke and E. R. Johnson, J. Chem. Phys., 124, 221101, 2006.
[7] P. Hohenberg and W. Kohn, Phys. Rev., 136 (3B), 864, 1964.
[8] W. Kohn and L. J. Sham, Phys. Rev., 140 (4A), 1133, 1965.
[9] S. Cottenier, Density Functional Theory and the family of (L)APW-methods: a step-by-step Introduction (Belgium: Insti-tuut voor Kern-en Stralingsfysica, K.U.Leuven), ISBN 90-807215-1-4, 2002.
[10] J. P. Perdew, S. Burke and M. Ernzerhof, Phys. Rev. Let., 77**,** 3865, 1996.
[11] F. Birch, Phys. Rev., 71, 809, 1947.
[12] G. Giesecke, H. Pfister, Acta Crystallogr , 11, 369, 1958.
[13] N. E. Christensen, S. Satpathy, Z. Pawlowska, Phys. Rev. B, 36, 1032. 1987.
[14] L. Pedesseau, J. Even, A. Bondi, W. Guo, S. Richard, H. Folliot, C. Labbe, C. Cornet, O. Dehaese, A. Le Corre, O. Durand and S. Loualiche, J. Phys. D: Appl. Phys., 41, 165505, 2008.
[15] Y. K. Vohra, S. T. Weir and A. L. Ruoff, Phys. Rev. B, 31, 7344, 1987.
[16] J. C. Jamieson, Science, 139, 845, 1963.
[17] S. K. Tewksbury, "Semiconductor Materials", Microelectronic System Research Center, Department Of Electrical And Computer Engineering, West Virginia University, Morgantown, WV 26506 (304), pp 293-6371, 1995.
[18] M. I. McMahon and R. J. Nelmes, Phys. Status Solidi (b), 198, 389, 1996.
[19] A. Mujica, R. J. Needs and A. Muñoz, Phys. Status Solidi (b), 198, 461, 1996.
[20] S. B. Zhang and M. L. Cohen, Phys. Rev. B, 35, 7604, 1987.
[21] R. K. Singh and Sadhna Singh, Phys. Rev. B, 39, 671. 1989.

International Journal of Innovation and Applied Studies
ISSN 2028-9324 Vol. 8 No. 1 Sep. 2014, pp. 382-393
© 2014 Innovative Space of Scientific Research Journals
http://www.ijias.issr-journals.org/

Density functional theory study on pressure induced structural transformation, elastic properties and electronic structure of gallium arsenide (GaAs)

Kh. Kabita[1], Jameson Maibam[1], B. Indrajit Sharma[1], R. K. Brojen Singh[2], and R. K. Thapa[3]

[1]Department of Physics,
Assam University, Silchar-788011,
Assam, India

[2]School of Computational and Integrative Sciences,
JNU, New Delhi 110067, India

[3]Department of Physics,
Mizoram University,
Tanhril, Aizawl-796 009, India

Copyright © 2014 ISSR Journals. This is an open access article distributed under the ***Creative Commons Attribution License***, which permits unrestricted use, distribution, and reproduction in any medium, provided the original work is properly cited.

ABSTRACT: The structural phase transformation under induced pressure of the GaAs- zinc blende (ZB) phase to rock salt (RS) phase, elastic properties and electronic structure of the stable (ZB) phase are studied under the framework of the density functional theory (DFT). When pressure is increased up to 10.7 GPa, transition from the GaAs-ZB to GaAs-RS structure occurs and the dependence of volume decrease of ZB to RS structure at the transition pressure is 14.11%. The elastic parameters such as elastic constants C_{11}, C_{12}, C_{33}, Zener anisotropic factor (A), Kleinmann parameter (ζ), Poisson's ratio (υ), Youngs modulus (Y) and energy band gap of GaAs-ZB structure shows a systematic variation with increase in pressure upto transition pressure. The results are found to be in consistent with other experimental and theoretical results.

KEYWORDS: Density Functional Theory (DFT); Energy band structure; Elastic properties; Phase transition.

1 INTRODUCTION

Gallium arsenide (GaAs) is a group III-V binary compound semiconductor utilized in the electronics and telecommunications industries and in the military science [1, 2]. Gallium arsenide chips are found in products such as night vision telescopes, discrete microwave circuitry, and room temperature lasers. It is superior semiconductors to silicon for optoelectronic devices due to its ability to handle signals at higher frequencies, at the same time generate lower noise [3, 4]. It is the most technologically important compound semiconductor material which has been intensively investigated in recent years. The study of electronic and structural properties helps us to understand, characterize and predict the mechanical properties of materials in the surroundings under extreme conditions. This study plays an important role in physical condensed matter [5]. With technological development, study of structural properties, phase diagram and high pressure phases of GaAs has aroused considerable scientific interest in the past decades. Froyen and Cohen [6] first reported the structural phase of GaAs in 1983. The structural transformation in GaAs was also investigated by Besson *et al* [7] and Weir *et al* [8] using the single-crystal x-ray absorption spectroscopy and elastic neutron scattering. Studies on electronic structures, high-pressure properties have been reported by various groups [9-12]. In literature, works on the phase transformation, band structure, density of states (DOS) and elastic properties with variation of pressure is still rare. To the best of our knowledge none of the papers in open literature has considered the variation of energy band gap and elastic properties from the induced pressure perspective and investigated the behavior of the same with the available experimental data. The present paper is mainly focused on study of the phase transition from the zinc-blende to rocksalt structure, band structure

Corresponding Author: B. Indrajit Sharma

and elastic properties of GaAs with increasing pressure using WEIN2K code based on DFT. This paper is organised as follows: Section 2 describes the theoretical and computational method used in this study. The results are discussed in section 3 and conclusions are given in section 4.

2 THEORETICAL AND COMPUTATIONAL METHOD

The calculation of GaAs has been performed with modified Becke-Johnson (mBJ) [13] exchange potential using full-potential linearised augmented plane wave (FP-LAPW) method [14] within the framework of density functional theory (DFT) [15, 16, 17] with Perdew-Bruke-Ernzerhof-Generalized Gradient Approximation (PBE-GGA) for the exchange correlation potential [18] as implemented in the WIEN2K code [19]. Within DFT formalism, the total energy can be expressed as a functional of density of electron system, ρ and can be written by the following functional,

$$E[\rho] = T_o[\rho] + V_H[\rho] + V_{xc}[\rho] + V_{ext}[\rho] \quad (1)$$

where, $T_o[\rho]$ is the kinetic energy of a non-interacting electron system, $V_H[\rho]$ and $V_{XC}[\rho]$ are the Hartree and exchange-correlation contributions to the energy and V_{ext} [ρ] is the energy due to the external potential of the system. Thus the corresponding Hamiltonian called the Kohn-Sham Hamiltonian is

$$\begin{aligned}\hat{H}_{KS} &= \hat{T}_o + \hat{V}_H + \hat{V}_{XC} + \hat{V}_{ext} \\ &= -\frac{\hbar^2}{2m_e}\vec{\nabla}^2{}_i + \frac{e^2}{4\pi\varepsilon_o}\int\frac{\rho(\vec{r}^{\,/})}{|\vec{r}-\vec{r}^{\,/}|}d\vec{r}^{\,/} + V_{XC} + V_{ext}\end{aligned} \quad (2)$$

The exact density of N electron system can be expressed in ground state by:

$$\rho(\vec{r}) = \sum_{i=1}^{N} \phi_i(\vec{r}) * \phi_i(\vec{r})$$

where the single particle wave functions $\phi_i(r)$ are the N lowest energy solutions of the Kohn Sham equation: $\hat{H}_{ks}\phi_i = \phi_i\phi_i$ of the N electron system.

These equations can be solved self consistently in an iterative process. In this method, the lattice is divided into non-overlapping spheres (called atomic or muffin tin sphere) surrounding each atomic sites and an interstitial region [20]. Inside the muffin tin (MT) region, the potential is a product of radial function and spherical harmonics and expanded up to order l = 10. For the interstitial regions that are outside the muffin tin spheres, the potentials are expanded in plane waves. 8000 k-points are used for the integration procedure as we find that above 8000 k-points the energy remains same and this 8000 k-points reduces to 256 irreducible k-points inside the Brillion zone including five high symmetry points W, L, Γ, X and K. Convergence is obtained at $R_{MT}K_{max}$ = 9.0 where R_{MT} is the atomic sphere radii and K_{max} gives the plane wave cut-off. The calculations are performed with the equilibrium lattice constants which are determined from the plot of the total energy against the unit cell volume by fitting to the Birch-Murnaghan equation of states [21].

3 RESULTS AND DISCUSSION

3.1 STRUCTURAL PROPERTIES

The total energy curve as a function of unit cell volume for GaAs in zinc-blende and rocksalt structure is shown in figure 1. It is clearly seen that ZB structure of GaAs is more stable than the RS structure which is in good agreement with previous results [22, 23, 24]. The obtained zero pressure equilibrium lattice constant (a_0) for GaAs-ZB structure is found as 5.74 A^o. This lattice constant corresponding to the optimized structure is slightly larger than experimental values as given in table 1. It has an error of about 1.8% which is quite acceptable under the 2% error and is used for further calculation. Thus the agreement between our result and other available theoretical and experimental data [25, 26, 27, 28, 29, 30] is well good indicating that our calculation can proceed for further study.

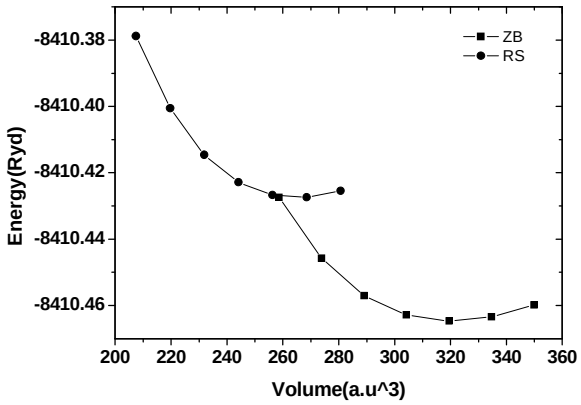

Fig.1. Energy versus volume for ZB and RS structure of GaAs.

Table 1. Lattice Constants, Bulk Modulus And Pressure Derivative Of Bulk Modulus Of ZB And RS Structure Of Gaas At Zero Pressure.

Structure		A_0 [A^0]	B_0 [Gpa]	B_0'
ZB	Present Work	5.74	61.08	4.86
	References	5.65[a], 5.64[b],5.59[c]	60.4[d],74.7[a]	4.8[e],4.71[c],4.56[f]
RS	Present Work	5.39	71.10	4.90
	References	5.32[g],5.31[h],5.28[i]	73.54[c],69.95[i]	4.05[c],4.77[g],4.87[i]

Ref[a] [22], Ref[25][B], Ref[26][C], Ref[27][D], Ref[28][E], Ref[29][F], Ref[23][G], Ref[24][H], Ref[30][I],

3.2 PHASE TRANSITION AND ELASTIC PROPERTIES

The zero temperature pressure induced phase transition between the GaAs-ZB structure and GaAs-RS structure has been determined using the usual condition of equal enthalpies i.e. H = E + PV. The enthalpy as a function of energy is shown in figure 2. The phase transition from ZB to RS structure is found to occur at a pressure of 10.7 GPa which is close to the experimental values [31, 32] and other theoretical results as shown in table 2.

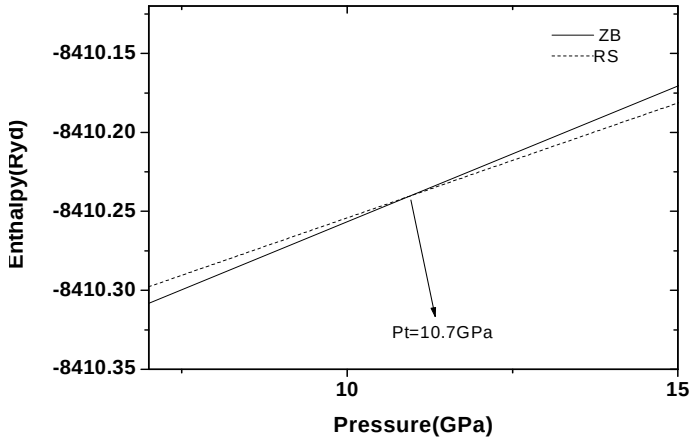

Fig.2. Enthalpy as a function of pressure.

Table 2. Transition pressure from ZB to RS in GaAs.

ZB-RS	Pressure [GPa]
Present work	10.7
Ref [7]	12±1.5
Ref [30]	10.5
Ref [31]	11.8
Ref [32]	12.3

To understand the volume collapse at the transition, the unit cell volume at different pressures (V_P) are normalised by dividing with volume at zero pressure (V_O). The normalised volume (Vp/Vo) of ZB and RS structure of GaAs at different pressure is shown in figure 3. With increase in pressure the relative volume is found to decrease for the two structures. During phase transition, the normalised volume of ZB phase is found to be occurring at 0.876 and for RS phase at 0.734. It is clearly seen that volume collapse occurs at 14.2% indicating that the ZB phase is more compressible than the RS phase.

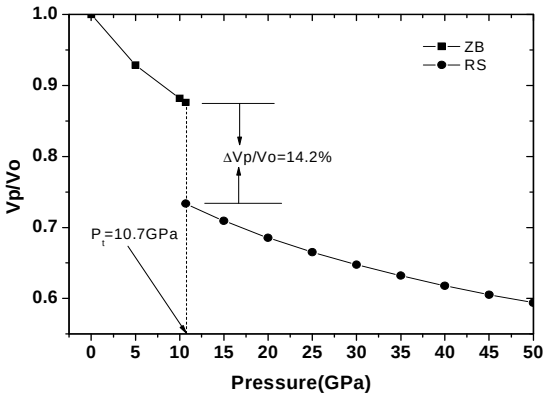

Fig. 3. Phase transition between ZB and RS structure of GaAs at 10.7 GPa pressure.

Since the transition pressure occurs at 10.7 GPa, the three independent observable elastic constants are obtained from 0 to 10 GPa pressure for ZB phase and 12 GPa to 25 GPa pressure for RS phase and is shown in figure 4. Figure 4 shows the linear increase in C_{11}, C_{12}, C_{44} value with increase in pressure for ZB phase. Also these values satisfy the mechanical stability conditions: $(C_{11}+2C_{12}) > 0$; $C_{11}C_{12} > 0$; $C_{44} > 0$; $C_{11} > 0$. In case of RS phase after transition pressure, even though there is a little variation in C_{44} value with linear increase in C_{11}, C_{12} values, and the stability conditions are found to be satisfied.

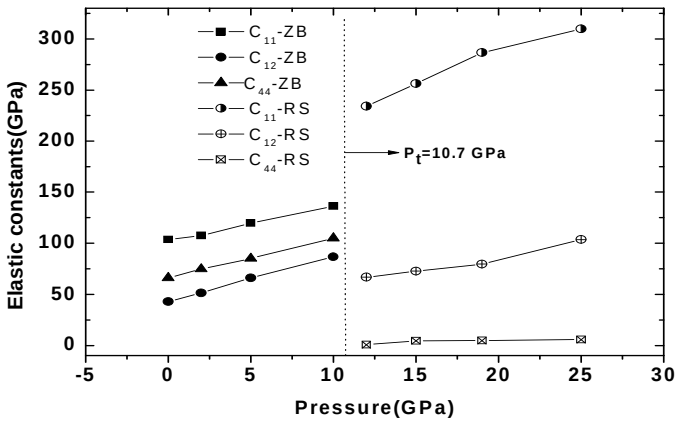

Fig. 4. Elastic constants (C_{11}, C_{12}, C_{44}) as a function of pressure for GaAs-ZB and GaAs-RS structure.

In this light of observations, we are confined our calculation for the elastic parameters on ZB structure up to a higher pressure of 10 GPa. The Zener anisotropic factor (A), Poisson's ratio (υ), Kleinmann parameter (ζ), Youngs modulus (Y), and Debye's temperature (θ_D) are important elastic parameters which determine the mechanical and thermal behaviour of a material.

The Zener anisotropic factor (A), Poisson's ratio (υ), Kleinmann parameter (ζ), Youngs modulus (Y) are calculated using the relation given by Mayer *et. al* [33]. The Zener anisotropy factor gives us an insight on the elastic isotropy of the material. For an elastically isotropic material, A = 1. If A > 1, it is stiffest along <111> plane body diagonals and when A < 1, it is stiffest along <100> cube axes. It is expressed as:

$$A = \frac{2C_{44}}{C_{11} - C_{12}} \tag{3}$$

Kleinmann parameter describes the relative position of the cation and anion sub-lattices and is given by the relation:

$$\zeta = \frac{C_{11} + 8C_{12}}{7C_{11} + 2C_{12}} \tag{4}$$

The Poisson's ratio gives us the stability of crystal against shear and provides a sharp criterion for differentiating the brittleness and ductility in solids and it is calculated using the relation,

$$\upsilon = \frac{1}{2}\left(\frac{B - (2/3)G}{B + (1/3)G}\right) \tag{5}$$

The Young's modulus is determined to measure the stiffness of the solid and is given by:

$$Y = \frac{9GB}{G + 3B} \tag{6}$$

where, $G = \frac{G_V + G_R}{2}$ is the isotropic shear modulus , G_v is the Voigt's shear modulus corresponding to the upper bound of G values, and G_R is the Reuss's shear modulus corresponding to the lower bound of G values. G_v and G_R can be expressed as

$$G_V = \frac{C_{11} - C_{12} + 3C_{44}}{5} \tag{7}$$

$$G_R = \frac{5(C_{11} - C_{12})C_{44}}{4C_{44} + 3(C_{11} - C_{12})} \tag{8}$$

Debye's temperature is an important parameter which determines the thermal characteristics of a material. Debye's temperature also gives us explicit information about lattice vibrations. It is calculated using the average sound velocity (υ_m) given by the common relation [34]

$$\theta_D = \frac{h}{k}\left[\frac{3n}{4\pi}\left(\frac{N_A\rho}{M}\right)\right]^{1/3}\upsilon_m \tag{9}$$

Where *h* is the Plank's constant, *k* is the Boltzmann constant, N_A is the Avogadro's number, *n* is the number of atoms per formula unit, *M* is the molecular mass per formula unit, *ρ* is the density and υ_m is given by [35]

$$\upsilon_m = \left[\frac{1}{3}\left(\frac{2}{\upsilon_t^3} + \frac{1}{\upsilon_l^3}\right)\right]^{-(1/3)} \tag{10}$$

where υ_t and υ_l are the transverse and longitudinal velocities respectively, which are obtained from Navier's equation [36] as

$$\upsilon_t = \sqrt{\frac{3B+4G}{3\rho}} \tag{11}$$

$$\upsilon_l = \sqrt{\frac{G}{\rho}} \tag{12}$$

The calculated elastic parameters for ZB phase with variation of pressure up to 10 GPa are shown in figure 5(a) and figure 5(b). A consistent pattern of linear increase in elastic parameters with increase in pressure can be observed from these figures.

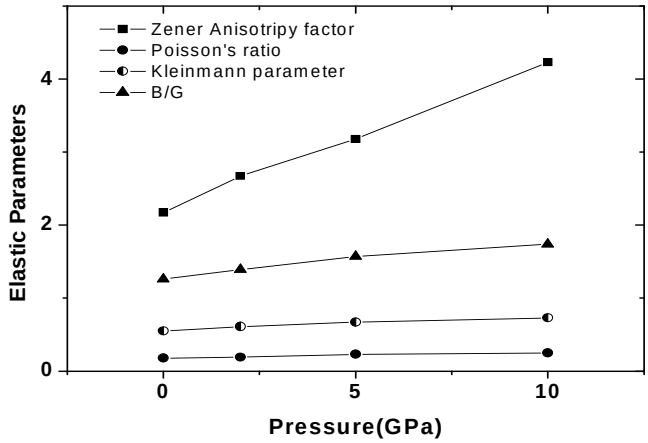

Fig. 5a. Elastic parameters (Zener anisotropic factor, Poisson's ratio, Kleinmann parameter and B/G ratio) as a function of pressure.

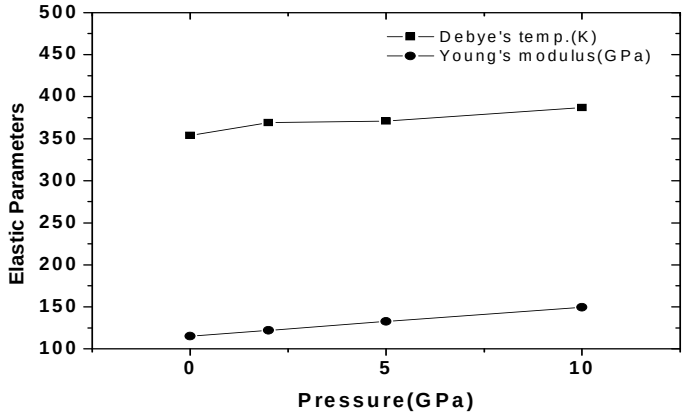

Fig. 5b. Debye's temperature and Young's modulus as a function of pressure.

The Kleimann parameter quantifies internal strain and thus indicates the relative ease of bond bending against the bond stretching. It also implies resistance against bond bending or bond angle distortion. In a system, minimizing bond bending leads to Kleinmann parameter, ζ = 0 and minimizing bond stretching leads to ζ =1. In the present study, the parameter ζ is found to be 0.55 to 0.73 with the variation of pressure, indicating the shrinkage in bond-stretching. Also the value of the Zener anisotropic factor varies from 2.17 to 4.23 with increase in pressure showing the degree of elastic anisotropy. The empirical malleability measure of a material is determined by the value of B/G [37]. A material is found to be brittle if B/G < 1.75 and ductile if B/G > 1.75. B/G value of the present studies varies from 1.26 to 1.74 with increase in pressure and hence it is found that GaAs-ZB structure is brittle and with increase in pressure it tends to become ductile. The larger the value of Young's modulus, the stiffer is the material and since the value of Y varies from 114.96 GPa to 149.456 GPa as pressure

increases, we find that GaAs-ZB pahse becomes more rigid. Poisson's ratio gives us the degree of directionality of the covalent bonds. For covalent materials, υ = 0.1, whereas for ionic materials, υ = 0.25 [38]. Our calculations show that with increase in pressure the value of υ varies from 0.18 to 0.25 showing that with increase in pressure the ionic contribution to inter atomic bonding becomes dominant. Fu *et al* [39] reported that for central force solids the lower and upper limits for υ are 0.25 and 0.5 respectively. Our values also indicates that as pressure increases, inter atomic forces tends to be more central. The value of Debye's temperature is also found to vary from 354K to 387K suggesting that with increasing pressure the Debye's temperature also increases indicating stiffer lattice and better thermal conductivity.

3.3 BAND STRUCTURE AND DENSITY OF STATES

The energy band diagram of GaAs-ZB structure and GaAs-RS structure at zero pressure and zero temperature is calculated using mBJ as it gives us more accurate results closer to the experimental values and the results are given in figure 6(a) and figure 6(b) respectively. From figure 6(a) we observed that the conduction band minimum as well as the valance band maximum is located at the middle of the Brillioun zone, Γ point. From these observations we can conclude that the band gap of GaAs-ZB structure is direct band gap with an energy band gap of 1.3eV while the experimental value is 1.4 eV. Again from figure 6(b) we find that the conduction band crosses the Fermi level and lies within the valance band making the GaAs-RS structure metallic in nature. The reason for the metallic nature in the RS structure is due to broadening of the band with increase in pressure and overlapping of the filled valance band and conduction band.

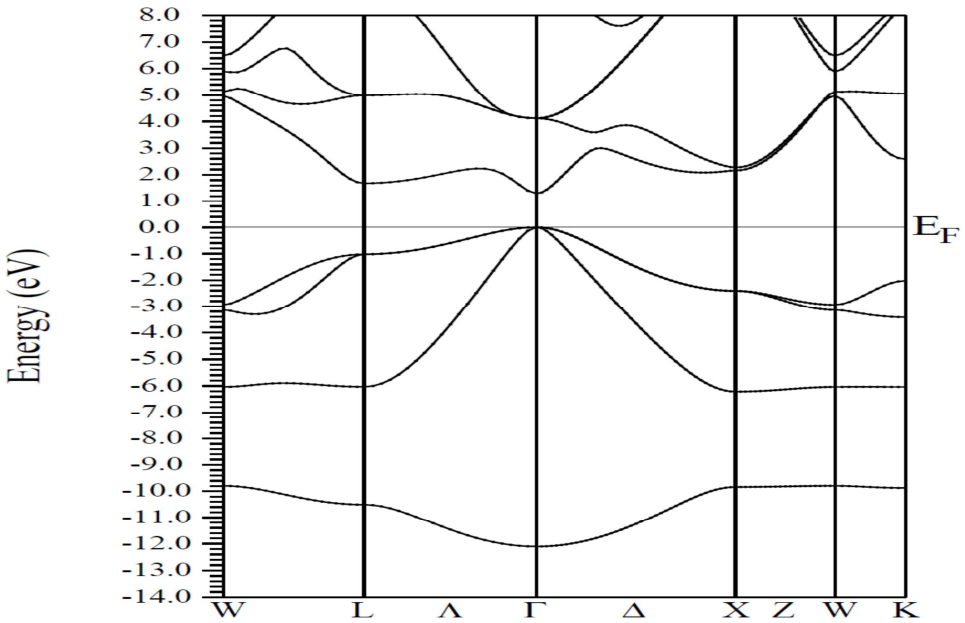

Fig. 6a. Band structure of GaAS-ZB structure.

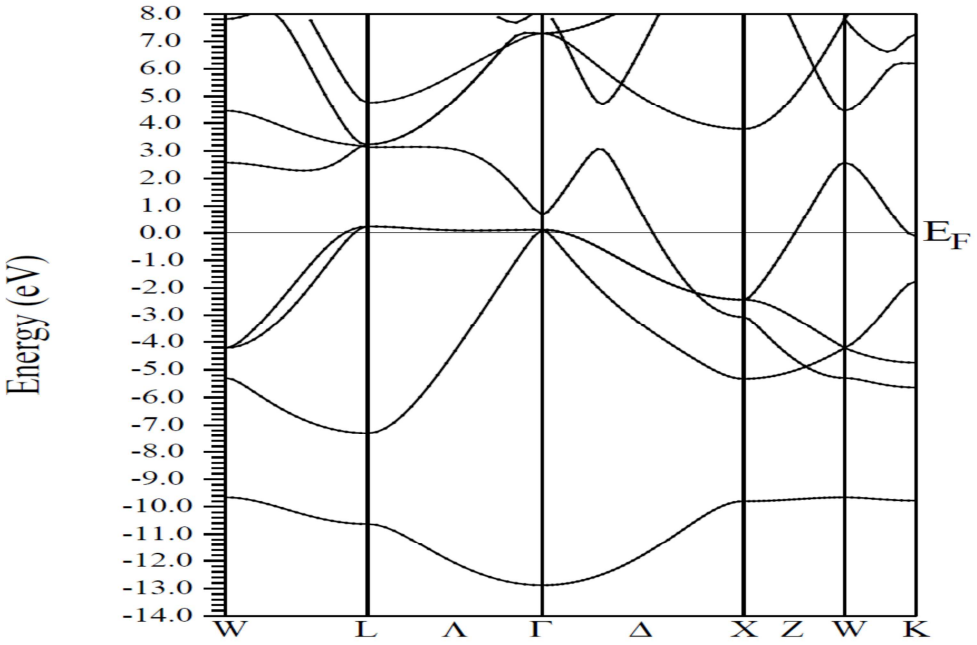

Fig. 6b. Band structure of GaAs-RS structure.

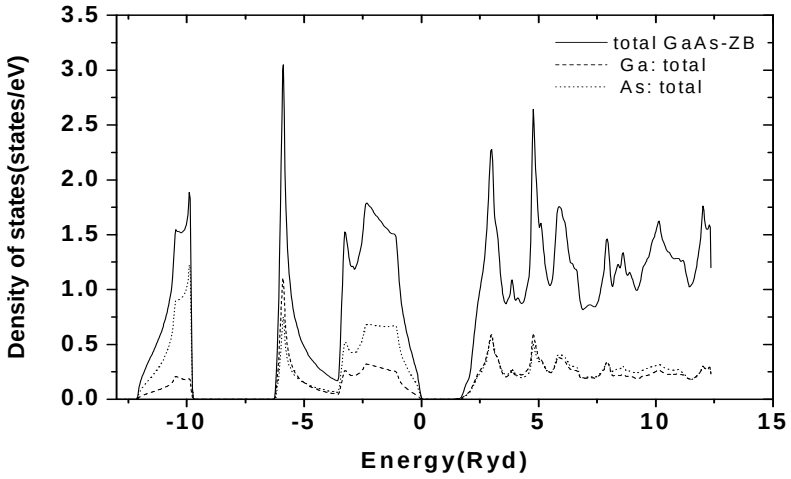

Fig. 7a. Total DOS of GaAs -ZB structure.

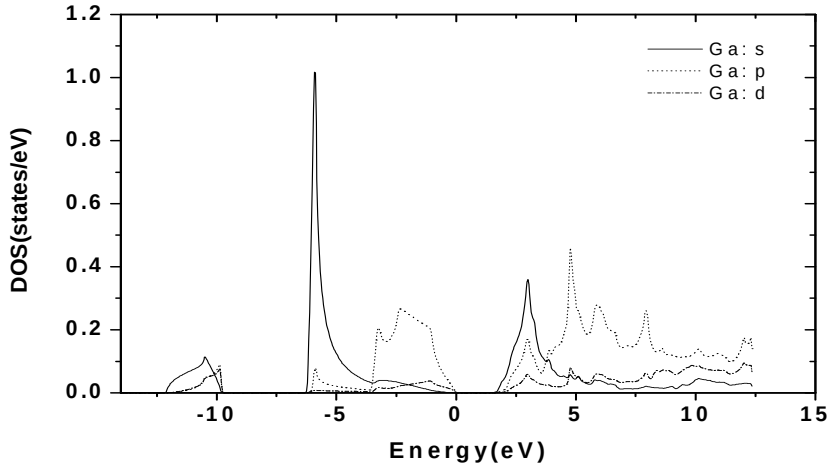

Fig. 7b. Partial DOS of Ga atom in GaAs-ZB structure.

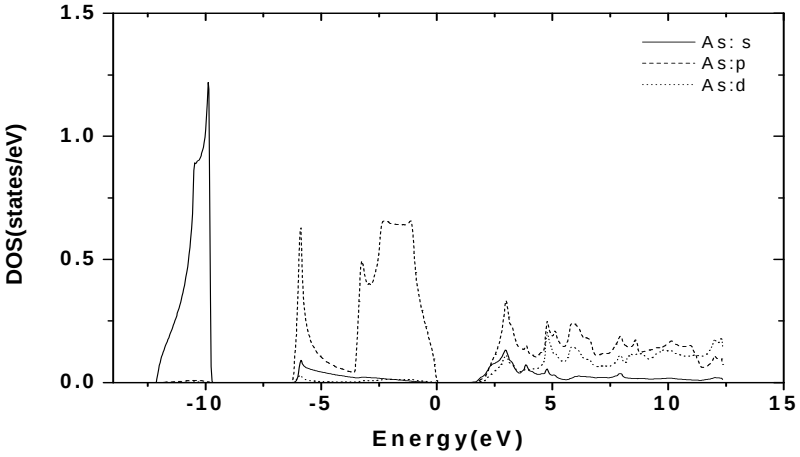

Fig. 7c . Partial density of As atom in GaAs-ZB structure.

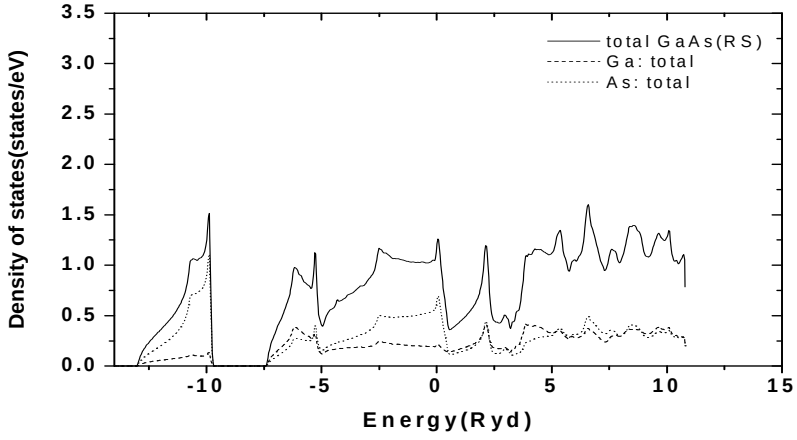

Fig. 8a. Total DOS of GaAs-RS structure.

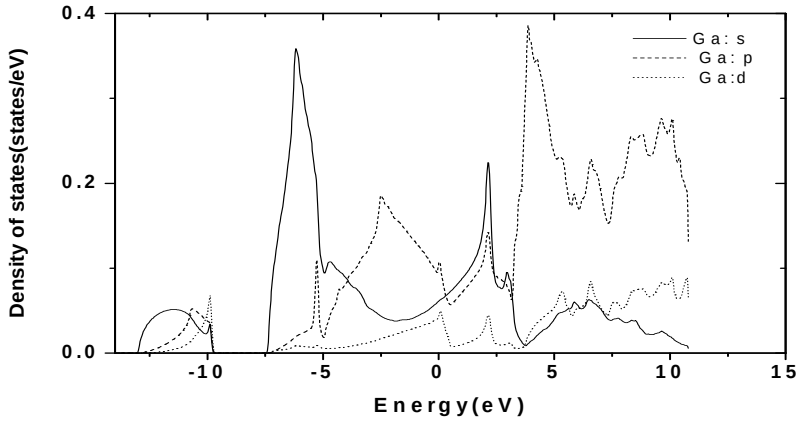

Fig. 8b. Partial DOS of Ga atom in GaAs-RS structure.

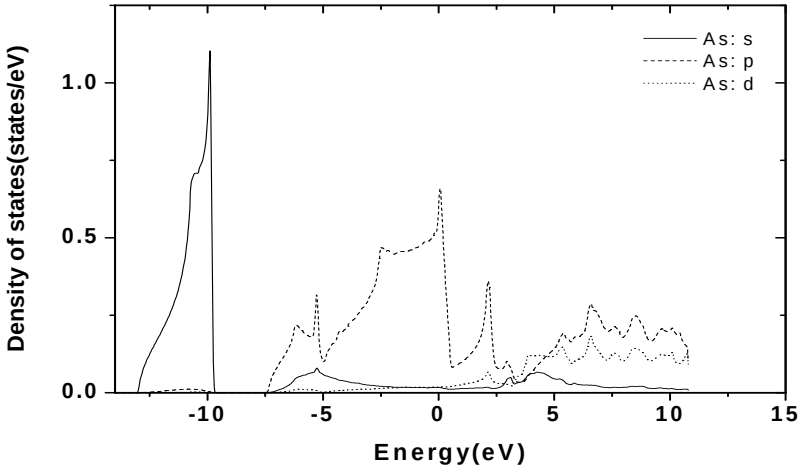

Fig. 8c. Partial DOS of As atom in GaAs-RS structure.

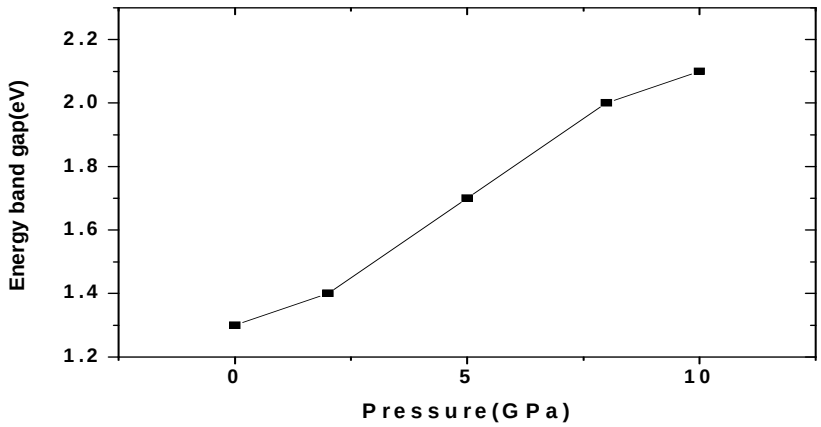

Fig. 9. Variation of energy band gap with pressure in GaAs ZB structure.

Figure 7(a,b,c) shows the total and partial DOS of GaAs in ZB phase and figure 8(a,b,c) shows the same in RS phase. From the partial DOS as shown in figure 7(b) and figure 7(c), one can observe that the lowest band appears in energy band diagram of ZB phase is mainly contributed from s-non metal (As atom) orbital and the valance band is mainly contributed by the s-metal (Ga atom) orbital and p-non metal (As atom) orbital with little contribution from the p-metal (Ga atom) orbital. The contribution of the s, p orbital of metal and non-metal in DOS in the lowest and valence band is found to decrease with increase in pressure. Similar behaviour is observed in partial DOS of GaAs-RS structure in figure 8(b) and figure 8(c) as the lowest band is mainly contributed by the s-non metal orbital while the valence band is mainly contributed by the p-non metal orbital and s- metal orbital with little contribution from the p-metal and d-metal orbital. An important observation in the energy band diagram of GaAs-RS structure is the crossing of the conduction band towards valence band and hence results in metalic nature. It is interesting to see the variation of band gap with pressure for the direct band gap in GaAs-ZB phase. These variations of the energy band gap with increase in pressure is shown in figure 9 and observe that with increase in pressure the band gap also increases. The resaon is that the energy eigenvalues corresponding to s, p, and d orbital's lies in the higher region with increasing pressure.

4 CONCLUSION

In this paper we present a detailed study of pressure induced structural transformation, elastic properties and electronic structure of GaAs. The phase transition from ZB to RS structure is obtained at 10.7 GPa and ZB structure is found to be more stable. During the phase transition, the relative volume of ZB structure occurs at 0.876 and the RS structure at 0.734 and volume collapses at 14.2% indicating that ZB structure of GaAs is more compressible as compared to RS structure. The calculated equilibrium lattice parameter, bulk modulus, pressure derivative of the bulk modulus and elastic constants are found to be in good agreement with the other experimental and theoretical studies. The elastic constants satisfy the mechanical stability condition from 0 to 10 GPa pressure for ZB structure and 12 GPa to 25 Gpa pressure for RS structure. The elastic parameters for the stable GaAs-ZB phase such as Zener anisotropic factor, Kleinmann parameter, Poisson's ratio and Youngs modulus show a systematic variation with increase in pressure up to 10 GPa pressure before transition. The GaAs-ZB structure is found to be direct band gap semiconductor of 1.3 eV and the band gap increases with increase in pressure.

REFERENCES

[1] A. L. Robinson, "GaAs readied for high speed microcircuit", *Science*, vol. 219, pp. 275-277, 1983.

[2] R. J. Harrison, "Gallium arsenide: state of the art reviews", *Occup. Med*., vol. 1, pp. 49-58, 1986.

[3] F. W. Smith, H. Q. Le, V. Diadiuk, M. A. Hollis, A. R. Calawa, S. Gupta, M. Frankel, D. R. Dykaar, G. A. Mourou and T. Y. Hsiang, "Picosecond GaAs based photoconductive optoelectronic detectors", *Appl. Phys. Lett*., vol. 54, no. 10, pp. 890-892, 1989.

[4] D. K. W. Lam and R. Macdonald, "GaAs optoelectronic mixer operation at 4.5 GHz", *IEEE Trans. Electron Devices*", vol. 31, pp. 1766-1768, 1984.

[5] E. Wachowicz and A. Kiejna, "Bulk and surface properties of hexagonal-close-packed Be and Mg", *J. Phys. Condens. Matter*., vol. 13, pp. 10767-10776, 2001.

[6] S. Froyen and M. L. Cohen, "Structural properties of III-V zinc-blende semiconductors under pressure", *Phys. Rev. B*, vol. 28, pp. 3258-3265, 1983.

[7] J. M. Besson, J. P. Itie, A. Polian, G. Weil, J. L. Mansot and J. Gonzales, "High pressure phase transition and phase diagram of gallium arsenide", *Phy. Rev. B*, vol. 44, pp. 4214-4234, 1991.

[8] S. T. Weir, Y. K. Vohra, C. A. Vanderborgh and L. A. Rouff, " Structural phase transitions in GaAs to 108 GPa", *Phys. Rev. B*, vol. 39, pp. 1280-1285, 1989.

[9] J. R. Chelikowsky, "High-pressure phase transitions in diamond and zinc-blende semiconductors", *Phys. Rev. B*, vol. 35, pp. 1174-1180, 1987.

[10] Kh. Kabita, M. Jameson, B. Indrajit Sharma, R. K. Thapa Singh, R. K. Brojen, "First principle calculation of pressure induced phase transition and band structure of Gallium phosphide", *Iraqi J Appl. Phys*., vol. 9, pp. 17-20, 2014.

[11] M. Durandurdu and D. A. Darbold, "Ab initio simulation of high pressure phases of GaAs", *Phys. Rev. B*, vol. 66, pp. 045209(1) – 045209(5), 2002.

[12] A. Mujica and R. J. Needs, "The Cmcm structure as a stable phase of binary compounds : application to GaAs-II", *J. Phys. Condens. Matter*., vol. 8, pp. L237 –L243, 1996.

[13] A. D. Becke and E. R. Johnson, "A simple effective potential for exchange", *J. Chem. Phys*., vol. 124, pp. 221101-221104, 2006.
[14] E. Wimmer, H. Krakauer, M. Weinert and A. J. Freeman, "Full-potential self-consistent linearized-augmented-plane-wave method for calculating the electronic structure of molecules and surfaces: O_2 molecule", *Phys.Rev. B*, vol. 24, pp. 864 -875, 1981.
[15] P. Hohenberg and W. Kohn, "Inhomogeneous electron gas", *Phy. Rev. B*, vol. 136, no. 3, pp. B864-B871, 1964.
[16] W. Kohn and L. J. Sham, "Self-Consistent Equations Including Exchange and Correlation Effects", *Phys. Rev*., vol. 140, no. 4A, pp. 1133-1138, 1965.
[17] S. Cottenier, *Density Functional Theory and the family of (L) APW-methods: a step-by-step introduction*, Belgium, ISBN 90-807215-1-4, 2002.
[18] J. P. Perdew, K. Burke and M. Ernzerhof, "Generalized Gradient Approximation Made simple", *Phys. Rev. Lett*., vol. 77, pp. 3865-3868, 1996.
[19] P. Blaha, K. Schwarz, G. K. H. Madsen, D. Kvasnicka and J. Luitz, *Wien2k. Techn. Universitat*, Wien, Austria, ISBN 3-9501031-1-2, 2001.
[20] O. K. Andersen, "Linear methods in band theory", *Phys. Rev. B*, vol. 12, pp. 3060-3083, 1975.
[21] F. Birch, "Finite Elastic Strain of Cubic Crystals", *Phys. Rev*., vol. 71, pp. 809-824, 1947.
[22] O. Madelung, M. Schulz, H. Weiss (Eds.), *Physics of II–VI and I–VII Compounds*, Landolt-Börnstein, Vol. 17b, Springer, Berlin, 1982.
[23] K. Albe, L. Nordlund, J. Nord and A. Korunen, "Modelling of compound semiconductors: Analytical bond-order potential for Ga, As and GaAs", *Phys. Rev. B*, vol. 66, pp. 035205(1)-035205(14), 2002.
[24] L. Y. Lu, X. R. Chen, B. R. Yu and Q. Q. Gou, "First-principles calculations for transition phase and thermodynamic properties of GaAs", *Chin. Phys*., vol. 15, no. 4, pp. 802-806, 2006.
[25] Cui Hong-Ling, Chen Xiang-Rong, J. I. Guang- Fu, "Structures and Phase Transition of GaAs under pressure", *Chin. Phys. Lett*., vol. 25, no. 6, pp. 2169-2172, 2008.
[26] A. Mujica, R. J. Needs and A. Munoz, "First-principles pseudopotential study of the phase stability of the III-V semiconductors GaAs and A1As" , *Phys. Rev. B*, vol. 52, no. 12, pp. 8881-8892, 1995.
[27] S. Lee, J. Kang and M. Kang, "Structural properties of semiconductors in the generalized gradient approximation", *Journal of the Korean Physical Society*, vol. 31, no. 5, pp. 811-814, 1997.
[28] R. Smith, "A semi-empirical many-body interatomic potential for modelling dynamical processes in gallium arsenide", *Nuclear Inst. and Methods in Physics Research B,* vol. 67, no. 1-4, pp. 335-339, 1992.
[29] D. Dunslan, *Properties of GaAs*, edited by M. R. Brozel and. G. E. Stillmann, Inspec, London, 1996.
[30] D. C. Gupta and Subhra Kulshrestha, "Pressure induced phase transitions and electronic structure of GaAs", *J. Phys. Condens. Matter*, vol. 20, pp. 255204(1)- 225204(7), 2008.
[31] A. Gracia and M. L. Cohen, "Effect of Ga 3*d* states on the structural properties of GaAs and GaP", *Phys. Rev. B*, vol. 47, pp. 6751-6754, 1993.
[32] J. Cai, N. Chen and H. Wang, "Atomistic study of the pressure-induced phase-transition mechanism in GaAs by Möbius inversion potentials", *J. Phys. Chem. Solids*, vol. 68, no. 3, pp. 445-457, 2007.
[33] B. Mayer, H. Anton, E. Bott, M. Methfessel, J. Sticht, J. Harris, P. C. Schmidt, "Ab-initio calculation of the elastic constants and thermal expansion coefficients of Laves phases", *Intermetallics*, vol. 11, no. 1, pp. 23-32, 2003.
[34] L. Johnston, G. Keeler, R. Rollins and S. Spicklemire, *Solid State Physics Simulations, The Consortium for Upper-Level Physics Software*, New York, John Wiley, 1996.
[35] O. L. Anderson, "A simplified method for calculating the Debye temperature from elastic constants", *J. Phys. Chem. Solids*, vol. 24, pp. 909-917, 1963.
[36] E. Schreiber, O. L. Anderson and N. Soga, *Elastic constants and their measurements*, New York, McGraw-Hill, 1973.
[37] S. F. Pugh, "Relations between the elastic moduli and the plastic properties of polycrystalline pure metals", *Philosophical Magazine*, vol. 45, pp. 823-843, 1954.
[38] V. V. Bannikov, I. R. Shein and A. L. Ivanovskii, "Electronic structure, chemical bonding and elastic properties of the first thorium containing nitride perovskite $TaThN_3$", *Phys Status Solidi Rapid Res. Lett*., vol. 3, pp. 89-91, 2007.
[39] H. Fu, D. Li, F. Peng , T. Gao, X. Cheng, "Ab initio calculations of elastic constants and thermodynamic properties of NiAl under high pressures", *Computational Material Science*, vol. 44, pp. 774-778, 2008.

Copyright © 2014 by American Scientific Publishers
All rights reserved.
Printed in the United States of America

AMERICAN SCIENTIFIC PUBLISHERS

Advanced Science, Engineering and Medicine
Vol. 6, pp. 354-358, 2014
(www.aspbs.com/asem)

ARTICLE

Density Functional Theory Study of Electronic Structure, Elastic Properties and Phase Transition of Gallium Phosphide (GaP)

Kh. Kabita[1], Jameson Maibam[1], B. Indrajit Sharma[1,*], R. K. Thapa[2], and R. K. Brojen Singh[3]

[1]*Department of Physics, Assam University, Silchar 788011, Assam, India*
[2]*Department of Physics, Mizoram University, Aizawl 796001, Mizoram, India*
[3]*School of Computational and Integrative Sciences, JNU, New Delhi 110067, India*

Using the first principle full-potential linearized augmented plane wave (FP-LAPW) method the electronic structure, elastic properties of GaP in zinc-blende (ZB) structure and its phase transition to rock-salt (RS) structure under different pressures are studied. The phase transition from ZB to RS structure is found to occur at a pressure of 21.9 GPa. It exhibits a 14.11% volume decrease of ZB to RS structure at the transition pressure. The energy band diagram of GaP ZB structure shows an indirect band gap of 2.33 eV. The partial density of states (DOS) shows the main contributions of *s*, *p*, and *p*, *d* atomic orbital states of non-metal *P* and metal Ga atom in the band diagram.

KEYWORDS: ELASTIC PROPERTIES; ELECTRONIC STRUCTURE; GALLIUM PHOSPHIDE (GAP); PHASE TRANSITION.

1. INTRODUCTION

Gallium phosphide is an important group III–V binary compound semiconductor. In quantum and optoelectronic devices, it is often used as a substrate.[1] It is a popular semiconductor material and is considered to be of wide-band gap and hence making it a good candidate for room-temperature device applications such as top junction solar cells in multi junction solar cell system. GaP is used as a substrate in low-cost red, orange, and green light-emitting diodes (LEDs) with low to medium brightness since the 1960s. It has a relatively short life at higher current and its lifetime is sensitive to temperature. Because of its many uses, the investigation of its physical properties has become of great interest. In 1983, Froyen and Cohen calculated the electronic band structure of GaP using the psedopotential total energy approach.[2] Many other groups have also calculated the electronic structure of GaP using different methods like the semi empirical pseudopotential, the tight binding method and full potential method.[3–6] Although there are more theoretical and experimental papers on GaP, to the best of our knowledge, there are not much paper on the study of electronic structure, elastic properties and phase transition. In this present work we have investigated the electronic structure, elastic properties as well as its phase transition from ZB to RS structure of GaP using the FP-LAPW method based on density functional theory (DFT). In this method the exchange-correlation potential was calculated with Generalised Gradient approximation (GGA) using the Perdew–Burke–Ernzerhof (PBE-GGA) scheme.[7] The paper is organised into the following sections, in Section 2 we briefly describe the computational technique used in the calculation of the electronic structure of GaP. In Section 3 we compare our results with the previous theoretical and experimental results. The conclusion of our work is given in Section 4.

*Author to whom correspondence should be addressed.
Email: indraofficial@rediffmail.com
Received: 9 September 2013
Accepted: 29 September 2013

2. COMPUTATIONAL METHOD

Within the formalism of DFT,[8–10] the total energy is expressed as a functional of density of the electron system, ρ as

$$E[\rho] = T_0[\rho] + V_H[\rho] + V_{xc}[\rho] + V_{ext}[\rho]$$

where, $T_0[\rho]$ is the kinetic energy of a non-interacting electron system, $V_H[\rho]$ and $V_{XC}[\rho]$ are the Hartree and exchange-correlation contributions to the energy and $V_{ext}[\rho]$ is the energy due to the external potential of the system. Thus the corresponding Hamiltonian called the Kohn-Sham Hamiltonian is

$$\hat{H}_{KS} = \hat{T}_0 + \hat{V}_H + \hat{V}_{XC} + \hat{V}_{ext}$$
$$= -\frac{\hbar^2}{2m_e}\vec{\nabla}_i^2 + \frac{e^2}{4\pi\varepsilon_0}\int \frac{\rho(\vec{r}')}{|\vec{r}-\vec{r}'|}d\vec{r}' + V_{XC} + V_{ext}$$

The exact density of N electron system can be expressed in ground state by, $\rho(\vec{r}) = \sum_{i=1}^{N} \Phi_i(\vec{r}) * \Phi_i(\vec{r})$ where the single particle wave functions $\Phi_i(r)$ are the N lowest energy solutions of the Kohn Sham equation: $\hat{H}_{ks}\Phi_i = \epsilon_i\Phi_i$ of the N electron system. This equation can be solved self consistently in an iterative process. DFT calculation is performed using the first principle FP-LAPW method as well as GGA as implemented in WIEN2K.[10–12] This method is used as it is one of the most accurate methods in electronic structure calculation of crystals. In this method, the lattice is divided into non-overlapping spheres (called atomic or muffin tin sphere) surrounding each atomic sites and an interstitial region.[13] Inside the muffin tin (MT) region, the potential is a product of radial function and spherical harmonics and expanded up to order $l = 10$. For the interstitial regions that are outside the muffin tin spheres, the potentials are expanded in plane waves. 8000 k-points are used as we find that above 8000 k-points the energy remains same for the integration part which reduces to 256 irreducible k-points inside the Brillion zone. Convergence is obtained at $R_{MT}K_{max} = 9.0$ where R_{MT} is the atomic sphere radii and K_{max} gives the plane wave cut-off.

3. RESULTS AND DISCUSSION

3.1. Structural Properties

The first important step in calculating the total energy of the system is to generate the optimized structure. So, the number of optimized k points used in the Brillouin zone is essential. Figure 1(a) shows the variation of k-points with energy per unit cell structure of GaP. One can see a lot of energy variations at different k values. It is observed that at around 7500 k-points onwards there is no much variation of energy. Thus taking 8000 k-points is well good enough for further calculations. In literature, there are two phases of GaP such as ZB and RS and shows phase transition under pressure.[14] Figure 1(b) shows the two curves of total energy as a function of primitive cell volume of ZB and RS structures of GaP to make a sense of more stable structure. A series of different lattice constants are used to calculate the total energy and the corresponding unit cell volume. From the figure one can see that the ZB structure of GaP is more stable in comparison to the RS structure which is in agreement with the other's previous work.[1, 14] The two curves are fitted with Birch-Murnaghan equation of state.[15] The obtained equilibrium lattice parameter (a_0), bulk modulus (B_0), and pressure derivative of the bulk modulus (B') are listed in Table I. These values are compared with the previous theoretical and experimental results as published by other groups.[14–21] It shows that our results are reasonably in agreement with the previous reported data.

3.2. Phase Transition and Elastic Properties

The phase transition pressure at absolute temperature is found out from the equal enthalpy condition i.e., the pressure at which the enthalpies of both ZB and RS structure

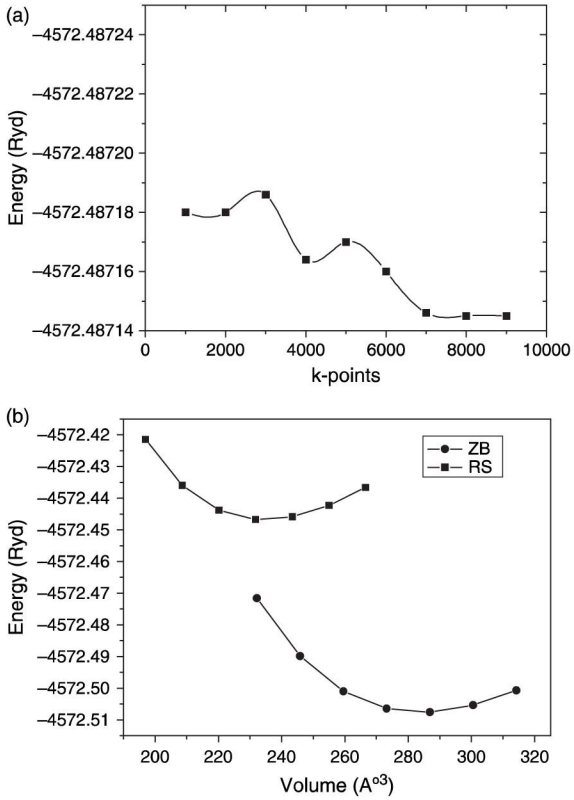

Fig. 1. (a) Total energy per unit cell of GaP verses number of k-points. (b) Total energy verses unit cell volume of GaP-ZB and RS structures.

is same. In Figure 2 the enthalpy as a function of pressure is shown. It is observed that the phase transition from the ZB to RS structure occurred at a pressure of 21.9 GPa which is in good agreement with the other's experimental and theoretical results as shown in Table II. Figure 3 shows the variation of normalised volume (V_p/V_o) with respect to equilibrium volume (V_o) with pressure of both the phases. It is observed that the normalised volumes of both the phases are found to decrease with increase in pressure. During the phase transition, V_p/V_o of ZB phase is found to occur at 0.8293 and of the RS phase at 0.6882. It clearly shows the volume collapses at 14.11%

Table I. Equilibrium lattice constant (a_0), bulk modulus (B_0), pressure derivative (B_0') of GaP ZB and RS structures.

Structure	a_0 (Å)	B_0 (GPa)	B_0'
ZB			
Present work	5.523	77.708	4.347
References	5.512;[a] 5.411;[b] 5.50;[c] 5.386[d]	76.0;[a] 90.0;[b] 77.21;[c] 86.8[d]	4.59;[a] 4.50;[b] 4.88;[c] 4.00[d]
RS			
Present work	5.181	88.342	4.814
References	5.165;[e] 5.160[f]	87.3;[e] 87.59[f]	3.78;[e] 4.54[f]

Notes: [a]Ref. [16]; [b]Ref. [17]; [c]Ref. [20]; [d]Ref. [19]; [e]Ref. [14]; [f]Ref. [1].

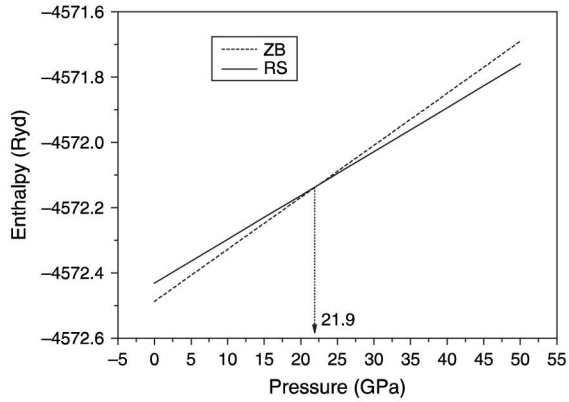

Fig. 2. Enthalpy per unit cell of GaP-ZB and RS structures as a function of pressure.

Table II. Transition pressure for ZB to RS structure of GaP under pressure.

ZB–RS	Pressure (GPa)
Present work	21.9
Ref. [14]	21.9
Ref. [24]	24 ± 0.3
Ref. [25]	22.0
Ref. [26]	21.5 ± 0.8

indicating that RS phase of GaP is more compressible as compare to ZB phase. Hence the elastic constants C_{11}, C_{12}, C_{44} of GaP ZB structure are calculated for the lattice volume corresponding to the pressure ranging from 0 GPa to 21.9 GPa using the stress–strain method.[22] For computing the elastic constants C_{ij}, the volume conserving technique is used.[23] The results are listed in Table III.

The results clearly show the mechanical stability conditions: $(C_{11}+2C_{12}) > 0$; $C_{11}C_{12} > 0$; $C_{44} > 0$ are satisfied and hence the stable GaP ZB structure can exists up to higher pressure of 22.3 GaP. The other elastic parameters

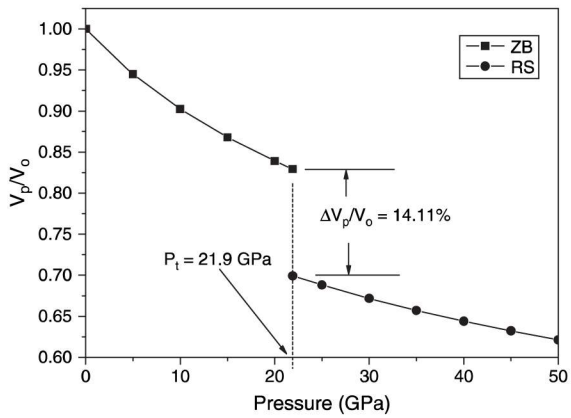

Fig. 3. Normalised volume under pressure verses pressure of GaP-ZB and RS structures.

Table III. Calculated elastic constants C_{11}, C_{12}, C_{44} of GaP ZB structure.

Structure:	P (GPa)	C_{11} (GPa)	C_{12} (GPa)	C_{44} (GPa)
Zinc-blende	0	124.1; 123.5;[e] 137.5[g]	54.9; 50.9;[e] 59.4[g]	84.1; 70.9;[e] 72.2[g]
	5	147.864	72.587	100.640
	10	171.107	90.325	117.443
	15	183.915	112.007	130.246
	20	201.757	130.358	144.158
	22.3	206.420	139.969	150.128

Notes: [e]Ref. [14]; [g]Ref. [27].

Table IV. Calculated values of density ρ, Zener anisotropy factor A, Poisson's ratio υ, Kleinman parameter ζ, Youngs modulus Y and Deby's temperature Θ_D of GaP ZB structure.

ρ (kg/m^3)	A	υ	ζ	Y (GPa)	G (GPa)	Θ_D (K)
3969.3279	2.43	0.197	0.567	141.069	58.9017	458.82

such as Zener Anisotropy factor A, Poisson's ratio υ, and Young's modulus Y are calculated at zero pressure lattice volume by using the relations given by Mayer et al.[28,29]

$$A = 2C_{44}/(C_{11}-C_{12})$$

$$\upsilon = (1/2)[B-(2/3)G]/[B+(1/3)G]$$

$$Y = 9GB/(G+3B)$$

where $G = (G_V + G_R)/2$ is the isotropic shear modulus,

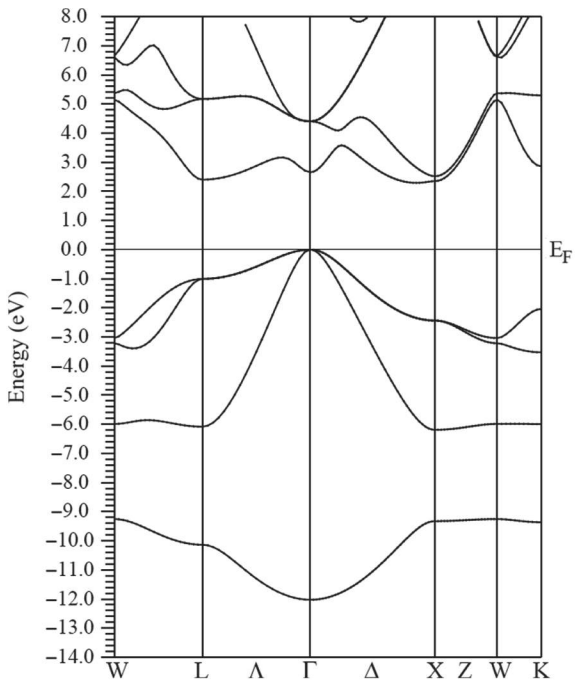

Fig. 4. Energy band diagram of GaP ZB structure.

ARTICLE

G_v is the Voigt's shear modulus and G_R is the Reuss's shear modulus and can be expressed as:

$$G_V = (C_{11} + C_{12} + 3C_{44})/5 \text{ and}$$
$$5/G_R = 4/(C_{11} - C_{12}) + 3/C_{44}$$

It is well understood that the relative positions of the cation and anion sub-lattices under volume conserving strain distortions, for which the positions are fixed by symmetry is described by the kleinman parameter ζ given by:

$$\zeta = (C_{11} + 8C_{12})/(7C_{11} + 2C_{12})$$

Also, from the bulk modulus and the isotropic shear modulus, the longitudinal elastic wave velocity (v_l) and the transverse elastic wave velocity (v_t) are calculated as follows:

$$v_l = [(3B + 4G)/3\rho]^{1/2} \text{ and } v_t = (G/\rho)^{1/2}$$

Now, the average sound velocity (v_m) is given by

$$v_m = [(1/3)\{2/v_t^3 + 1/v_l^3\}]^{-1/3}$$

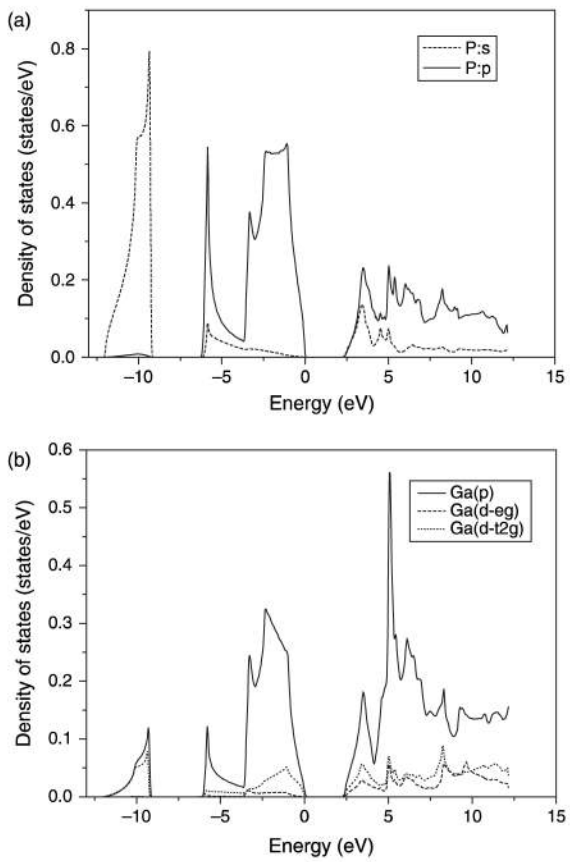

Fig. 5. (a) Partial DOS of P (s, p) in GaP ZB structure. (b) Partial DOS of Ga (p, d) in GaP ZB structure.

Using the average sound velocity v_m, the Debye's temperature θ_D is calculated from the elastic constants data as given by:

$$\theta_D = (h/k)[(3n\rho N_A)/(4\pi M)]^{1/3} V_m$$

where h is the Plank's constant, k is the Boltzmans constant, N_A is the Avogadro's number, n is the number of atoms per formula unit, M is the molecular mass per formula unit, ρ ($= M/V$) is the density. Thus computed elastic parameters are listed in Table IV.

3.3. Band Structure and Density of States

Figure 4 shows the band diagram of GaP ZB structure. In this band diagram, one can observe that the valance band maximum occurs at the Γ point and the minimum conduction band occurs at L point. Hence GaP is found to be an indirect band gap material with the band gap of 2.33 eV which is in quite agreement with the theoretical and experimental values of 2.09 eV–2.74 eV as reported by other groups.[5, 20, 21, 30] Figures 5(a) and (b) shows the partial DOS of the non metal P atom and metal Ga atom in GaP respectively. From the partial DOS as shown in Figures 5(a) and (b), one can observe that the lowest band appears in energy band diagram (in Fig. 4) is mainly contributed from 2s-non metal (P atom). This band is distributed in a width of approximately 3 eV. Above this band, there lies valence band of width of approximately 6 eV. This valence band is contributed together from the 2p non-metal orbital, and 2s, 2p metal orbital with a little contribution from d metal orbital.

4. CONCLUSION

In this paper we present a detailed study of electronic structure and elastic properties of GaP along with its phase transition from ZB to RS structure under pressure using the full-potential linearized augmented plane wave method. The exchange correlation potential was calculated within the generalized gradient approximation using the Perdew–Burke–Ernzerhof (PBE-GGA) scheme. The phase transition from ZB to RS structure is found to occur at 21.9 GPa and GaP ZB phase is more stable. At the transition, the volume collapses at 14.11% indicating the RS phase of GaP is more compressible as compare to ZB phase. The band diagram of GaP in ZB structure exhibits an indirect band gap of 2.33 eV. The partial DOS shows the main contributions from s, p orbital of non metal P atom and p, d orbital of metal Ga atom in the band diagram of GaP. The calculated equilibrium lattice parameter, bulk modulus and pressure derivative of the bulk modulus are found to be in good agreement with the other experimental and theoretical studies. Also using the stress–strain method, the elastic parameters such as Zener anisotropy factor, Poisson's ratio, Kleinman parameter, Young's modulus and Deby's temperature Θ_D are found to be 2.43, 0.197, 0.567, 141.0693 GPa and 458.82 K respectively.

References and Notes

1. L. Sukit, P. Reunchan, A. Janotti, and G. V. W. Chris, *Phys. Rev. B* 77, 195209 **(2008)**.
2. S. Froyen and M. R. Cohen, *Phys. Rev. B* 28, 3258 **(1983)**.
3. Y. Al-Douri and H. Aourag, *Physica B* 324, 173 **(2002)**.
4. Y. Al-Douri, S. Mecabih, N. Benosman, and H. Aourag, *Physica B* 325, 362 **(2003)**.
5. M. Rabah, Y. Al-Douri, M. Sehil, and D. Rached, *Mater. Chem. Phys.* 80, 34 **(2003)**.
6. A. H. Reshak, *Eur. Phys. J. B* 47, 503 **(2005)**.
7. J. P. Perdew, S. Burke, and M. Ernzerhof, *Phys. Rev. Lett.* 77, 3865 **(1996)**.
8. P. Hohenberg and W. Kohn, *Phys. Rev. B* 136, 64 **(1964)**.
9. W. Kohn and L. J. Sham, *Phys. Rev. A* 140, 1133 **(1965)**.
10. S. Cottenier, Density functional theory and the family of (L) APW-methods: A step-by-step introduction (Belgium, Insti-tuut voor Kern-en Stralingsfysica, K. U. Leuven ISBN 90-807215-1-4) **(2002)**.
11. E. Wimmer, H. Krakauer, M. Weinert, and A. J. Freeman, *Phys. Rev. B* 24, 864 **(1981)**.
12. P. Blaha, K. Schwarz, G. K. H. Madsen, D. Kvasnicka, and J. Luitz, Wien2k.Techn.Universitat, Wien, Austria, ISBN 3-9501031-1-2 **(2001)**.
13. O. K. Andersen, *Phys. Rev. B* 12, 3060 **(1975)**.
14. L. Liu, J. J. Wei , X. Y. An, X. M. Wang, H. N. Liu, W. D. Wu, *Chin. Phys. B* 20, 106201 **(2011)**.
15. F. Birch, *Phys. Rev.* 71, 809 **(1947)**.
16. R. Rashid Ahmed, F. Aleem, S. J. Hashemifar, and H. Akbarzadeh, *Physicab. Conden. Matter.* 403, 1876 **(2008)**.
17. A. Mujica, R.J. Needs, *Phys. Rev. B* 55, 9659 **(1997)**.
18. B. Bouhafs, H. Aourag, and M. J. Cartier, *Phys: Conden Matter.* 12, 5655 **(2000)**.
19. S. B. Zhang and M. L. Cohen, *Phys. Rev. B* 35, 7604 **(1987)**.
20. Y. Al-Douri and A. H. Reshak, *Applied Phys. A* 104, 1159 **(2011)**.
21. N. Bouarissa, H. Baazis, and Z. Charifi, *Phys. Status Solidi (b). Basic Solid State Phys.* 231, 403 **(2002)**.
22. F. Birch, *J. Appl. Phys.* 9, 279 **(1938)**.
23. D. C. Wallace, Thermodynamics of Crystals, Wiley, New York **(1972)**.
24. J. P. Pinceaux, J. M Besson, A. Rimsky, and G. Weil (eds.), High pressure in research and industry, *Proceedings of the 8th AIRAPT Conference*, Institute of Physical Chemistry, University of Uppsala, Sweden, August **(1981)**.
25. A. J. Miller, G. A. Saunders, and Y. K. Yogurtcu, *Philos. Mag. A* 43, 1447 **(1981)**.
26. M. Baublitz and A. L. Ruoff, *J. Appl. Phys.* 53, 6179 **(1982)**.
27. D. Gehrlich and M. Wolf, High Pressure Science and Technology, Pergamon, Oxford **(1980)**.
28. H. Mayer, E. Anton, M. Bott, J. Methfessel, J. Sticht, and P. C. Schmidt, *Intermetallics* 11, 23 **(2003)**.
29. M. Jamseson, B. I. Sharma, R. Bhattacharjee, R. K. Thapa, and R. K. B. Singh, *Physica B* 406, 4041 **(2011)**.
30. S. K. Tewksbury, Semiconductor materials, edited by C. J. Whitaker, Microelectronic System Research Center, West Virginia University **(2005)**.

ARTICLE

Kh. Kabita [1]
Jameson Maibam [1]
B. Indrajit Sharma [1*]
R.K. Brojen Singh [2]
R. K. Thapa [3]

[1]Department of Physics, Assam University, Silchar-788011, Assam, INDIA
[2]School of Computational and Integrative Sciences, JNU, New Delhi, INDIA
[3]Department of Physics, Mizoram University, Aizawl, Mizoram, INDIA
** Corresponding author: indraofficial@rediffmail.com*

First Principle Calculation of Pressure-Induced Phase Transition and Band Structure of Gallium Phosphide

A first principle study of the electronic, structural and phase transition of the III-V binary compound semiconductor gallium phosphide (GaP) is performed under the framework of density functional theory (DFT). Structural transformation from the zinc-blende (ZB) to rocksalt (RS) structure is observed at a pressure of about 21.9 GPa and the dependence of the volume decrease of ZB to RS structure at the transition pressure is 14.11% . The variation of the energy band gap, elastic constants and debye's temperature with pressure are also obtained successfully. Our results are found to be in consistent with other experimental and theoretical results.

Keywords: Density Functional Theory, Density of states (DOS), Band structure, Phase transition
Received: 27 November 2013, **Revised:** 8 December 2013, **Accepted:** 15 December 2013

1. Introduction

Gallium phosphide is an important III-V compound semiconductor which has increasingly attracted attention theoretically and experimentally and can be used advantageously in a variety of technological areas. It is also considered to be of wide-band gap and hence making it a good candidate for room-temperature device applications such as top junction solar cells and multi junction solar cell system. The variation of band gap of GaP with pressure is important for the identification of some of the luminescent processes and for a better understanding of their origin. In recent years the study of the structural properties, phase diagram and effect of pressure has aroused considerable scientific interest. Two phases of GaP such as zinc-blende (ZB) and rock-salt (RS) has been found with phase transition taking place under pressure [1]. The ZB to RS structure phase transition has been found to occur around 18.8 GPa with unstable RS structure [2]. Using the density functional theory (DFT) Rashid et al. [3] have studied the structural and electronic properties of GaP and compared the lattice parameters, bulk modulus, pressure derivative of the bulk modulus with earlier data. A. Mujica and R. J. Needs [4] found that the simple cubic phase of GaP should be stable between 14.7 GPa and 20.3 GPa. The High-pressure properties of the zinc-blende structure have been determined by Raman scattering, ultrasonic measurements, fundamental absorption, and refractive-index measurements [5-7]. Even though GaP has been well known for a long time, calculations on the elastic properties and pressure variation of GaP are still very rare. In the present work, the phase transformation from zinc-blende to rocksalt structure along with the electronic structure, density of states (DOS), change in band gap, and variation in mechanical properties is studied for better understanding of the semiconductor.

2. Computational Method

The calculation of GaP was performed within the framework of density functional theory (DFT) using the full potential linearised augmented plane wave (FP-LAPW) method [8]. The exchange-correlation effects are treated within the generalised gradient approximation of Perdew-Burke-Ernzerhof (PBE-GGA) scheme [9] as implemented in wien2k code [8,10,11]. This method is used as it is one of the most accurate methods in electronic structure calculation of crystals. In this method, the lattice is divided into non-overlapping atomic spheres surrounding each atomic sites and an interstitial region [12]. Inside the muffin tin (MT) region, the potential is a product of radial function and spherical harmonics and expanded up to order l = 10. For the interstitial regions that are outside the muffin tin spheres, the potentials are expanded in plane waves. 8000 k-points are used for the integration part which reduces to 256 irreducible k-points inside the Brillion zone. Convergence is obtained at $R_{MT}K_{max}$ =9.0 where R_{MT} is the atomic sphere radii and K_{max} gives the plane wave cut-off.

3. Results and Discussion

3.1 Structural properties

The ground state lattice parameter of ZB and RS structure of GaP are obtained by optimisation of the structures. The total energy and the corresponding primitive cell volume are calculated by setting a series of different lattice constants for both the structures and the energy versus volume curves are shown in figure 1. From figure 1 it is clearly seen

 All Rights Reserved

that the ZB structure of GaP is more stable as compared to RS structure which is in good agreement with other previous results [1,4]. The zero pressure, lattice constant a_o, bulk modulus B_o, pressure derivative of the bulk modulus $B_o^{/}$ are obtained by fitting the calculated energy-volume points to the Birch-Murnaghan equation of states [13] and the obtained results are listed in table 1. It shows that our results are reasonably in agreement with the previous reported data [1, 4, 14-16].

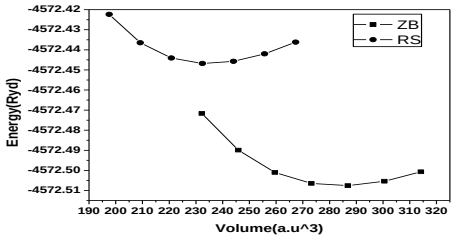

Fig. (1) Energy versus volume for different structure of GaP

Table (1) Lattice constants a_o, bulk modulus B_o, and pressure derivative of bulk modulus $B_o^{/}$ for ZB and RS structures of GaP at zero pressure

Structure		a_0 (A^0)	B_0 (GPa)	$B_0^{/}$
ZB	Present work	5.523	77.709	4.347
	References	5.411[a]; 5.50[b]; 5.386[c]	90.0[a]; 7.21[b] ; 86.8[c]	4.50[a];4.88[b]; 4.00[c]
RS	Present work	5.181	88.303	4.84
	References	5.165[d]; 5.160[e]	87.3[d]; 87.59[e]	3.78[d]; 4.54[e]

[a]Ref. [4]; [b]Ref. [14]; [c]Ref. [15]; [d]Ref. [1]; [e]Ref. [16].

3.2 Phase transition and Elastic properties

For the determination of phase transition pressure at zero temperature, the usual condition of equal enthalpies i.e. H=E+PV is used. The enthalpy as a function of pressure is shown in figure 2. The phase transition of GaP from ZB to RS is found to occur at 21.9 GPa pressure. The obtained transition pressure is found to be in good agreement with other experimental and theoretical results which are shown in table 2. In figure 3, the normalised volume (Vp/Vo) of ZB and RS of GaP at different pressure is shown. The relative volume is found to decrease as pressure increases for the two structures. During the phase transition, V_p/V_o of ZB phase is found to occur at 0.8293 and the RS phase at 0.6882. It clearly shows that the volume collapses at 14.11% indicating that ZB phase of GaP is more compressible as compare to RS phase. Hence the elastic constants C_{11}, C_{12}, C_{44} of GaP-ZB structure are calculated for the lattice volume corresponding to the pressure ranging from 0 GPa to 21.9 using the stress-strain method [20].

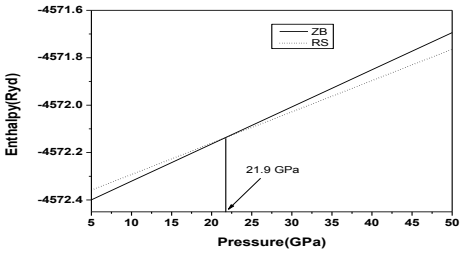

Fig. (2) Enthalpy as a function of pressure

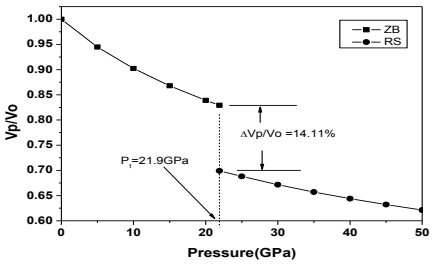

Fig. (3) Phase transition between ZB and RS structure of GaP at 21.9 GPa

For computing the elastic constants C_{ij}, the volume conserving technique is used [21]. The results are shown in figure 4. The results clearly show the mechanical stability conditions: $(C_{11}+2C_{12})>0$; $C_{11}C_{12}>0$; $C_{44}>0$ are satisfied and hence the stable GaP-ZB structure can exists up to higher pressure of 21.9 GaP. Using the calculated elastic constants (C_{11}, C_{12}, C_{44}), the Debye's temperatures of the ZB phase at different pressures are obtained. Form figure 4 and figure 5, it is also observed that the elastic constants as well as the Debye's temperature increases with increasing pressure.

Table (2) Transition pressure from ZB to RS in GaP

ZB - RS	Pressure (GPa)
Present work	21.9
Ref.1	21.9
Ref.17	24±0.3
Ref.7	22.0
Ref.18	21.5±0.8
Ref.19	21.7

© Iraqi Society for Alternative and Renewable Energy Sources and Techniques (I.S.A.R.E.S.T.)

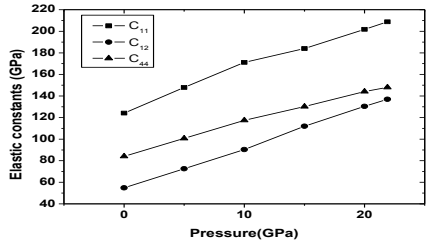

Fig. (4) Elastic constants (C_{11},C_{12},C_{44}) as a function of pressure

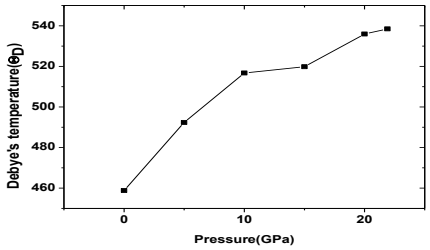

Fig. (5) Debye's temperature as a function of pressure

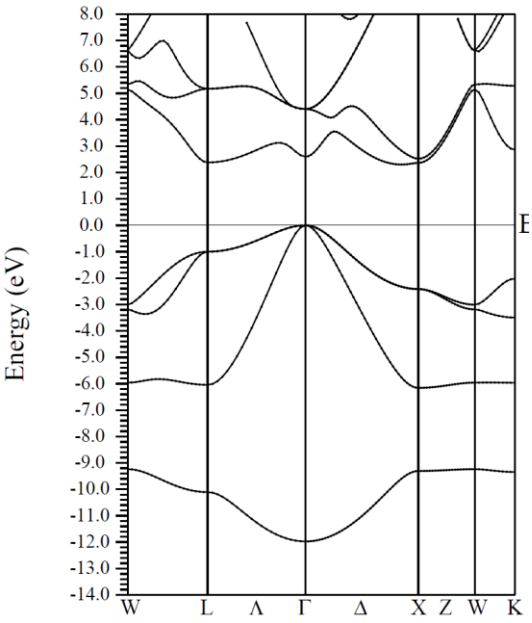

Fig. (6) Energy band diagram of GaP ZB structure at zero pressure

3.3 Band structure and Density of states

The energy band diagram of GaP-ZB at zero pressure is shown in figure 6 and the partial DOS of Ga and P in GaP-ZB are shown in figure 7 (a) and 7 (b) respectively. In the band diagram, one can observe that the valance band maximum occurs at the Γ point and the minimum conduction band occurs at L point. Hence GaP-ZB is found to be an indirect band gap semiconductor material of 2.3 eV. From the partial DOS one can observe that the lowest band appears in energy band diagram is mainly contributed from s-non metal (P atom) orbital and the valance band is mainly contributed by the s-metal (Ga- atom) orbital and p-non metal orbital with little contribution from the p-metal orbital. The contribution of the s, p orbitals of metal and non-metal in Density of States (DOS) in the lowest and valence band is found to decrease with increase in pressure. The variation of band gap of GaP-ZB structure under pressure ranging from 0 GPa to 21.9 GPa is shown in figure 8 and observed that there is increase in band gap with increase of pressure.

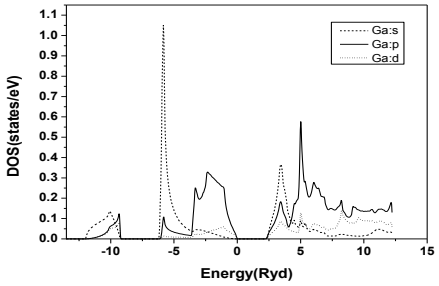

(a)

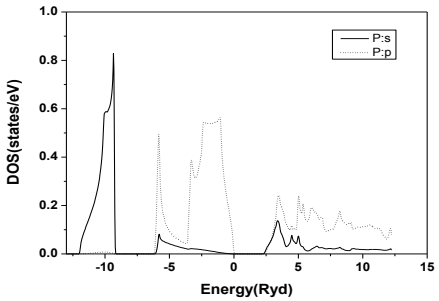

(b)

Fig. (7) (a) Partial DOS of Ga in GaP, (b) Partial DOS of P in GaP

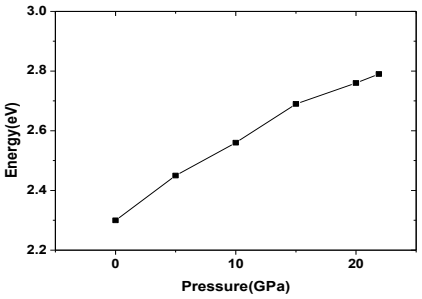

Fig. (8) Pressure versus energy band gap in GaP

4. Conclusion

In this paper we present a detailed study of pressure induced phase transition and electronic structure of GaP from ZB to RS structure. The phase transition from ZB to RS structure is obtained at 21.9 GPa and ZB phase is found to be more stable. During the phase transition, the relative volume of ZB phase is occured at 0.8293 and the RS phase at

 All Rights Reserved

0.6882 and volume collapses at 14.11% indicating that ZB phase of GaP is more compressible as compare to RS phase. The calculated equilibrium lattice parameter, bulk modulus and pressure derivative of the bulk modulus are found to be in good agreement with the other experimental and theoretical studies. The Debye's temperature calculated from the elastic constants is increased with increase in pressure. GaP-ZB phase is found to be an indirect band gap semiconductor material of 2.3eV and band gap increases with increase in pressure. The partial DOS shows the main contributions from s, p orbital of non metal-P atom and p, d orbital of metal-Ga atom in the band diagram of GaP.

References

[1] L. Lui et al., *Chinese Physics B*, 20(10) (2011) 106201-106206.
[2] A. Garcia, and M. L. Cohen, *Phys. Rev. B*, 47 (1993) 6751-6754.
[3] A.R. Rashid et al., *Physica B: Condens. Matter*, 403 (2008) 1876-1881.
[4] A. Mujica and R. J. Needs, *Phys. Rev. B*, 55 (1997) 9659-9670.
[5] J.P. Itie et al., *Phys. Rev. B*, 40 (1989) 9709–9714.
[6] A. Bernard, Weinstein and G.J. Piermarini, *Phys. Rev. B*, 12 (1975) 1172–1186.
[7] A.J. Miller, G.A. Saunders and Y.K. Yogurtcu, *Philos. Mag. A*, 43 (1981) 1447-1471.
[8] E. Wimmer et al., *Phys. Rev. B*, 24 (1981) 864-875.
[9] J.P. Perdew, K. Burke and M. Ernzerhof, *Phys. Rev. Lett*., 77 (1996) 3865-3868.
[10] P. Blaha et al., Techn. Universitat, Wien, Austria, ISBN 3-9501031-1-2, (2001).
[11] S. Cottenier, "Density Functional Theory and the family of (L) APW-methods: a step-by-step Introduction" (Belgium, Instituut voor Kern-en Stralingsfysica, K. U. Leuven., ISBN 90-807215-1-4, (2002).
[12] O.K. Andersen, *Phys. Rev. B*, 12 (1975) 3060-3083.
[13] F. Birch, *Phys. Rev*., 71 (1947) 809-824.
[14] Y. Al-Douri, and A.H. Reshak, *Applied Physics A*, 104 (2011) 1159-1167.
[15] S.B. Zhang and M.L. Cohen, *Phys. Rev. B*, 35 (1987) 7604-7610.
[16] L. Sukit et al., *Phys. Rev. B*, 77 (2008) 195209-1952015.
[17] J.P. Pinceaux et al., "High pressure in research and industry", Proc. of the 8th AIRAPT Conf.; August 17-22; Institute of Physical Chemistry, University of Uppsala, Sweden, (1981).
[18] M. Baublitz and A.L Ruoff, *J. Appl. Phys*. 53 (1982) 6179-6186.
[19] J. Sjakste, N. Vast and V. Tyuterev, *Phys. Rev. Lett*. 99 (2007) 236405-236409.
[20] F Birch, *J. Appl. Phys*., 9 (1938) 279-288.
[21] D.C. Wallace, **"Thermodynamics of Crystals"**, Wiley, New York, (1972).

© Iraqi Society for Alternative and Renewable Energy Sources and Techniques (I.S.A.R.E.S.T.)